The Climatology of heat waves in the North West Province, South Africa

N Mkiva

orcid.org 0000-0003-4878-4943

Dissertation accepted in fulfilment of the requirements for the degree Master of Science in Geography at the North West University

Supervisor: Prof TA Kabanda

Graduation ceremony: April 2020

Student number: 26788330

Declaration

I declare that the dissertation that I hereby submit for the degree Master of Science in Geography at the North West University is my own work and has not been previously submitted by me for degree purposes at any other university or institution.

Acknowledgements

I would like to express my deep gratitude to my supervisor Professor T.A. Kabanda for his guidance, encouragement and constructive suggestions throughout the writing of this dissertation. Different data sources are acknowledged for making this study a success, these include, the South African Weather Service (SAWS) that provided the temperature data and the National Centers for Environmental Prediction (NCEP), where other meteorological data was obtained. The financial assistance from the North West University Staff bursary is also much appreciated.

Special thanks goes to Prof T.M. Ruhiiga - thank you so much for your words of encouragement. My acknowledgement would be incomplete without thanking my family, and in particular my brothers (Lunga, Xolisile and Zimasa) for their encouragement. I would also like to extend my gratitude to all the other staff members of the Department of Geography and Environmental Sciences. I would also like to show my deep appreciation to Prof S.J. Piketh for his support and assistance in preparation of final submission. To my friends and colleagues, I will forever be grateful for the support you gave me. In the same breath I would like to extend my appreciation to my cousin Lwandlekazi Guzana for her endless words of inspiration- thanks for renewing my energy and purpose of obtaining this degree.

I dedicate this work to my beloved daughter Emihle – I had to spend time away from you in obtaining this degree, it was not fair but worth sacrificing for, and also to my late mother Nokuzola (Snowe) Mkiva- *ndiyabulela ngayo yonke imizamo yakho Dlamini, Zizi, Zitha, Somnt, Maphiko kunga ungaphumla ngoxolo.*

Abstract

The overall objective of this dissertation was to develop a heat wave climatology in North West Province (NWP) of South Africa (SA) through analysing maximum temperature and subsequent atmospheric parameters during the heat wave episodes. The main challenge in studying heat wave is the lack of uniform definition. However, in South Africa, the South African Weather Service (SAWS) has defined it as a condition when mean maximum temperatures for the hottest month are exceeded by 5°C and persist for a minimum of three consecutive days. Based on the statistical analysis of maximum temperatures above a station threshold, 25 heat wave events across 13 stations in NWP were identified. The study domain was extended to include the adjacent oceans (10° - 40°S, 0° - 60°E); in order to monitor the evolution of the large- scale circulation as the heat waves develops. The reanalysis of vector winds, humidity, Outgoing Longwave Radiation (OLR), and geopotential heights at 200 hPa, 500 hPa and 850 hPa from NOAA/OAR/ESRL PSD, Boulder Colorado USA through their website at http://www.esrl.noaa.gov/psd were used.

Cyclic patterns associated with the recurrence of heat waves in NWP were discovered through the application of spectral analysis. Three signals were identified at different periodicities, namely 12years, 4.8 years, and 2.1 years. These cycles were associated with sunspot activity, El Nino-Southern Oscillation (ENSO), and quasi-biennial oscillation (QBO) respectively. The significant findings that relate large-scale atmospheric circulation and heat waves occurrences were found to include:

(i) persistent clear skies over the study area identified by higher OLR values; (ii) existence of strong subsidence as observed from vertical motion patterns and (iii) lower specific humidity and corresponding wind patterns over the South West Indian Ocean (SWIO) and the South Atlantic Ocean (SAO). From this study, the concept and methodology applied in this dissertation should provide the basis for further heat waves scientific research in order to enhance a better understanding about this phenomena. The outcomes derived from this study could be used in various practical applications that include formulating policy developments and several sectoral preparedness and response.

Table of Contents

List of Figures

List of Tables

Acronyms

AMSL: Above mean Sea Level
AO: Atlantic Ocean
AOA: Atlantic Ocean Anticyclone
DEA: Department of Environmental Affairs
DWAF: Department of Water Affairs and Forestry
ENSO: El Niño – Southern Oscillation
EVT: Extreme Value Theory
IO: Indian Ocean
IOA: Indian Ocean Anticyclone
IPCC: Intergovernmental Panel on Climate Change
NCEP: National Centres for Environmental Prediction
NOAA: National Oceanic and Atmospheric Administration
NWP: North West Province
OLR: Outgoing Longwave radiation
PDF: Probability Density Function
POT: Peaks over Threshold
QBO: Quasi –Biannual Oscillation
SABC: South African Broadcasting Corporation
SAO: South Atlantic Ocean
SAWS: South African Weather Service
SEAO: South East Atlantic Ocean
SH: Southern Hemisphere
SIO: South Indian Ocean
SST: Sea Surface Temperatures
SWIO: South West Indian Ocean
TTT: Tropical Temperate Through
UNECA: United Nations Economic Commission for
Africa WMO: World Meteorological Organization

CHAPTER 1

Introduction

1.1. Overview of the Study

The changes in weather and climate extremes have significant impacts and are among the most serious challenges to the society in coping with a changing climate. Meehl *et al*. (2009) indicated that the kinds of extreme weather events that would be expected to occur more often in a warming world are indeed increasing. There is still a global challenge in defining an extreme weather event, as most extremes are qualified on the basis of how rare they are, how intense they are and the impacts they have on the society, which involve excessive loss of life, economic or monetary losses or both (Easterling *et al.,* 2000). However, none of those qualifying options is satisfactory (Beniston & Stephenson, 2004). It is therefore, a necessity to give much attention to these extreme climatic events so as to also detect the occurrence of changes in the environment.

Among the investigated climate extremes is; heat waves. Generally, heat waves are referred to as prolonged extreme temperature conditions, where the term “extreme conditions, according to Deo *et al.* (2009), denotes the infrequent events at the very high or very low end of the range of values of a particular climate variable. Lucio *et al.* (2010) appended the topic of extremes and stated that “an extreme weather event” is an event that is rare within its statistical reference distribution at a particular place. However, the definition of “rare” varies as well, but an extreme weather event would normally be as rare as or rarer than the 10^{th} or 90^{th} percentile. When dealing with climatic events, the extremes are those that are rare both in their intensity and in the frequency of their occurrence (Hinze *et al.,* 1997). Further, Hennessy and Pittock (1995); Katz and Brown (1992) claimed that a small change in the average value can produce a much larger impact on the frequency and intensity of climate extremes.

Although the heat wave phenomenon is not easy to define, due to its spatial distribution and time aspects, the South African Weather Service (SAWS) (2016) has defined a heat wave condition as an atmospheric event when the maximum and minimum temperatures rise above the normal threshold (long term mean) for a particular region, and continues for about 3 days consecutively. The SAWS further states that heat wave exists when for three consecutive days, the maximum temperature is 5 degrees higher

than the maximum for the hottest month. Robinson (2001) defines a heat wave slightly differently by adding that the mean maximum daily temperature during the heat wave period reaches the threshold value at least 1 day and continues at least for 3 days consecutively.

This research intended to study the heat wave climatology in NWP of South Africa. The province is land-locked and therefore prone to continental climate influences. The main purpose of the study is to analyse the synoptic weather associated with heat waves in the region, which might be precursors or provide strong influence on the prevailing temperatures during heat wave episodes. High temperature extremes, because of their impacts on society, are one of the most-investigated meteorological phenomena and are the focus of many studies (Meehl *et al*., 2000; Frich *et al*., 2002).

Therefore, describing heat waves in terms of temperature and the corresponding synoptic conditions for major events can enhance the existing knowledge of these extreme temperature events. The understanding of these extreme events is crucial for local, regional and global stakeholders and decision makers to prepare appropriate adaptation and mitigation plans in areas where these events are common and persistent.

1.2. Background of the study

In general, heat wave definitions differ from one country to another, location to location, because each area has its own physical features, geographical orientation and weather circulation patterns; but the centre of the definitions is generally based on the minimum and maximum temperatures observed at a given location. In this study, the identification of these events were determined based on the daily maximum temperatures. Robison, (2001) indicated that, a heat wave can be registered when there is hot weather for several days. Various causes of a heat wave have been identified, these include the warming of the troposphere (Unkaševica and Tošic 2009). Brabson *et al*. (2005) added that a lack of convective rainfall and high summer temperatures could lead to soil moisture deficit, which could further result in heat wave occurrences.

According to Zittis *et al.* (2014), in most cases heat waves are connected with high pressure systems detected at 500 hPa geopotential heights. At these heights, it has been found that the anti-cyclonic circulation favors most of the extreme heat waves and can extend to >1000 km in radius. Sfîcă *et al.* (2017) have revealed that heat waves do not occur independently of circulation conditions, but their occurrence is

favored by certain flow configurations while unlikely under other ones. Therefore, a relationship between circulation and occurrence of prolonged extreme events is thus an important component of a climate system. Certainly, the synoptic behavior of cyclones and anticyclones is an important manifestation of how large scale circulation can interact with weather extremes (Pezza *et al.,* 2012). During heat wave conditions, other climate features tend to resonate with these changes in temperature (mean maximum temperature); therefore, this study has explored the behavior of such parameters during the evolution of the heat wave (before, during and after the heat wave). The studied climate parameters included: sea surface temperature (SST), pressure, wind (direction and speed), air humidity.

Recent studies in South Africa have applied various climate indices to quantify the heat wave duration and severity based on night-time minima or daytime maxima (Perkins & Alexander, 2013). However, all these indices have been found to have limited convenience when applied for comparing the severity of heat waves based on their spatial and temporal distribution. It is recommended, therefore, that when studying heat waves, different factors should be considered. These include frequency, duration and intensity of temperatures that rise above the normal threshold (long-term mean of maximum temperatures). Min *et al.* (2011); Coumou and Rahmstorf (2012) and IPCC (2013) envisaged that in a future warmer climate, with increasing mean temperatures, heat waves will not only become more frequent, but also their duration and intensity are very likely to increase.

Heat waves in southern Africa are not unusual; the most recent events have been registered in January 2016 (SAWS, 2016) and covered much of the eastern half of South Africa. However, these events in South Africa remain little studied, so this study aimed at examining these heat waves further and reduce this knowledge gap.

1.3 Problem Statement

Earlier studies reveal that South Africa has been under the stress of increasing temperatures and droughts (Fisher *et al.,* 2015). For example, an abnormal increase in temperatures was observed towards the end of the 2015 summer season in South Africa, which resulted in 11 deaths in NWP in just one month (Department of Health & Department of Environmental Affairs (DH & DEA), 2016; (South African Broadcasting Corporation (SABC), 2016. Such unusual heat waves gave rise to questions related to

the future course of the climate and whether this recent event was merely an extreme anomaly or part of an ongoing trend toward more extreme heat waves. Short duration episodes of extreme heat or cold are often responsible for major impacts on society (Trigo *et al.,* 2005; Trigo *et al.,* 2006).

According to Rusticucci *et al.* (2016), the frequency and severity of heat waves are projected to increase in the future due to variation in climate. However, in South Africa there is still scarcity of research given to understanding the climatology of heat waves. Part of the problem is that heat waves are silent killers that do not leave a trail of destruction in their wake. They are, therefore, unlike other known natural climate/weather extremes disasters. Such known disasters include floods, tropical cyclones and tornadoes, that leave visible signs of societal and infrastructure impacts. Usually, heat waves gain attention only while they last; after they pass, memories quickly fade. Therefore, this study committed to explore a climatology of heat waves in NWP of South Africa; thereby initiating the process of understanding the occurrence and importance of such phenomena by exploring and analyzing the physical features and climate of NWP, and the intensity and duration of heat waves.

1.4 Research Aim and Objectives

1.4.1 Aim

The aim of this research was to study a climatology of heat waves in NWP of South Africa over a range period of 1960 to 2016.

1.4.2 Objectives

In order to accomplish the above mentioned aim, the following objectives were set

- To analyse spatial and temporal variations of heat waves in NWP.
- To determine the frequency of heat waves at selected sites in the NWP.
- To analyse the synoptic-scale atmospheric circulation characteristics associated with heat wave conditions.

1.5 Description of the Study Area

This section describes the environmental setting of the study area, focusing on the physical components that highly determine the climate of the area. Also, the location of the stations used in this study are presented in Figure 1.1.

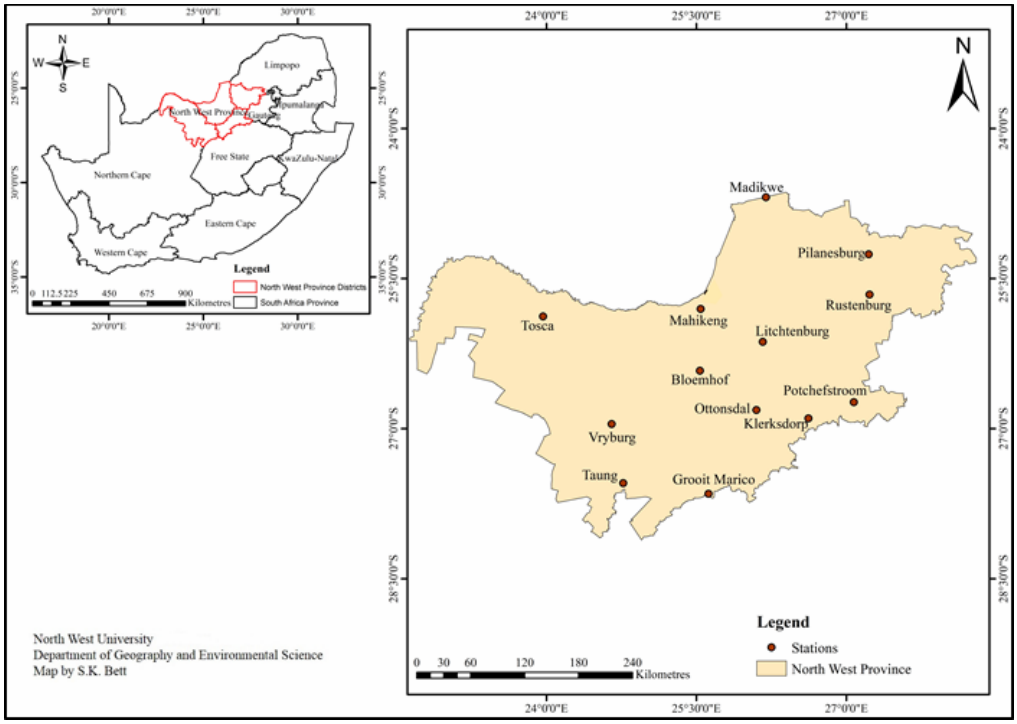

Figure 1.1: Location of the study area (North West Province) for this research. Red dots on the enlarged right hand side map indicates the location of the automatic weather stations collecting hourly data in NWP as part of the SAWS national network.

1.5.1 Location and Physical Characteristics

This study was conducted in the NWP (Figure 1.1). This province is one of the smallest provinces in South Africa and is entirely landlocked by four other South African Provinces, namely Northern Cape (west), Free State (south), Gauteng (east) and Limpopo (north-east), and forming a border with Botswana as a neighboring country to the north (de Villiers & Mangold, 2002). Geographically, it is centered at 26°S and 25°E. According to de Villiers and Mangold (2002), the NWP occupies a total land area of 116 320km^2 and Mafikeng serves as the capital city of the province. It also features one of the driest regions in South Africa, in the plateau which covers a large part of the province.

The NWP landscape has an altitude ranging between 920-1780 m above mean sea level (AMSL) (de Villiers & Mangold, 2002). Much of the area of the province consists of flat areas of scattered trees and grasslands. The Magaliesburg mountain range is situated in the northeast, and extends 130 km from Pretoria to Rustenburg. This affects the climate of the eastern side of the province, giving it a very fine, temperate weather compared to the rest of the province.

1.5.2 Climate

It has been argued that climate is largely influenced by location and its physical characteristics (Iizumi & Ramankutty, 2015). According to Hewitson and Crane (2006), topography and land-water boundaries can define a fixed local climate for the area. The climate of the province is characterized by well-defined seasons with hot summers and cool sunny winters. The climate and rainfall vary from the more mountainous and wetter eastern region to the drier, semi-desert plains of the Kalahari in the west. In the NWP, this rainfall pattern is enhanced by the irregularity of topography across the province. In South Africa and during the winter months (June to August), it is agreed by Engelbrecht and Landman (2014) that the subtropical high-pressure belt is well established over the country (South Africa). As a matter of fact, winter rainfall over the interior is sparse during this season and the dominant weather encompasses sunny days, clear skies and cold nights. Situated at the interior of the country, the NWP is prone to these weather systems as well. Further, the rainy season usually occurs in spring, typically caused by weather systems of the westerly wind regime known as “westerly waves” in concurrence with ridging high-pressure systems in the lower levels of the atmosphere. The moisture transport from the Indian Ocean into the interior is dependent on these two weather systems (Engelbrecht & Landman 2014).

The automatic weather stations used in this study are the; Madikwe, Pilenesburg, Potchefstroom, Rustenburg, Mafikeng, Lichtenburg, Bloemhof, Klerksdorp, Ottonsdal, Marico, Taung, Vryburg and Tosca, which are well distributed over the province. Considering the wide geographic scope of the area and the distribution of stations in the analysis, conducting this study represents an important step towards the accumulation of heat wave frequency, duration, and intensity for the province, thereby providing another step ahead to comprehensive heat wave evolution.

1.5.2.1 Temperature distributions

Temperature affects a wide range of processes and is used as an index of the energy status of the environment. It is one climatic variable for which there is a high degree of confidence that it will increase in the future. The NWP is well known for its unique seasonal and daily variations in temperature, often being extremely hot in summer, with an average of 32°C, and dropping to a cold of 0.9°C during the winter months (de Villiers & Mangold, 2002). The Vaal River flows along the southern border of the province, with other small river channels in different areas of the province. There is a small number of large water bodies in the province and these have a great impact on

the distribution of temperature and circulation patterns regulating the weather. The observed increases in warm extremes are consistent with predictions of a temperature increase in the western half, as well as parts of the north east and east of South Africa (Kruger & Sekele, 2013b), with evidence of an increase in warm extremes. The North West Province has revealed a true correlation to that during the extreme temperature events that were observed in the 2015 summer season. A significant annual increase in frequency of high temperature extremes and a decrease in low temperatures across all areas of the country has been noted by the DEA (2013), particularly in the western and northern interior. The atlantic high pressure system, which is situated near the west coast, is a source of drier air, which moves into the subcontinent from the southwest and southeast (Kruger *et al.,* 2010). As for the geographical setting of North West, temperature distribution is highly affected by the movement of these systems.

1.5.2.2 Rainfall

NWP, which centred on the plateau of South Africa and boarded by escarpments, has a distinct rainfall variability from the rest of the country. The rain brought by the humid sea winds falls over the weather side of the mountain slopes, so that the leeward side stays basically dry. This precipitation gets even lighter towards the Kalahari side of the province, causing evaporation to be more than precipitation rates in many areas of the province. Generally, the distinct hot and summer climate dominating the whole of South Africa is largely affected by the atmospheric systems that dominate the regional climate, namely the anti-cyclonic high pressure and low pressure system. The low pressure normally sits over the eastern side of the landmass, resulting in greater rainfall on the eastern side than the western side, with moisture adverted from the tropical Indian Ocean by the northern limb of the Indian Ocean anticyclone. The anticyclone tends to shift and merge over the continent and largely creates dry conditions over much of the continent (Taljaard & Phil, 1996). The latter system is associated with subsidence and limited cloud development, hence the limitation of rainfall in the province.

1.5.2.3 Water bodies (hydrology)

Surface waters in the province are in the form of rivers, dams, pans, wetlands and dolomitic eyes fed by aquifers. Perennial surface water resources are generally scarce, particularly in the semi-arid western region (Department of Water Affairs and Forestry (DWAF), 2004). The western part receives about <300 mm of rain per year, the semi-arid central part 500mm per year and the moderate eastern part geting about 600 mm per year (READ, 2014). Thus temperatures tend to be high because there are few

surface water bodies to modify the climate. The main rivers are the Crocodile, Groot Marico, Hex, Elands, Vaal, Mooi, Harts and Molopo and this also being the only major river in the drier north-western part of the province.

1.6 Chapter Summary and Organization of the work

This chapter highlights major challenges in defining heat waves. In NWP, recent heat waves have caused significant mortality and environmental impact, showing the need to study and understand these events. Such major challenges in defining heat waves have been highlighted in this chapter. The area's geographical location, its continental climate and the quasi-stationary anticyclone over the subcontinent are likely to influence heat waves.

A review of relevant literature is presented in Chapter 2. Chapter 3 discusses the data involved, how it was used to achieve the objectives of the study. Then, Chapter 4 represents the results of all methods used in this study, except the synoptic analysis of atmospheric parameters, which appear in Chapter 5. Chapter 6 features the overall summary and conclusion.

CHAPTER 2

Literature Review

2.1 Introduction

A review of related literature is provided in this section at a global and national scale, including the different characteristics that have been identified in analysing heat waves. The NWP produces about 18% of South Africa's total maize, a crop whose yield has been shown to be highly sensitive to atmospheric changes (Blignaut *et al.,* 2009). Sunflower and other agricultural products are also produced in the province and abnormally high temperatures can adversely affect yields, causing significant economic harm. It is not only for these reasons that the climatology of heat waves needs to be studied, but also to expand the knowledge about these phenomena and what to expect in future in within the context of a changing climate.

Meehl *et al*., (2000); Radinović and Ćurić (2012) documented in great detail that heat waves have direct consequences on society and the environment, as well as the indirect consequences affecting different domains such as agriculture, water resources, energy demand, regional economies and human health. The developed studies over the past three decades focused on particular types of impact, especially on human health, thermal and air quality conditions (Giles *et al.,* 1990; Matzarakis & Mayer, 1997). Cases of mortality and morbidity due to excess heat were also reported (Pantavou *et al.,* 2008 & Theoharatos *et al.,* 2010).

2.2 Global Temperature Extremes

Prolonged temperature extremes can result in large societal and economic consequences. A general increasing trend in temperature has already been observed globally with an increase of about 0.8°C since 1880 (Hansen *et al.,* 2010; Sánchez-lugo et al., 2018). Associated with this tendency, it is increasingly recognised that extreme weather events might increase in number, intensity and duration (IPCC, 2013). The modelling studies indicate that a 5 to 10% probability of frequent and severe heat waves will occur in a 40-year timeframe (Barriopedro *et al.,* 2011). Extremely high-temperature summer heat waves have been occurring with increasing frequency in recent decades. Some of these extreme temperature changes have been studied by Wang *et al.,* (2015), examining three summers (2003, 2006, and 2013) in Central China. During their study, the synoptic-scale characteristics of heat waves and associated atmospheric circulation

anomalies were investigated. The partial results were that large-scale atmospheric circulation changes, moisture deficiencies, dry conditions and downslope winds were the common features of all the investigated heat wave episodes.

More intense and frequent heat waves have been predicted by Meehl and Tebaldi, (2004) and Beniston, (2004) on the basis of greenhouse simulations. However, they stated that there is clearly a need to quantify pre-greenhouse climate in order to differentiate it from greenhouse influences. Also addressing the greenhouse phenomenon, Planton *et al*., (2008) mentioned that an increase in frequency or intensity of extreme events is commonly associated with distinctive changes in climate due to greenhouse gases and aerosol anthropogenic emissions. They went on to explain how a shift of the probability density function (PDF) of a climatic parameter towards one side of the distribution would indeed induce an increase in the probability of occurrence and the intensity of the extremes on the same side. Thus, it is likely that warming should lead to an increase in frequency and intensity of heat waves, just as a decrease in mean summer rainfall would lead to more frequent and severe drought episodes.

Although most heat waves are defined in terms of days, they can have extended durations. In the United States, heat waves in 1995 and 1996 were confined to a few extreme days in July (Kunkel *et al.,* 1996), and most heat waves seem to be in this category globally. However, a heat wave that occurred in Europe in 2003 had an extended period, where it was sustained over the months of June, July and August (Hunt, 2007). The influence of sea surface temperature (SST) anomalies in the Atlantic and Mediterranean on these heat waves in Europe were investigated, and SST anomalies were found to provide predictability for the occurrence of heat waves (Della-Marta *et al.,* 2007). The frequent synoptic pattern associated with these extreme events in Europe is the omega blocking, typically characterized by a low-high-pattern arranged in the west-east direction, also with the blocking of high pressure system over the same area for long time (Hernández-Ceballos *et al.*, 2016). That in return limits the arrival of the Northern low-pressure systems over Europe.

Chang and Wallace (1987) list heat waves with durations of up to 3 months for the United States. Summer heat waves with extreme high temperatures have been occurring with increasing frequency and these have had disastrous consequences for human health, economies and ecosystems. It is also expected that such events will become more common in the context of global warming (Hunt, 2007). It is with this

regard that, even though a heat wave is a meteorological event, it cannot be fully assessed without reference to human impact.

A combination of weather elements related to the human experience of heat must be used. Over 500 people died from heat-related illness in Chicago during the 1995 heat wave (Karl & Knight, 1997). Many scientific reports about death tolls due to heat waves have been published in many parts of the world. A heat wave that occurred in South Korea in 1994 was clearly exceptional, leaving the city with a death toll exceeding 3000 (Kysely & Kim, 2009). Deaths have also been reported in India due to heat waves over the years. In that country, a heat wave in 1998 caused 2042 deaths, and one in 2015, caused 3054 deaths (Ratnam *et al*., 2016).

2.3 Africa Temperature Extremes

The African continent mainly spans the inter-tropical zone between the Tropic of Cancer and the Tropic of Capricorn. Outside the tropics, the northernmost and southernmost fringes of the continent have a Mediterranean climate (Russo *et al*., 2016). Owing to this geographical location, where solar radiation intensity is always high, extreme events like heat waves can occur in any season in Africa. This is in contrast to European counties, where these events are predominantly in the summer. According to Solomon (2007), Africa is one of the most vulnerable regions to weather and climate variability, and extreme events such as heat waves have an adverse impact on public health, water supplies and food security.

In northern Africa, the northern Sahara experienced 40-50 hot days per year in the period 1989-2009 (Vizy and Cook, 2012) while in South Africa and for the last 15 years, the probability of austral summer heat waves has increased with respect to the period 1961-1980. This was found to be associated with deficient rainfall conditions that tend to occur during El Nino events (Lyon, 2009). In northern Africa, there is a projected increase in number of hot days in the coming decades (Patricola & Cook, 2010; Vizy & Cook, 2012). A recent study by Ceccherini *et al*. (2017) analysed African heat wave regimes by identifying the most important heat waves during the period 1981-2015. The analysis drew attention to the spatial distribution of decades. The complete results gave a clear indication that both intensity and spatial distribution of maximum temperatures are increasing. They further stated that specifically from 1996 onwards, it was possible to observe a positive increase in heat waves, with the maximum presence during 2011-2015.

Scientists have found a decrease in the diurnal temperature range in many parts of the world, although a few exceptions have been found, where the range has actually increased (Karl *et al*., 1993). In South Africa, Muhlenbrunch-Tegan (1992), for the period of 1940-1989, found a decrease in maximum temperature and an increase in minimum temperatures. Hughes (1995) did a re-analysis on the study done by Karl *et al*. (1993) for the period of 1951-1991, and looked at the data for large towns and small towns for the 1960-1990 period. The analysis results showed a maximum temperature increase of about the same across the whole of South Africa regardless of the station location or urban- area size. In Kruger (2004) study, the rate of increase in maximum temperature was found to be +0.11°C decade^{-1} in the small towns and +0.12°C decade^{-1} at the largest city locations.

2.4 Southern Africa Temperature Extremes

Previous studies on temperature trends for 1960–2003 and 1961-2000 in Southern Africa, includes that of Kruger and Shongwe (2004) and New *et al.* (2006), showing a general positive trend in the annual mean, maximum and minimum temperatures. In addition, the results of a study by Kruger and Sekele (2013a) have shown that warm extremes have increased while cold extremes have decreased. However, the trends vary on a regional basis, and their statistical analysis indicated a stronger increase in warm extremes in the western half of South Africa, as well as parts of the east and north-east, than in other areas of the country. According to SAWS (2016), in the month of January 2016, the highest temperatures were recorded in Marico (in the NWP) with a high of 45°C on the 7th of January 2016, breaking a 43-year long record of 41°C, which was recorded on 19 January 1973.

During the inception of this study, the years 2011-2015, have been the hottest on record globally (NOAA, 2015) and in South Africa, they were the driest years since 1904. This can be attributed to variability in weather patterns due to changes in mean values of climate parameters and a very strong El Niño event. NOAA (2015) explains El Nino and La Nina as two opposite phases of what is known as the El Nino-Southern Oscillation (ENSO) cycle. The ENSO cycle is explained as a scientific term that describes the fluctuations in temperature between the ocean and the atmosphere in the east-central Equatorial Pacific (approximately between the International Date Line and 120°W). La Niña is sometimes referred to as the cold phase of ENSO while El Niño is referred to as the warm phase of ENSO. These deviations from normal surface

temperatures can have large-scale impacts not only on ocean processes but also on global weather and climate in specific areas around the world. The two events occur on an average of every two to seven years but El Nino occurs more frequently than La Nina. Two years later, another scientific report was published claiming the 2017 global surface temperatures to be the second or third highest globally since the records began in the mid to late 1800s (Sánchez-Lugo *et al.,* 2018).

Although the southern part of Africa generally receives below-normal rainfall during the El Niño years and La Nina usually bringing normal or above-normal rainfall, it cannot be accepted as a rule. Southern Africa can be divided into numerous rainfall regions, each region having a different correlation with ENSO. Also, ENSO explains only approximately 30% of the rainfall variability, which means that other factors should also be taken into account when predicting seasonal rainfall. For example; the 1997-98 El Nino was the strongest on record but not all of South Africa received below-normal rainfall. Some regions had an abundance of rain because of the moist air that was imported from the Indian Ocean (SAWS, 2016). This is in agreement with Tyson and Preston - Whyte (2000) that once enough moisture is brought onto the continent from the adjacent oceans, a diurnal cycle of rainfall can then develop even in the absence of the large scale forcing provided by the synoptic scale systems such as TTTs (Hart *et al*., 2013). Thus, there is no definite rule for rainfall and temperature changes in ENSO years over southern Africa.

A detailed analysis of other climate parameters was necessary especially in this study. During the 2015 period, SAWS further analysed a percentage of normal rainfall for the season June 2014 – June 2015, and it showed that almost all of the central and eastern South Africa had already experienced below-normal rainfall over the previous year (2013) but the North West and eastern KwaZulu-Natal were, especially dry with only between 50-75% of their average annual rain having fallen (SAWS, 2016).
This has contributed to numerous drought episodes and has caused wide-spread misery and economic hardship in South Africa, and has also been associated with an extraordinary frequency of heat waves (SAWS, 2016). South Africa recorded 48.4°C in Vredendal in October 2015 (the highest recorded temperature in the world for October), while 31 maximum temperature records were shattered during the month of January 2016. Furthermore, January and February 2016 were hottest month yet (SAWS, 2016). Most of the work which has been done in South Africa incorporates heat waves with

drought or any other interrelated climate extremes (Lyon & Mason, 2007; Lyon, 2009 & Fischer, 2014). There are few studies which dealt with heat waves in isolation. Lyon and (Mason, 2007) argued that higher probabilities of heat waves conditioned on drought are largely seen in the interior sections of South Africa, away from coastal locations. They also established that these inland areas also show enhanced heat wave probabilities during El Niño events, which are often accompanied by drought as well as above-average tropospheric temperatures during the austral summer.

During the heat wave episodes, daily maximum temperatures usually rise to values over 40°C in most areas of South Africa, and minimum temperatures above 26°C, for a period of at least two consecutive days (Robinson, 2001). High level of discomfort is experienced as soon as temperature values are higher than 35°C and average relative humidity is more than 25%. This principle is considered particular since heat waves are rare per decade (Robinson, 2001). The national challenge as observed by Hughes (1996) is the period of the available climate records for stations in South Africa, where some larger cities have mean temperature data extending more than a century and many smaller towns have digitized maximum and minimum temperature records from 1960 onwards.

2.5 Future Temperature Extremes for South Africa

Between the years 2006 and 2015, the frequency and spatial average of extreme heat waves had increased to 24.5 observations per year (60.1% of land cover) as compared to 12.3 per year (37.3% of land area) in the period from 1981 to 2005 (Ceccherini, 2017). It is predicted therefore that all African cities are anticipated to face more exceptionally hot days in the future with respect to the rest of the world (Ceccherini *et al*., 2017).

The warming is likely to be greater over the subtropical regions of the continent than over the tropical regions. Currently, there is evidence from observations that a strong warming trend has already manifested itself over southern Africa (Kruger & Shongwe, 2004 & New *et al.,* 2006). They further stated that, in South Africa, the increase in air temperature is likely to be higher over the interior and lower over the coast and eastern escarpment areas. With regards to the African continent, double the global rate of temperature increase is displayed in studies of Engelbrecht *et al* (2015) and Garland *et al* (2015). For North West Province, which is situated in the interior, this could mean that

temperatures will reach a regime never observed before in the recorded climate of the province.

Studies by Meehl and Tebaldi (2004); Coumou and Rahmstorf (2012) and Perkins *et al.* (2012), suggest that at both the global and regional scales, heat waves are of interest to research due to the impact they pose on human health, agriculture, ecosystems and national economy. The NWP produces about 18% of South Africa's total maize, a crop whose yield has been shown to be highly sensitive to atmospheric changes (Blignaut *et al.,* 2009). Sunflower and other agricultural products are also produced in the province and abnormally high temperatures can adversely affect their yields, causing significant economic harm. It is not only for these reasons that the climatology of heat waves needs to be studied but also to expand the knowledge about these phenomena and what to expect in future in within the context of a changing climate.

2.6 Formation of heat waves

Surprisingly, heat waves lack a uniform meteorological definition; rather, different definitions have been applied in different climates. According to WMO, as climate differs from location to location, the definition of extreme event (weather or climate) and its threshold also differs. In other words, what is considered an extreme value of a given climate element in one location can be considered as being within the normal range in another different location. Thus, heat waves can be defined by locally-specific criteria, based on absolute values for a given area, or according to some generally applicable, standardized measure of deviation from normal.

2.6.1 Heat waves over temperature thresholds

In this approach, relative or fixed thresholds are usually employed (Croitoru *et al.* 2014), whereby fixed selected value would only be determined by the climate of a given area. A few studies have revealed extreme values in temperature and some giving an in-depth information on individual events (Karl & Knight, 1997). In a comparable study, Kunkel *et al.* (1996) investigated the 1995 heat wave in Chicago within a climatic perspective by comparing the most extreme temperatures (over five consecutive days) during the event with other very warm maximum temperatures from past events in the records. Such studies analyzed heat waves duration and frequency, which provide more details in displaying an anatomy of heat waves by examining various climatic parameters during the individual events. This is in agreement with Robinson (2000),

who specified that individual events are considered only where required, to refine or to test the definitions.

2.6.2 Heat waves based on percentile thresholds

According to Robinson (2000), the sociological components of a heat wave are dependent on the local climate and can be expressed by some measure of departure from the expected or mean conditions. The applicable definition is that of WMO, which is also cited by Met Office, that a heat wave occurs when daily maximum temperatures in more than five consecutive days exceeds the average maximum temperatures by 5°C, the normal period being 1961-1990 (Barbu *et al.,* 2014). For example, Lyon (2009) investigated the possible behavior of drought and heat waves in South Africa both separately and together. He defined a heat wave as occurring, when for three consecutive days, the daily maximum temperature values exceed the 90th percentile during the southern summer months of December, January and February. However, events exceeding the 95% percentile were also identified. Therefore, using criteria based on percentiles, rather than on direct maximum-temperature values, a uniform standard can be applied at different locations under different conditions. With respect to that, Lyon also argued that a uniform temperature threshold for all stations would not be as meaningful as percentile threshold since the climatology can vary between stations across a region. Different quantitative definitions based on other atmospheric parameters like temperature and humidity have been studied by Grundsteuin *et al*. (2012)

Due to a range of definitions proposed for defining heat waves, there is an obvious incentive for the research communities as well as the public and private sectors to focus on heat wave research. Also, more research is needed on other extreme climatic events so as to access the possible shifts in frequency and intensity of events like floods, storms and heat waves, following climatic changes that are projected by IPCC (2001) to take place in the course of the 21st century. Currently, extremes are qualified on the basis of how rare they are, how intense they are and the impacts they exert on the environment. However, none of those qualifying options is satisfactory (Beniston & Stephenson, 2004). For example, the IPCC (2001) based its definition on the frequency of occurrence of the event, i.e., an event that is as rare as 10% or 90% quantile of a particular distribution of an atmospheric variable such as temperature.

Apparently, ad in terms of extreme temperature impacts on human health, the heat stress of the same 10% upper extreme temperatures in two locations will have a greater human health and environmental impact despite the rareness of the event. Thus, the two approaches used by IPPC for qualifying an extreme event are met in both locations irrespective of the climatic factors they display. This agrees with Beniston *et al*. (2007), explaining that extremes that are generally considered in the impact studies of changes in the climate regime are either rare, typically corresponding to the 10^{th} or 90^{th} percentile (thresholds with 10% of values lower or higher), intense even if not rare or severe through their consequences. The multiplicity of definitions for heat waves reveals a range of reasons that these events are studied.

2.6.3 Heat wave structure

Studies over the southern Hemisphere revealed that, anticyclones have known to be an important feature of the general circulation (Taljaard and van Loon 1963; Taljaard 1967). Most heat wave occurrences in southern Africa tend to feature this circulation. Furthermore, anticyclones are governed by different atmospheric dynamics, according to their scale. Planetary-scale anticyclones, such as the semi-permanent subtropical cyclones, are associated with the descending branch of the Hadley cell. Intermediate-scale anticyclones, as exemplified by blocking highs, are persistently slow-moving systems that grow due to the transport of vorticity and energy by transient eddies. Whereas, mesoscale anticyclones can be triggered by an uplift of air masses over a mountain barrier or by an intense low-level cooling over continental regions during winter (Bluestein, 1992; Ioannidou & Yau, 2008).

Anticyclones can also be classified according to their vertical thermal structure into cold core, warm core or mixed - warm core results from convergence in the upper troposphere and air subsidence beneath (Musk, 1988). This produces warmer than normal temperatures in the middle and lower tropospheres, and because of this, such deep highs intensify with height (Kurz, 1998). Warm-core anticyclones develop in the subtropics and mid-latitude regions with the subtropical high pressure cells to be located at approximately 30°N/S latitude (Hatzaki *et al.,* 2014). With the presence of westerlies, these may be associated with blocking high action and producing extra-warm temperatures.

From an atmospheric perspective, heat events tend to feature the following: (1) subsidence of air and the associated warming and drying of air from adiabatic compression; (2) clear skies, which support warming (latent and or sensible heat fluxes) during the high insolation summer; (3) advection of warm air (Horton *et al.,* 2016). In many locations, the advection will particularly be a poleward wind, but there are two common exceptions involved: the peripheries of large continents, where a day-time wind from the interior will often be warmer than a wind of maritime origin, and regions near higher mountains (such locations can experience their highest temperatures when dry mountain winds descend, compress and warm the valleys) (Lau & Nath, 2012).

2.7 Summary

Owing to the complexity of defining heat waves, several approaches of identifying and defining these extreme events were discussed in this chapter. Since climate differs from location to location, having a uniform definition of extreme events like heat waves and their thresholds is challenging, mainly because what may be considered as being an extreme in a given climate might be within the normal range in another region. A SAWS definition for heat wave was adopted for this study. Most studies in the literature have addressed heat waves together with drought, since prolonged drought episodes are likely to result in an intensification of extreme temperatures, constituting heat waves.

CHAPTER 3

Data and Methodology

3.1 Introduction

This chapter presents the data and methods used in the analysis to determine a climatology of heat waves in the NWP.

3.2 Data Sources and Description

3.2.1 Maximum Temperature

Daily maximum temperature data for 13 stations (Table 3.1) in NWP was obtained from the South African Weather Service (SAWS). Variations in spatial and temporal availability of climatic measurements usually influence the completeness of climate data sets. Gaps in the time series were filled through mean substitution, in the manner of Kotsiantis *et al*. (2006). However, the station data used has varying period ranges from 1960-2016, 1984-2016, 1991-2016, 1992-2016, 1993-2016, 1996-2016,1997-2016, 2005-2016 and 2007-2016 for the newest stations. This variation did not affect the progress of the study, considering that heat waves are rare events, a period of thirty years might even lapse without the occurrence of any single heat wave event (Huber & Gulledge, 2011). However, in climate studies, a 30-year period is a recommended period to observe climatic changes.

Station name	Station Number	Position (Lat/long)		AMSL (meter)	Period of record
Madikwe	0585341 8	-24.6880	26.1960	1027	2005-2016
Pilanesburg	0548375A4	-25.2570	27.2230	1085	1995-2016
Bloemhof	0362189 7	-25.6510	25.6210	1225	1993-2016
Rustenburg	0511399 X	-25.6600	27.2320	1150	1992-2016
Mafikeng	0508047 0	-25.8030	25.5420	1281	1984-2016
Tosca	0504833 6	-25.8780	23.9660	1124	2007-2016
Lichtenburg	0472278 0	-26.1330	26.1640	1497	1993-2016
Potchefstroom	0437104A4	-26.7350	27.0750	1351	1997-2016
Ottonsdal	04350019AX	-26.8140	26.0100	1498	1991-2016
Klerksdorp	0436204 1	-26.8980	26.6200	1329	1993-2016
Vryburg	0432237 3	-26.9540	24.6520	1245	1960-2016
Taung	0360453A0	-27.5450	24.7680	1115	1996-2016
Grooit Marico	0362189 7	-27.6510	25.6210	1225	1960-2016

Table 3.1: List of stations used in the analysis

3.2.2 Re-analysis Dataset

The atmospheric field data that were used in this study are produced by the National Centre for Environmental Prediction (NCEP) and National Centre for Atmospheric Research (NCAR). The field variables used include the climatological means, anomalies and composites of meteorological data. These data were obtained from NOAA/OAR/ESRL PSD, Boulder, Colorado, USA through their website at http://www.esrl.noaa.gov/psd.

The NCEP/NCAR, in collaboration with the National Oceanic and Atmospheric Administration (NOAA), have established a reanalysis using a frozen, state of the art analysis (Kalnay *et al*., 1996). The reanalysis project produced a retroactive record of more than 50 years of global analyses of atmospheric fields in an effort to support research needs and those of climate monitoring communities (Kistler *et al*., 2001). These reanalysis data are generated using a "frozen, state of the art" global numerical weather forecasting model, which assimilates past observation data onto a global three dimensional grid. Past observational data used for assimilation were obtained from ships, rawinsonde, pibal, aircraft, satellite and land based stations; additional global observational data were supplied by participating international organisations and countries. The output variables have been classified into four classes, depending on the degree to which they are influenced by observations and/or the model (Kalnay *et al*.,

1996). The first class of variables (A), which include the upper air temperatures, zonal and meridional wind components and geopotential height, are strongly influenced by the available observations and therefore, considered to be the most reliable product of the reanalysis. The second class of variables (B) such as moisture variables, divergent wind and surface parameters, are influenced both by the observations and the model, and categorized as less reliable. The third class of variables (C) such as surface fluxes, heating rates and precipitation are entirely determined by the model, thus, they are derived from the assimilation of other observed variables. The fourth class of variables (D) are derived from climatological data and are not dependent on the model.

NCEP reanalysis data are quality controlled and assimilated with a data assimilation system that is kept unchanged over the reanalysis period and in order to eliminate apparent climate jumps resulting from changes in the operational data assimilation system (Kalnay *et al*., 1996; Kistler *et al.,* 2001). These NCEP reanalysis gridded atmospheric data fields have been extensively used by researchers (e.g. Randel, Wu & Gaffen, 2000; Kostopoulou, 2003; Mulenga *et al*., 2003; Todd *et al*., 2004; Cook *et al*, 2004; Viguad *et al*., 2007; Fauchereau *et al*., 2008; Hart *et al*., 2010).

However, a number of concerns regarding the consistency and accuracy of outputs have been raised. Kalnay *et al*. (1996); Newman *et al*. (2000); Marshall and Harangozo (2000); Kistler *et al*. (2001); Reid *et al*. (2001) and Trenberth *et al*. (2001) assessed the consistency of the reanalysis output data. The noted inconsistencies have been linked to two major changes in the observing system on the reanalysis. Firstly, there is the establishment of the upper air network that occurred from 1948 to1957; consequently, the reanalysis prior to 1958 is considered to be the least reliable, especially in the Southern Hemisphere, because of the lack of observations during that period. Thus, the reanalysis for this period is entirely based on the model prediction. Secondly, the introduction of satellite data in 1979 resulted in a significant change in the climatology, and as a result, the climatologies based on the years 1979 to present are considered most reliable (Kalnay *et al*., 1996; Kistler *et al*., 2001). This is supported by Tennant (2004), who quantified the extent to which the introduction of satellite data in 1979 impacts both the daily and inter-annual scales of variability, and reported difference in the daily circulation statistics before and after 1979. The study mainly focused on the identification of possible atmospheric circulation associated with the evolution of heat waves in North West Province. For a study of this nature, mainly it is the anomalies that

are important. Atmospheric anomalies are given by the mean for 1980–2009 minus total mean of variables from NCEP/NCAR reanalysis (1968–1996) as obtained from NOAA/OAR/ESRL PSD, Boulder, Colorado, USA through their website at http://www.esrl.noaa.gov/psd.

The parameters used in this analysis include the geopotential height at 850 hPa, 500 hPa and 200 hPa; specific humidity, vector winds, Outgoing longwave radiation (OLR) and vertical velocity (omega). The geopotential height is used in synoptic-scale analysis of weather maps, and facilitates the locating of troughs, ridges, cyclones and anticyclones. The relationships between upper air ascent/descent, mass and water vapour convergence and divergence in connection with these systems are fairly well understood (Holton, 1979), so the role of these systems in enhancing heat wave can be detected from geopotential height analysis, especially when air mass compression and warming are detected. According to Rohini (2016), heat waves are unusual occurrences with extremely high surface air temperatures, lasting for several days with serious consequences. Therefore, a study of heat waves can be viewed through the lens of land-atmospheric interactions as well (Horton *et al*., 2016). The near surface layer (850 hPa) was considered in this study for such reasons because, as temperatures rise, soil moisture declines, reduce latent heat flux, allowing temperatures to rise further (Fischer *et al.,* 2007; Zampieri *et al.,* 2009), thus creating a more stable environment/layer. Over the inland areas of South Africa, the first absolutely stable layer develop at ~850 hPa (Tyson and Preston-Whyte, 2000). In addition, contour plots of geopotential height can be used to visualize the state of the atmospheric circulation. Low pressure systems are characterized by convective activities and typically bad weather, while high pressure systems are characterized by typically fair weather. According to Ragone *et al*. (2017), heat waves are associated with persistent high pressure systems. Humidity and vector winds play a significant role in enhancing or reducing the heat wave phenomenon. Wind plays an important role in transporting the moisture into or away from the reference point. Thus, sources of both evaporated and advected moisture can best be explained by wind motion. In dry areas where moisture is transported away, levels of low humidity are likely to occur with increased surface temperatures.

On the other hand, the OLR is widely considered as a representation for the deep convection and used for precipitation estimation, mainly in the tropics. Chikoore (2016) states that regions of high OLR are regions of high surface temperatures, clear skies (or

few clouds) and dry weather. While reduced emissions of OLR generally occur in association with deep convection, rain-producing clouds (Hartmann & Recker, 1986). The OLR data was used in this work to assist in analysing variations in convection and subsidence over NWP. Also, positive anomalies of OLR over a region are believed to correspond with large temperature anomalies (Ratnam *et al*., 2016). Vertical velocity (omega) is added in the analysis so to assist in area identification of rising and sinking air. These areas are well identified by different omega values, where negative values indicate the uplift of air and positive ones indicating the subsidence of air.

a) Geopotential height

Geopotential height approximates the actual height of a pressure surface above mean sea level. Therefore, a geopotential height observation represents the height of a pressure surface on which the observation was taken (Wallace and Gutzler, 1981). The geopotential is defined as having a magnitude of 0 at the Earth's surface and is represented by the symbol Φ. The Φ at any given height above the Earth's surface is equivalent to the distance travelled, multiplied by the gravity at each integration of height. The following formula was thus used (Wallace & Hobbs, 2006).

$$\Phi(z) = \int_0^z g\,dz \qquad (3.1)$$

Where z = height above the surface, and g is the gravitational acceleration at each height. It should be noted therefore, that the gravity is not constant throughout the atmosphere, it decreases as the distance from the centre of the earth increases. Then the geopotential height is thus measured in geopotential meter (gpm) and it is then represented by a capital 'Z'.

$$z = \frac{\Phi(z)}{g0} = \frac{1}{g0}\int_0^z g dz \qquad (3.2)$$

g0 is acceleration of gravity with a constant (≈9.8 ms^{-2}). In the lower atmosphere, Z is very close to z (called the geometric height). Geopotential height was used in this study in order to determine the elevation to which the extreme temperatures on the surface

are observed. The use of geopotential height is mainly due to its valuable advantage of locating troughs, ridges, cyclones and anticyclones.

b) Atmospheric Humidity

Generally, this climate variable is expressed in three measurements; absolute, relative and specific humidity. Specific humidity is the one of the most important variables in climatology, because of its direct relation to the radiative forcing (Peixoto & Oort, 1996). Given the highlighted meteorological importance of specific humidity, it was adopted in this study as one of the measures to be analysed during the heat wave occurrences. The subsidence and adiabatic warming above can trap the warm and humid air in the surface layer, leading to positive feedback to the abnormally hot surface condition (Kueh *et al*., 2017). In the lower levels of the atmosphere, atmospheric humidity is found to be an important quantity (Laderach & Raible, 2013) for its role in the development of precipitation. At the surface, humidity is also an important meteorological and climate variable that affects human comfort (Dai, 2006) as it governs the manner in which animals and humans cool themselves through evaporation. During dry seasons, when water vapour in the subsurface soil is depleted as well as in the boundary layer of the atmosphere, most plant species die (Kabanda, 2004). According to Bengtsson (2010) humidity is given by the amount of water vapour per amount of air and is determined by evaporation, advection and precipitation. On the study of drought studies by Kabanda (2004), specific humidity was carried out at 700 hPa due to its maximum values that are around 700 hPa. This was found relevant to be used in this study, since droughts are linked to heat waves.

Over the tropics, the greater part of horizontal transfer of water vapour occur in the lower- troposphere of the atmosphere, i.e. below the 700 hPa (Pearce, 1989; Asnani, 1993). In general, specific humidity is the mass of water vapour in a given mass of air, normally expressed in grams of water vapour per kilogram of air (g kg^{-1}) at a given specific temperature (Black, 1996). According to Peixoto and Oort (1996); Ross and Elliot (1996), specific humidity is calculated as follows:

$$q = \epsilon \frac{e}{p + (1-\epsilon)\, e} \tag{3.3}$$

Where ϵ = Rd/Rv (≈ 0.622) and *Rd and Rv* are the gas constants for dry air and water vapour respectively. It can be simplified to;

$$q \approx \epsilon - \frac{e}{p} \tag{3.4}$$

then

$$q = \frac{0.622e}{p - 0.378e} \tag{3.5}$$

c) Outgoing Longwave Radiation (OLR)

Outgoing long wave radiation is explained by Salby (1996) as the emission of terrestrial radiation to space from the top of the earth's atmosphere. In physical terms, OLR is strongly controlled by three main meteorological variables. These include; the temperature of the earth and the atmosphere above it, the presence of water vapour in the atmosphere and the presence of clouds (which may completely block all outgoing infra-red radiation from the surface if the cloud is dense and overcast). OLR is the infra-red component of the Earth's energy balance, together with the solar net radiation flux. This further helps to describe the changes in energy availability by clouds through the difference between a clear sky and the observed radiative balances (Ceballos *et al*., 2003).

Sarazin *et al*. (2006) observed that the highest OLR values are found above the warm, dry, clear regions whilst regions of low OLR are regions of deep convection, frequent cloud and high rainfall. Thus, some drought studies e.g., Kabanda (2004); Chikoore, 2016), used OLR as a proxy for convection and precipitation. The OLR data used in this work was to assist in analysing the variations in subsidence over the NWP. Regions of subsidence are derived from positive OLR anomalies while areas of convection are denoted by negative OLR anomalies. OLR mean was used in this study using the uninterpolated OLR data.

d) Vertical Motion (Omega)

Outgoing long wave radiation in the previous section is fairly explained, indicating areas of convection (low OLR values) and subsidence (high OLR values). However, high and low values do not suggest the extent to which the surface/atmosphere is dry to enhance extreme temperatures. Therefore, the use of vertical motion enables area identification of rising and sinking air, which might help in further explaining the dry and moist conditions during heat waves events in NWP. In general terms, rising air in the atmosphere leads to the development of clouds and possibly, precipitation occurs. On the other hand, sinking air is associated with warm and dry conditions, which are also indicative of less or no clouds in the atmosphere, thus increased temperatures. This is relevant if the season in question is assumed to be a summer season, where heat waves occur the most. Feng *et al*. (2014) also emphasized that, dry conditions are usually associated with an anomalous subsidence of air. During heat wave formation, the subsiding air intensifies the anticyclonic motion (high pressure). Within such high

pressure systems, vertical air motion is generally downwards, causing adiabatic heating and warming at the surface (Schulze & Maharaj, 2006).

Vertical velocity ω is given by the following formula and is expressed in Pa s^{-1}.

$$\omega = \frac{Dp}{Dt} \quad (3.6)$$

Where p is pressure and t is time.

Vertical velocity values are negative for rising motion (uplift) and positive for sinking motion (subsidence). With this reason, strong positive values of ω over large areas, are commonly associated with dry conditions (Chikoore, 2016). Vertical velocity (omega) was analysed at 500 hPa. This level is important as it is considered as the level of non-divergence (Barry & Chorley, 2003) separating the areas of divergence from convergence. In addition, Fauchereau *et al*. (2008) stated that the 500 hPa level for omega represents the center of mass for the troposphere and allows for an insight on large-scale vertical movements in the whole troposphere.

e) Vector Winds

A study by Miralles *et al.* (2014) has proven that during the daytime, heat is supplied in an area by large scale horizontal advection. This points to a possible relationship between the advection of warm air over a region and the occurrence of a heat wave. The movement of air masses are well represented by the wind vector, which is defined by both the wind direction and wind speed. In a similar study of heat waves, areas of convergence and divergence are widely established through the analysis of wind vector (Adames and Wallace, 2014). Wind is an agent that transports moisture inland from major water bodies such as oceans, tropical rain forests and other moisture sources. The study area is located inland far away from moisture sources; therefore, moisture, clouds and precipitation reach inland mainly by means of wind transport. According to Kabanda (2004), that is the positive role played by wind in the study area. In this study wind patterns were used in order to establish whether there was a pattern of either dry or wet air being associated with heat waves occurrences. On the other hand, that wind can transport moisture from the area and deposit it far away, leaving the area dry.

3.3 Methods of Analysis

The methods which were used in this study include the following: Time series analysis; extreme value analysis; spectral analysis; and reanalysis. Each of these methods are explained in the following sub-sections:

3.3.1 Summer Season identification

This statistical analysis was employed in order to detect maximum temperature trends and other extreme heat related conditions. The series was performed per station, as different stations have records over different time spans. Most of the available stations are in the hot arid climate zone. Heat waves most commonly occur in summer when high-pressure systems are dominant and moving slowly. A seasonal temperature time series for 13 stations was performed to observe the changes over the course of the season for the time of recording in each station. This may further allow to study the patterns that may arise, which may give further atmospheric detail on the behaviour of maximum temperatures.

To determine the period of analysis, rather than selecting summer-season data for the NWP by pre-determined, fixed start and end dates for the seasons, the summer season was defined by the months, where extreme high-temperature events were concentrated. This was done by plotting the mean monthly maximum temperatures for each station (using Microsoft Excel 2013) to identify the periods of interest. Only those months were further analysed. The series gave an indication of where the extreme temperatures were concentrated, then that represented the summer season of the NWP.

As shown is in the illustration in Figure 3.1, the daily data was converted into monthly data and in order to select the period within which extreme values were found. This was performed using a composite of maximum-temperature data from all stations. The summer season, when high temperature spikes and heat waves are most likely to occur, was taken to be the warmest months of the year. The season (September, October, November, December, January, February and March) was identified from the NWP monthly-mean maximum temperature plot as presented in Figure 3.1.

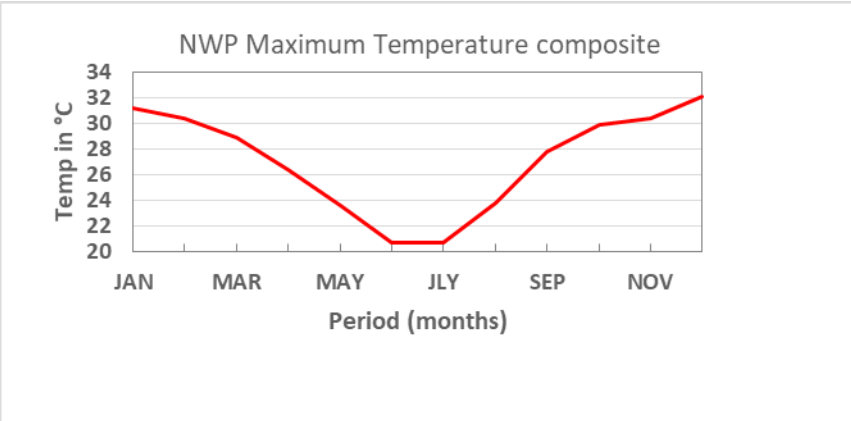

Figure 3.2: The identified summer season for North West Province

3.3.2 The Extreme value theory

The statistical theory of extreme values is a branch of statistics appropriate for studying meteorological extreme events such as heat waves, floods etc. (Coles, 2001). Extreme value theory (EVT) is frequently used in environmental studies (Katz *et al.* 2002) and in financial studies (McNeil and Frey, 2000) to produce distributions to fit data consisting of the maxima and minima samples. Numerous studies of climate extremes using EVT have been published in recent years (e.g. Kharin & Zwiers, 2000; van de Brink *et al*., 2004 & Fowler *et al*., 2005). However, these studies used only one aspect of EVT; which is the block maxima approach, and that does not exactly address heat waves as it only picks one data point in a block or period. To enhance similar studies, Katz (2010) and Furrer *et al.* (2010) proposed an EVT perspective, which is suitable for studying heat waves and hot spells by using a peak-over-threshold (POT) approach.

3.3.2.1 Peaks over threshold approach (POT)

POT is the approach that was used in this study based on its advantage of picking all values that are above a certain threshold, so that in some years, there may be several heat waves picked up. This also allows an individual event analysis, which was the main purpose of this study, by determining the synoptic weather associated with heat waves in the NWP. The use of POT also revealed information about the frequency, duration and intensity of the above normal temperatures within the data. The peaks-over-threshold (POT) approach is preferred over the annual maxima method in studies such as that by (Coles, 2001).

An appropriate threshold value needs to be determined, based on the full set of raw data. Gong (2012) listed three general points to select a threshold, which are empirical quantile, mean excess plot and stability checking of shape parameters. The threshold selection used in this study followed the South African Weather Service threshold for a heat wave definition, which states that a heat wave has occurred when for three consecutive days, the daily maximum temperatures are five degrees above the mean in that particular place at that time of the year. This has been widely used as a threshold that must be crossed to start and end a heat wave event. The first step in the application of POT is to select a reasonable threshold *(u).*

According to Coles (2001), the statistical distribution of the excess over a threshold *u* for a random variable *X* with distribution function *F* is defined as:

$$Fu\ (x) = \quad [X - u \quad \leq x | X > u] \tag{3.7}$$

3.3.2.2 Determining the heat wave threshold

The choice of threshold selection is not straightforward and is a very important step in the data analysis of extremes (Walshaw, 1994). The threshold needs to be high enough to distinguish extremes, but not so high as to exclude too much data (Bommier, 2014). Setting the value too high risks excluding some of the most important values within the data. Setting a threshold for events like heat waves, which are defined based on the climatological means of the region, can be very challenging due to variations of topography and other physical environmental elements. Another challenging factor is that heat waves do not occur uniformly throughout the year but tend to follow a seasonal pattern, occurring mostly in the summer.

However, to avoid a loss of data, which may constitute heat waves in NWP, the general Southern Hemisphere summer season was not used as an indication of where heat waves could be experienced. Instead, a summer season period for NWP was defined based on the local temperature data. This was performed through a composite of all daily maximum temperatures for each month for all stations. Following that, a monthly mean plot representing NWP was plotted in such a way as to highlight a period of significantly high mean max in which extreme temperatures could be found. The highlighted months were set to correspond to a summer season in the NWP for the purpose of this analysis. For each month in the NWP summer season, the threshold for

significant events was set at 5°C above the monthly mean max temperature at each station, based on the SAWS criteria mentioned above. All values above this threshold were then counted as critical events, which were then checked to determine if they met the heat wave criteria. Those that met the standards were then declared as significant events in the NWP.

3.3.3 Spectral analysis

Spectral analysis was performed using STATISTICA (StatSoft, Inc., 2015). Spectral analysis is concerned with the exploration of cyclical patterns in the data of interest, in this study, it was the maximum atmospheric temperatures. It might uncover just a few recurring cycles of different lengths in the time series of interest, which at first, looked more or less like random noise (Hill, 2006). In this study, spectral analysis will be employed to determine a statistically significant recurrence of heat waves (abnormal maximum temperature). Maximum temperature data was analysed and the significant periodicities of abnormal maximum temperature were isolated. The identified periodicities were then used to compare with other known oscillations of the climate variables such as the ENSO, quasi-biennial oscillation (QBO), sunspot cycle and others not yet established, in order to determine any related signal that could be used in developing a forecasting model of heat waves in future.

3.4 systematic summary of data analysis

The data analysis procedure applied in this study is as shown in the systematic diagram below (Figure 3.2).

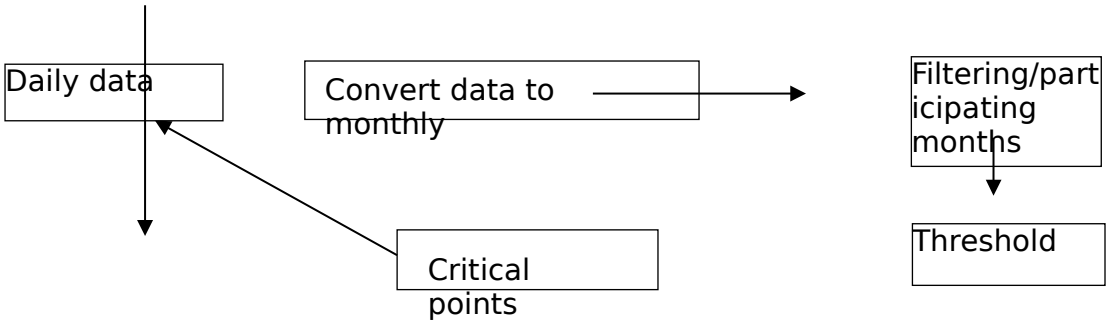

Figure 3.3: Systematic summary of data analysis and presentation

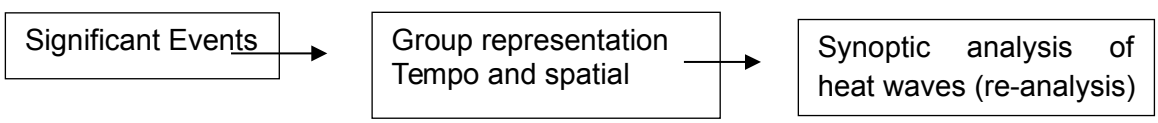

3.5 Chapter Summary

The data, data sources, and analyses performed in this study were described in this chapter. Several data analysis methods have been discussed with possible rationales for their selection. These include monthly series for all stations for establishing the summer season, and station daily maximum time series throughout the months of the summer season. The literature from the previous chapter paved the way for choosing POT method confidently, to be the main method in identifying heat waves; the decision was based on the statement by IPCC (2002) for POT as the best method in studying extreme events. Following the results of POT, more characteristics of heat waves were investigated by the application of spectral analysis and the cyclical patterns of these events were then studied in relation to those of other oscillation patterns. Lastly, a climatology of heat waves was drawn from the analysis of other atmospheric circulations through the NOAA re-analysis dataset.

CHAPTER 4

Evolution of Summer Temperatures and Associated Heat Waves over North West Province

4.1 Introduction

Although in climate studies, 30 years is an ideal period to be used, this may not be applicable in studying heat waves because they are rare events – in some instances, 30 years might elapse before a heat wave event is experienced (Huber & Gulledge, 2011). Therefore, heat waves studies of a period of few years (<30 years) are not unusual (Hern´andez-Ceballos *et al.*, 2016). Assessing the return period of these extreme events can also be a complicated process of analysis. This is well illustrated by Karl and Knight (1997), who obtained a value of 100 years for the Chicago heat wave of 1995. However, four years later (1999), another heat wave of the very same magnitude struck Chicago. In this study, the station data used varied from those that ranged from 1960-2016, 1984- 2016, 1991-2016, 1992-2016, 1993-2016, 1996-2016, 1997-2016, 2005-2016 and 2007-

2016 for the newest stations. This approach was used in order to capture any event which might have been recorded in NWP. The lack of long term climate data suitable for analysis of extremes is the single biggest obstacle to quantify whether extreme events have changed over the 20th century, either worldwide or on a regional basis (Easterling *et al*., 1999). This includes temporal and spatial observations of extremes of high temperature, precipitation, humidity, winds and atmospheric pressure for many parts of the world.

4.2 Maximum temperature analysis

In this section, monthly maximum temperatures per station (Figure 4.1) are presented. Prior to the analysis of the prevailing patterns in each station, it should be noted that the stations feature different periods of record, based on when the station started to observe and retain the temperature data. There are two longest reporting stations (1960-2016) and the shortest period was from 2007-2016. One station (Tosca) reported the highest temperature of 46°C in January 2016. Rustenburg observed 44.9°C; Taung's highest temperature was 44.6°C while Vryburg recorded 43.7°C. The other stations (Madikwe, Bloemhof and Pilanesburg) observed 42.1°C, 42.5°C and 42.9°C respectively. The station that observed the lowest maximum temperature is Mafikeng (41.5°C). The maximum temperatures maintained a quasi-stationary trend at around

35°C for all stations except Madikwe, which had a negative trend with a gradient of -0.03.

Marico reported a maximum temperature of 46.0°C, Klerksdorp 42.6°C. The other stations in the order of their maximum temperatures are Ottonsdal (42.3°C), Potchefstroom (40.8°C) and Lichtenburg (39.5°C). Generally, most stations showed a similar trend of temperature increase although Lichtenburg maintained lower maximum temperatures and the time series from most stations are highly correlated with each other, especially for stations that are located close to each other. This typical behaviour of temperatures among stations in the same vicinity was also observed by Kruger and Shongwe (2004) in their study of temperature trends in South Africa.

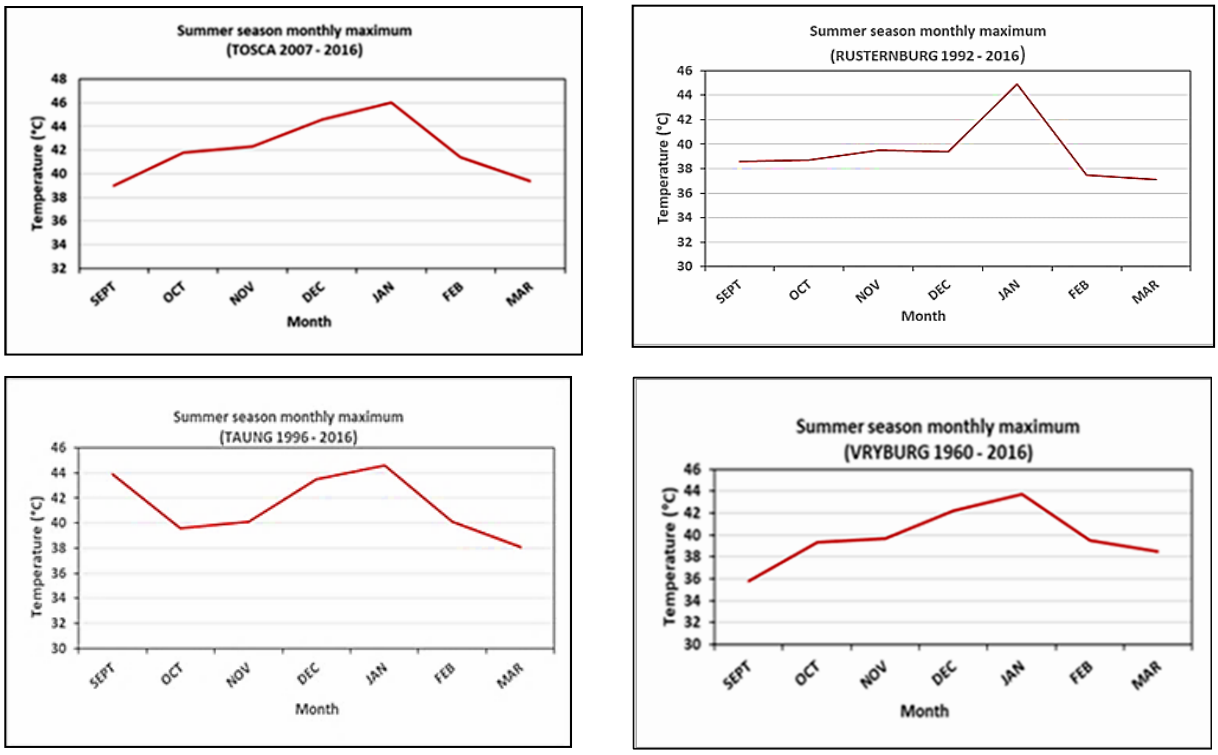

Figure 4.4: Monthly maximum temperatures for summer season for the 13 stations in the North West Province

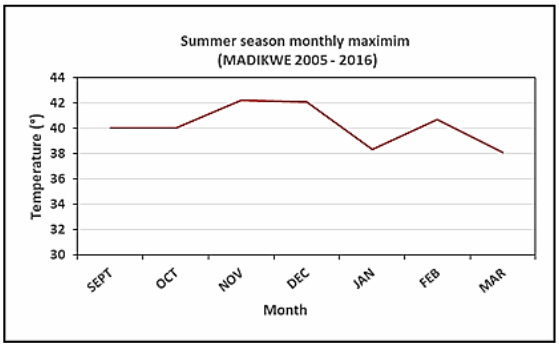

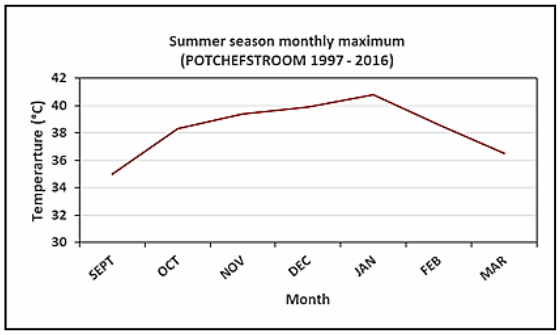

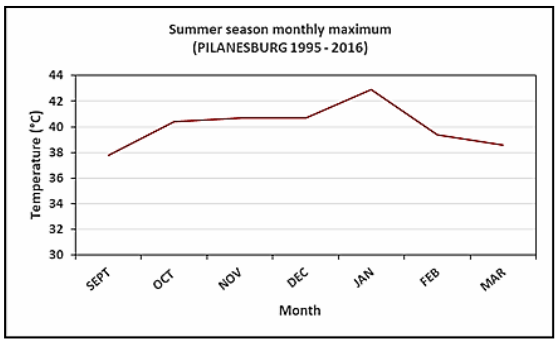

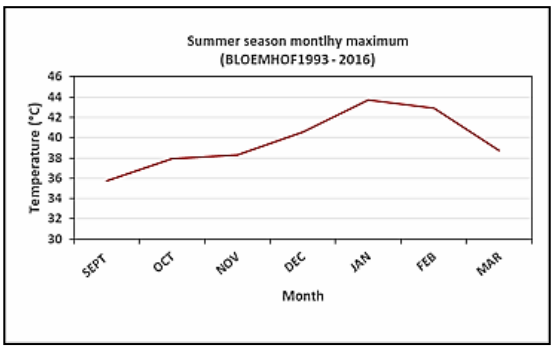

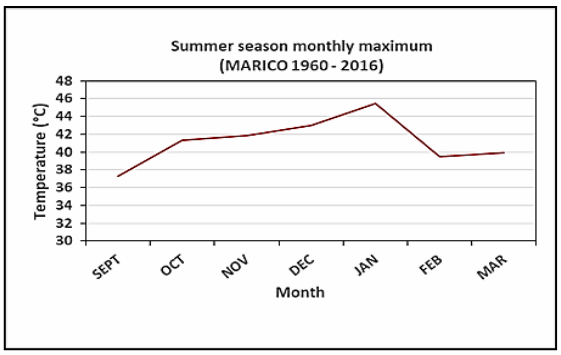

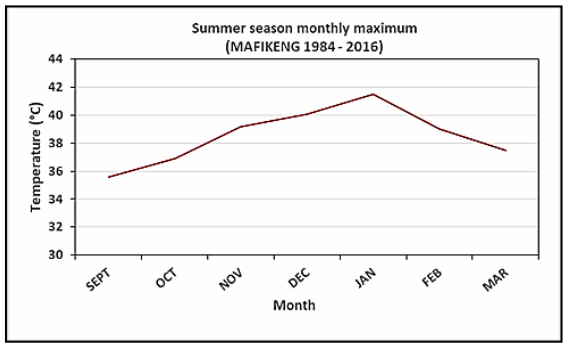

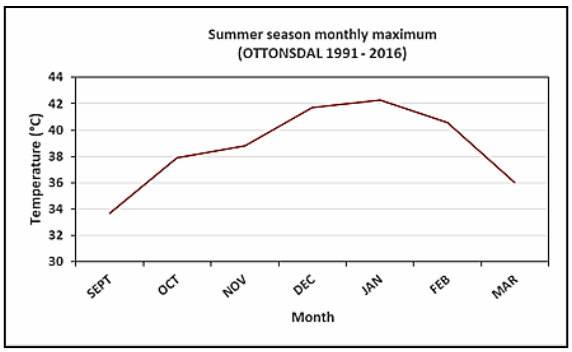

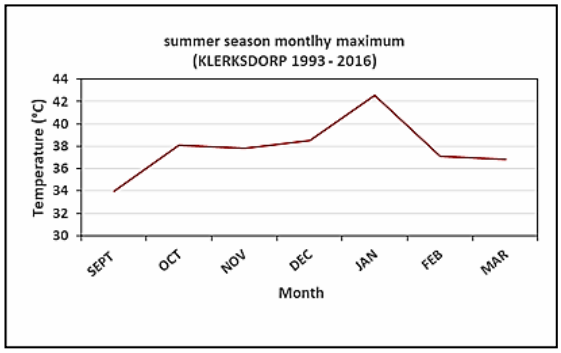

Figure 4.1: Continued’

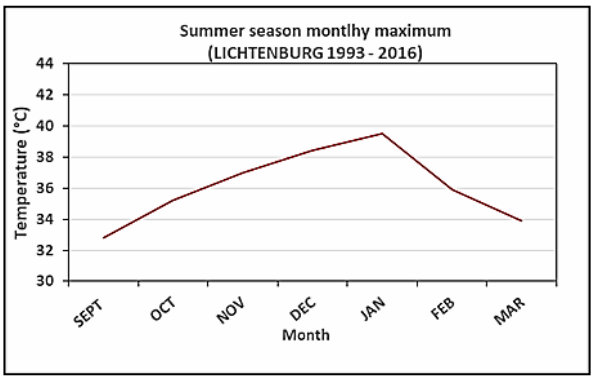

Figure 4.1: Continued'

4.3 Spatial and Temporal Variations of maximum temperature anomalies

This section represents the temporal and spatial variations of the above normal maximum temperatures in the NWP. Stations having the same period of observation were grouped into a single plot and those with different periods, such periods of record were plotted individually. Marico and Vryburg were two stations with the longest observations (1960-2016) followed by Mafikeng (1984-2016). The three other stations are Lichtenburg, Bloemhof and Klerksdorp, which had observations from 1993-2016 and Tosca, which only started in 2007. The plots for each group showed strong similarities with each other (not shown), and since no extreme temperatures were observed prior to 1996; the composite time series of nine stations was displayed (Figure 4.2).

Maximum temperature data were normalised using the long-term mean and divided by the standard deviation to produce a time series that showed normal to extreme seasonal maximum temperature events. In this study, persistent extreme positive events mean heat wave. The Figure shows that a high season-to-season variability exists. It is also evident from the same Figure (Figure 4.2) that in many cases, a number of the below-normal seasons tended to follow each other (i.e., 1999-2001, 2003-2005 and 2007-2010). Persistently, extreme maximum temperatures started in 2011 and climaxed in the 2015 season that ended in March 2016. This was the hottest season in a more than 50-year period from 1960 to 2016, departing from normal by ≈3.0.

The spatial distribution of the above normal maximum temperatures is defined here as the total number of all heat wave events throughout the summer seasons per station. Figure 4.3 shows the spatial distribution of summer season heat waves for each station in the study.

Among the 13 stations, 6 of them experienced at least one heat wave event. While, maximum occurrence was experienced in two stations, Tosca and Marico with 4 to 5 events. It is evident from these results that in a summer season, more than one heat wave event can be observed in one station while nothing will be observed on the other. In this study, only Lichtenburg did not report any heat wave event.

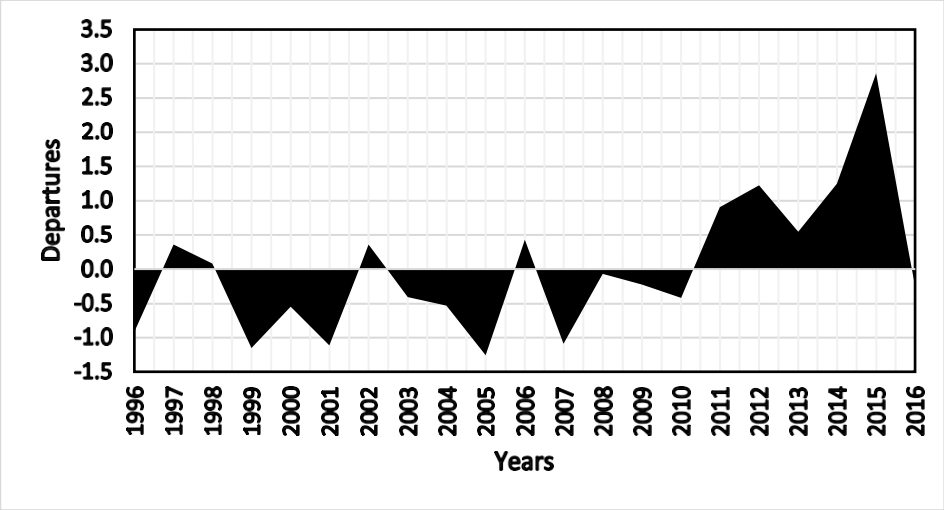

Figure 4.5: Temporal variations of maximum temperatures anomaly from 1996–2016

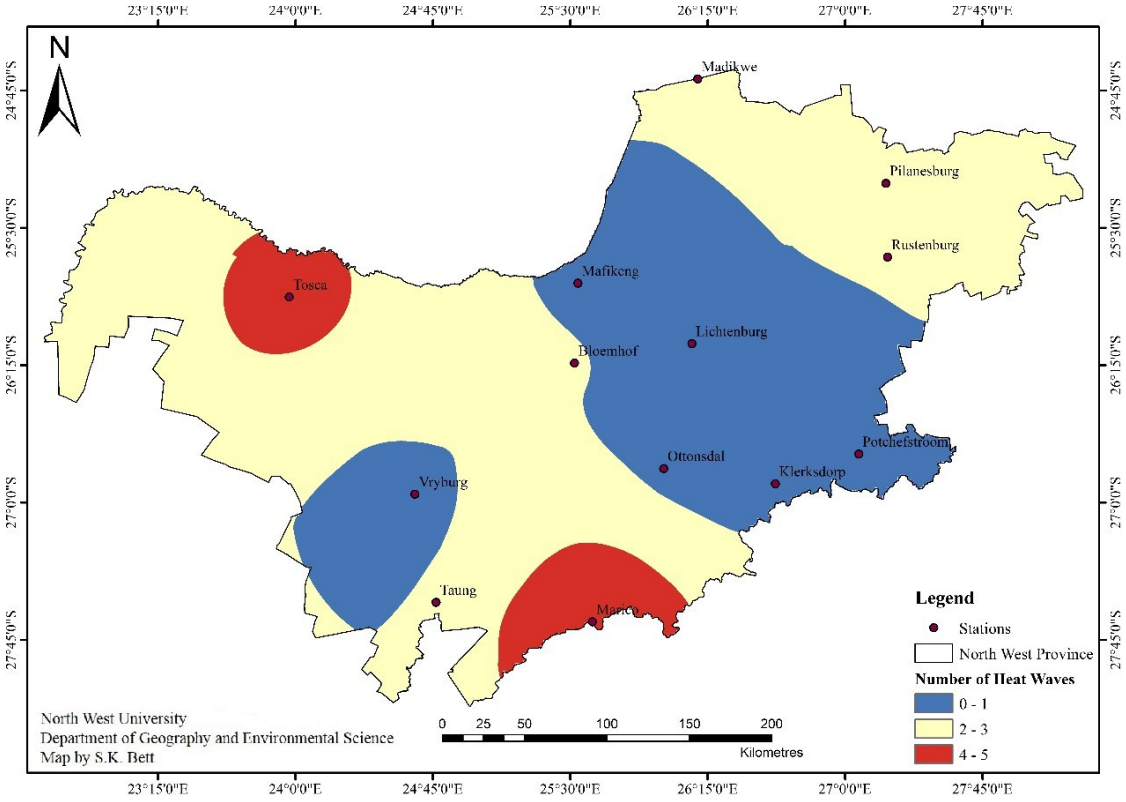

Figure 4.6: Spatial distribution of heat wave events over the North West Province (from 1960 – 2016)

4.4 Significant Heat Wave Events and their spatial occurrence

In this section, heat waves were identified based on the South African Weather Service criteria – which says that a heat wave occurs when, for three consecutive days, daily temperatures exceed the monthly mean by 5°C. The significant heat wave events experienced in the NWP since 1960 to 2016, are shown Table 4.1 below. In column 1, there is a list of stations which reported heat waves, column 2, represents the mean temperature of the month for a particular station. The third column, represents the summer season while the fourth column is the month in which heat wave episodes occurred during the matching season. In column five, heat wave persistence is presented. The threshold temperature (i.e., 5°C above the monthly mean maximum) for each station is presented in column six. In column 6, temperature threshold for the particular heat waves are shown and in agreement with Tan *et al*. (2007). Lastly, column 7 contains the highest maximum temperatures during a heat wave episode. In most cases, the highest maximum temperature during a heat waves exceeded 40°C. This observation concurs with that of Robinson (2000), who observed that during heat wave episodes in South Africa, the daily maximum temperatures usually rose to values over 40°C for a period of at least two consecutive days.

From Table 4.1, the longest-reporting station (Marico, which started in 1960) in NWP, registered the first heat wave in March of the 1983-84 summer season. During this period, temperatures exceeded the threshold (36.0°C) for three consecutive days and reached a maximum of 39.5°C. For almost two decades, there was no noticeable heat wave observed in NWP – although the observation network had increased to 12 stations. Eventually, in the 2004-05 summer season, Pilanesburg experienced a four-day heat wave, in November, with temperatures reaching 40.7°C. The following heat wave episode was reported in the November 2007-08 season, followed by another one in the September 2008-09 season as registered in Madikwe and Rustenburg respectively. After those heat waves, there was just one summer without a heat wave, followed by two more summers with heat waves (2010-11: October in Marico; and 2011-12: November in Marico, and December in Tosca). The maximum temperature in those stations exceeded 40°C. It should be noted that in all these events, heat waves were experienced in isolated areas (a single station).

Table 4.2: Significant heat waves which were experienced in the North West Province from 1960 to 2016

Station	Average max In °C	Heat wave events			Average max +5°C (Threshold Temperature)	Max temp In ° C
		Season	Months	heat wave duration(days)		
Marico	31.0	1983-84	Mar 1984	3	36.0	39.5
Pilanesburg	32.3	2005-06	Nov 2005	4	37.3	40.7
Madikwe	31.3	2007-08	Nov 2007	4	36.3	40.1
Rusternburg	29.8	2008-09	Sept 2008	3	34.8	38.6
Marico	33.0	2010-11	Oct 2010	3	38.0	41.3
Marico	34.2	2011-12	Nov 2011	3	39.2	40.8
Tosca	31.6	2011-12	Dec 2011	3	36.6	40.5
Tosca	30.7	2014-15	Sept 2014	4	35.7	39.0
Marico	34.4	2014-15	Nov 2014	3	39.4	41.9
Madikwe	34.4	2014-15	Nov 2014	5	39.4	42.2
Tosca	35.3	2014-15	Nov 2014	3	40.3	42.3
Pilanesburg	33.3	2014-15	Nov 2014	4	38.3	40.5
Taung	37.5	2014-15	Dec 2014	3	42.5	43.5
Bloemhof	36.5	2014-15	Feb 2015	4	41.5	42.9
Marico	34.9	2015-16	Jan 2016	4	39.9	44.5
Vryburg	35.3	2015-16	Jan 2016	3	40.3	43.7
Mafikeng	32.7	2015-16	Jan 2016	4	37.7	41.5
Ottonsdal	31.5	2015-16	Jan 2016	5	36.5	42.3
Rustenburg	32.5	2015-16	Jan 2016	3	37.5	41.6
Bloemhof	33.6	2015-16	Jan 2016	5	38.6	43.6
Klerksdorp	30.9	2015-16	Jan 2016	5	35.9	40.6
Pilanesburg	33.3	2015-16	Jan 2016	3	38.3	42.9
Taung	35.3	2015-16	Jan 2016	7	40.3	44.6
Potchefstroom	31.8	2015-16	Jan 2016	3	36.8	40.8
Tosca	37.2	2015-16	Jan 2016	4	42.2	46.0

In the 2014-15 summer season, there was a widespread heat wave, affecting six stations in the province (Tosca, Marico, Madikwe, Pilanesburg, Taung and Bloemhof). Maximum temperatures varied between 39 and 43.5°C as indicated in Table 4.1. The heat wave duration ranged from three days at some stations to five days at others.

The most striking heat wave phenomena recently are the widespread events in the 2015- 16 summer season. From Table 4.1, it is observed that in January 2016, eleven stations out of thirteen in the province, reported temperatures of >40°C in three consecutive

days. Of those stations, temperatures exceeded 40°C in four consecutive days at six stations, five consecutive days at three more stations, and seven consecutive days at another station (Taung, with a maximum of 44.6°C and its highest temperature reaching 44.6°C). During that period, the highest temperature was observed in Tosca (46°C), which registered four consecutive days of >40°

4.5 Heat Waves Frequency and Duration

Figure 4.4 shows the occurrence of seasonal significant heat waves in NWP since 1960. The number of columns represent heat wave events that occurred during the particular year. The heat wave events are represented by coloured bars, and successive events within a season are numbered sequentially. Their durations are represented by the number of days an event persisted. The first notable heat wave event occurred in 1984 and persisted for 3 days. The second heat wave episode was observed in 2005 and continued for four days; the period between the two episodes was 21 years. Thereafter, events of heat waves occurred 2 to 3 years apart. Over the 2012-2016 seasons, heat waves occurred at double the frequency seen in 1984-2011.

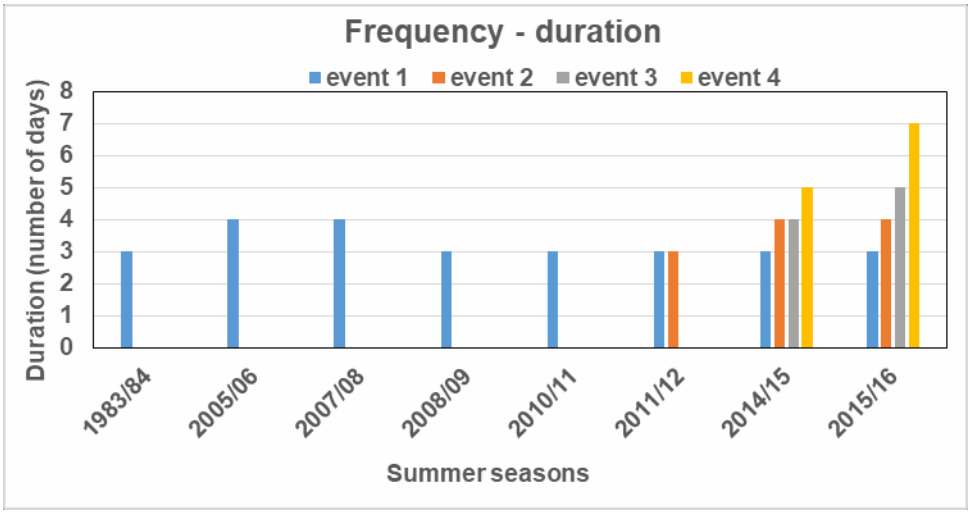

Figure 4.7: Frequency-duration of significant heat waves in North West Province from the 1983/84 to 2015/16 summer seasons

In relation to frequency, it was found that from 1984 to 2011, single events were identified as heat waves in the seasons indicated in (Figure 4.4). There were also single events in 2005 and 2008, and these had a longer duration than the others. As previous studies stated, in a changing climate, heat waves will not only become more frequent; their duration and intensity will also likely to increase as well (Min *et al.*, 2011; Coumou & Rahmstorf, 2012; & IPCC, 2013). The most outstanding feature of the

temporal distribution of these events is the high frequency between the years 2015 and 2016, compared to all the other seasons. The frequency, intensity and duration intensified during these two seasons. It is important to note that the longest duration of heat wave event could be a significant indicator of heat wave intensity.

4.6 Cyclic signals of heat waves in North West Province

The recurrence times between extreme events have been the central point of statistical analyses in many different areas of science (Makarau, 1995; Kabanda, 2004; Tularam and Ilahee, 2010; Sun *et al*., 2014). Jentsch and Beierkuhnlein (2008) maintained that, extreme weather events are rare in occurrence and that their effects are out of proportion to their shot period of duration and their predictability is still low. They further stated that, extreme events are hardly ever explicitly addressed in current numerical climate models. This may be due to the fact that causal explanations for connections between large-scale climatic circulation patterns and the local occurrences of extreme weather events are still missing.

In seeking meaningful recurrence intervals of heat waves in NWP, a more intense analysis of significant heat waves events was implemented through a single spectrum analysis. The aim was to examine periodicities as represented in Figure 4.5. Three significant peaks were observed: the first one which corresponds to a period of 12 years, second to 4.8 years, and the third to 2.1 years.

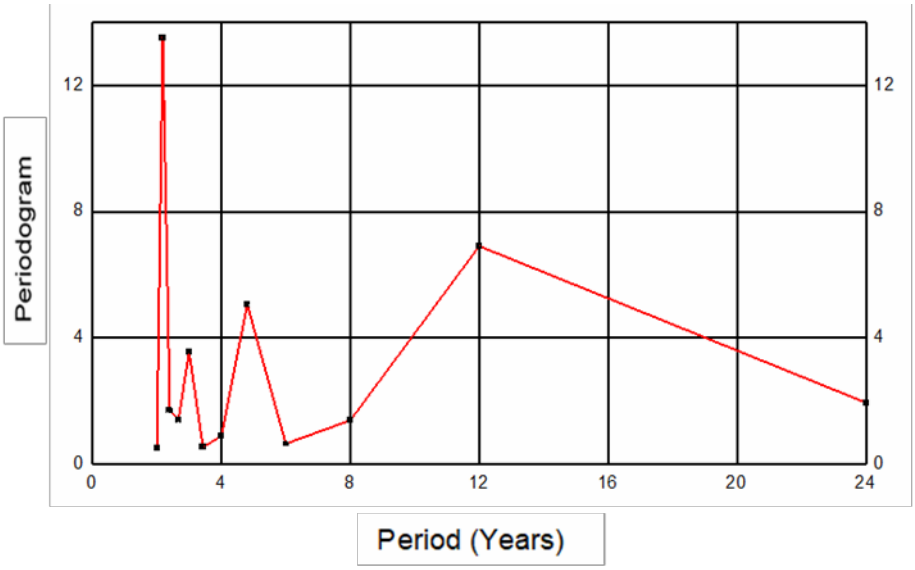

Figure 4.8: Spectral analysis of heat waves in North West Province

Several studies have revealed that a strong 11-year solar cycle exists in the atmosphere (van Loon and Labitzke, 2000; Tsiropoula, 2002 & Meehl *et al*., 2009). However, an average number of visible sunspots vary over time, increasing and decreasing on a regular cycle of between 9.5 to 11 years, on average about 10.8 years (Zhang, 2009). The 11-year cycle is actually half of a longer 22-year cycle of solar activity. The 12-year period peak observed in this study, suggests a modulation of the 11-year solar cycle, and therefore, it could be ascribed to the sun's activity as supported by literature.

The second peak of 4.8 years found in this study is associated with the El Nino-Southern Oscillation (ENSO). It is generally agreed that El Nino has a return period of 4-5 years and a duration of 12-18 months (Makarau, 1995; Puckridge *et al*., 2000; Kabanda, 2004). Also, the evolution of El Nino events in 1896-1982 by Quinn and Neal (1987), indicated some mean return period of 4.8 years.

The last peak (2.1 years) maybe ascribed to quasi-biennial oscillation (QBO). According to Osprey *et al*. (2016), QBO is one of the most repeatable phenomenon seen in the atmosphere, which is best observed in the stratospheric winds above the equator, where the zonal winds are changing between east and west. The period of the QBO varies in space and time, but it lies on an average near 28 months at all levels (Ogallo *et al*., 1993; Labitzke & van Loon 1999 & Baldwin *et al*., 2001).

4.7 Chapter Summary

Various methods were applied in this chapter in the process of identifying significant heat wave events. The identification was based on the definition of heat waves as stated by SAWS. Time series analysis for the stations was performed in order to identify a season, which may be taken as summer season for the purpose of further analysis. The extreme temperatures were found to have occurred mainly in September, October, November, December, January, February and March - months that constitute the austral summer. The greater values of positive seasonal anomalies have shown that maximum temperatures had the greatest increase. This positive change was especially high during the 2014-2015 summer season. The increase in mean maximum was seen in all stations (longest period of record, the middle and the newer stations) in different seasons.

Monthly maximum time series for each station was performed and showed a similar pattern, especially in stations of close proximity and within the same climate zone.

In terms of tempo-spatial variations, all stations showed a clear positive change of the above normal temperatures in various seasons. Although the reporting periods of stations differ from each other, the highest maximum temperatures were registered in January 2016 in all stations. This is also supported by the great number of heat waves registered in January 2016. Eleven stations out of thirteen stations registered heat wave events during this period, all with maximum temperatures >40°C.

As climate studies have predicted, under the influence of climate change more intense heat waves will be experienced in the future. The most remarkable duration of the heat wave in the presented seasons was the 7-days consecutive event during the 2015 summer season. Additionally, three significant circulation patterns, which in this study are associated with the occurrence of heat waves, were observed.

CHAPTER 5

Mean and Anomaly Atmospheric Characteristics associated with heat waves in North West Province

5.1 Introduction

In this chapter, large-scale atmospheric circulations that prevail during the identified significant heat wave events are analysed. The study domain to observe the synoptic circulation features was in the range of 10°S to 40°S and from 0°E to 60°E. The adjacent oceans (southwest Indian Ocean in the east and southeast Atlantic Ocean in the west) are included. According to Kabanda (2004) and Nenwiini (2017), it is necessary to consider such a large domain because the weather systems that influence Southern Africa, especially those of the synoptic scale, seldomly form *in situ*. They suggested that monitoring a larger area would capture and highlight the geographical and temporal characteristics of the weather systems (especially their sources). In this study, it means the characteristics of the weather systems would be associated with the evolution of a particular heat wave episode. The analysis will display both the mean and anomaly patterns. Both patterns were computed using NCEP/NCAR reanalysis dataset for the following parameters - geopotential height, specific humidity, vector winds, outgoing longwave radiation (OLR) and vertical velocity (omega). The long term means (climatologies) as obtained from https://www.esrl.noaa.gov/psd/data, are calculated based on the 1968–1996 standard.

5.2 Meteorological Parameter analysis: 9-13 November 2014 heat wave at Madikwe

Under this section, meteorological parameters that prevailed during the November 2014 summer season were analysed in addressing the evolution of heat waves. From Table 4.1, the November 2014 heat wave episode periods were chosen to feature in this analysis because that month experienced more than one heat events as compared to the other years, which only reported one event. Six stations reported different heat wave magnitudes and durations, with the longest event of 5 consecutive days that was reported in Madikwe. The patterns of geopotential heights at 850 hPa, 500 hPa and 200 hPa and other parameters for the selected heat waves that occurred during the 2014/15 summer season in the month of November, are presented in the corresponding figures. These levels are known as the lower, middle and upper levels of the troposphere respectively. The plots contain the analysis of the following; (A) one day prior to-the heat wave, (B) during the first day of heat wave, (C) is the composite of all of the heat wave

days for that particular heat event and (D) one day after the last heat wave. The days that constitute the composite plot are diverse, depending on the length of the heat wave episode in terms of days. In some instances, the heat wave occurrence lasted for ≥ 5 days while in others < 5 days.

5.2.1 Mean Geopotential Height - 850 hPa

The main patterns that are worth of mentioning in Figure 5.1 are the low-level circulations characterized by the ridging of the Atlantic Ocean Anticyclone (AOA) into south-west South Africa. This characteristic is observed in (A), (B), (C) and (D), although its axis varied with time; its common oscillation is between 24 and 36°S. The meridional trough linking the tropical trough (Congo trough) with that from south of southern Africa was maintained throughout the A, B, C and D stages. While at the same time, the Indian Ocean Anticyclone (IOA) ridged into southeast southern Africa.

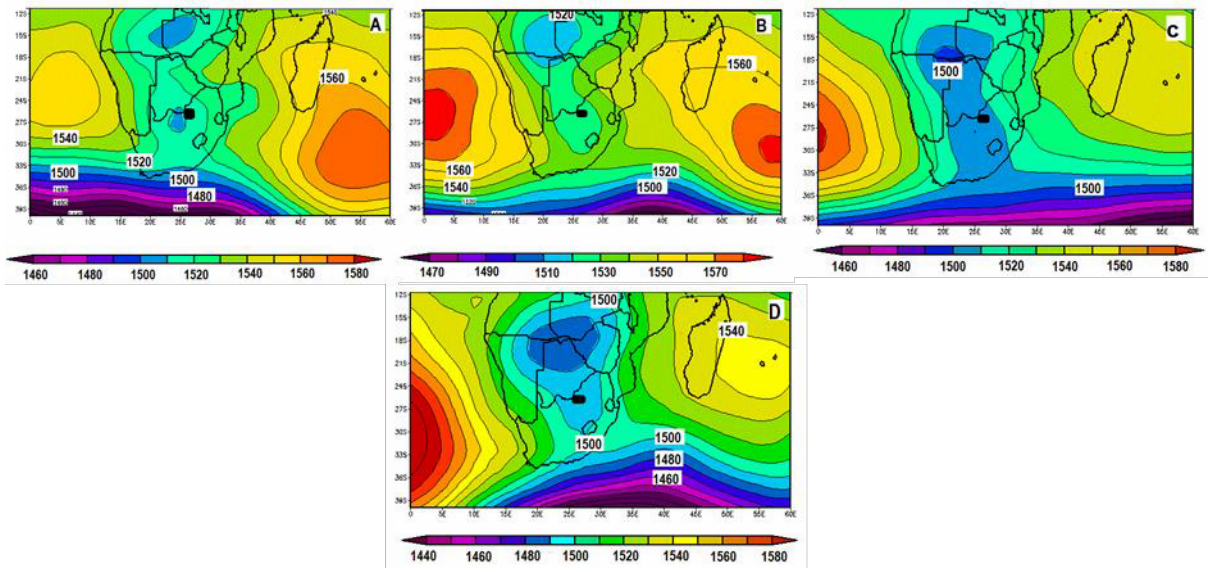

Figure 5.9: Geopotential height (gpm) at 850 hPa over the North West province during the 5- day lasting heat wave (9-13 November 2014) over Madikwe. (A) - One day prior to the heat wave, (B) - during the first day of the heat wave, (C) - the composite of all of the heat wave days and (D) - a day after the heat wave cessation. Contours are drawn at 20 m intervals.

The most conspicuous observation is the intensification of both the AOA and IOA during the heat wave onset (B) to reach the central value of ~1580 hPa. The composite (C) pattern resembles the patterns during the period of heat wave days (B, and other days between B and C) though with a broad trough extending from the southern ocean

(Atlantic and Indian Oceans) to equatorial Africa. Its centre is in the Caprivi Strip in Namibia. The general pattern resembles the Greek letter, Omega.

5.2.2 Geopotential height anomalies – 850 hPa

Geopotential anomalies at 850 hPa are presented in Figure 5.2. At stages A and B, centres of positive anomalies with magnitude between 30 and 50 gpm dominated large areas over the two adjacent oceans. On the other hand, weak positive anomalies occupy most of the sub-continent (including the study area). The other important development observed is that - in all stages (A-D), there are negative geopotential heights anomalies over the SWIO, which deepened to reach -40 gpm south of the Mozambique Channel at stage D. The pattern of the composite anomalies for all heat wave days is in C, it depicts an omega-like shape of negative departures from the mean. The NWP experienced negative values of -10gpm. From the individual daily anomalies (not shown here) that make up the composite, it is shown that the study area maintained the falling pressures throughout the heat wave episode. While at the same time (D - day of cessation), a weakness (-20 to -30gpm) is centred over most parts of southern Africa and the study area experienced the same patterns.

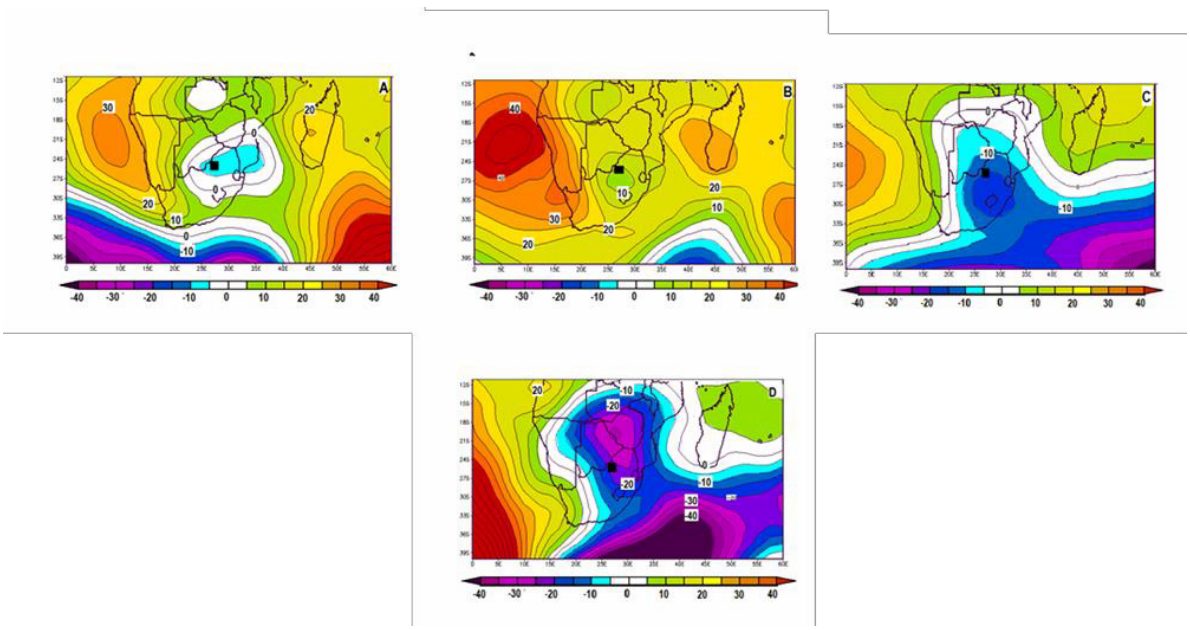

Figure 5.10: Geopotential height anomalies (gpm) at 850 hPa over the North West province during the 5-day lasting heat wave (9-13 November 2014) over Madikwe. (A) - One day prior to the heat wave, (B) - during the first day of the heat wave, (C) - the composite of all of the heat wave days and (D) - a day after the heat wave cessation .Contours drawn at 5m contour intervals.

5.2.3 Mean Geopotential Height - 500 hPa

During the November 2014 heat wave, the dominating climate system was the anticyclone that originated from the southeast Atlantic Ocean one day prior to heat wave onset (Figure 5.3A). It features the central value of 5900gpm, a weak trough also existed in the Mozambique Channel. In the course of the start of the heat wave event (Figure 5.3B), the high pressure from the southeast Atlantic Ocean intensified and extended to engulf the study area. Adjacent to it, a hanging strong low-pressure trough is evident – thus creating a Rex block, where air flowing from the southeast Atlantic Ocean, curved around the ridge and then around the trough in the Mozambique Channel. The hanging feature of the trough slowed down the movement of the corresponding weather systems. The composite (Figure 5.3C) features a mid-latitude high that extended from the Atlantic Ocean with a central value of 5900gpm.

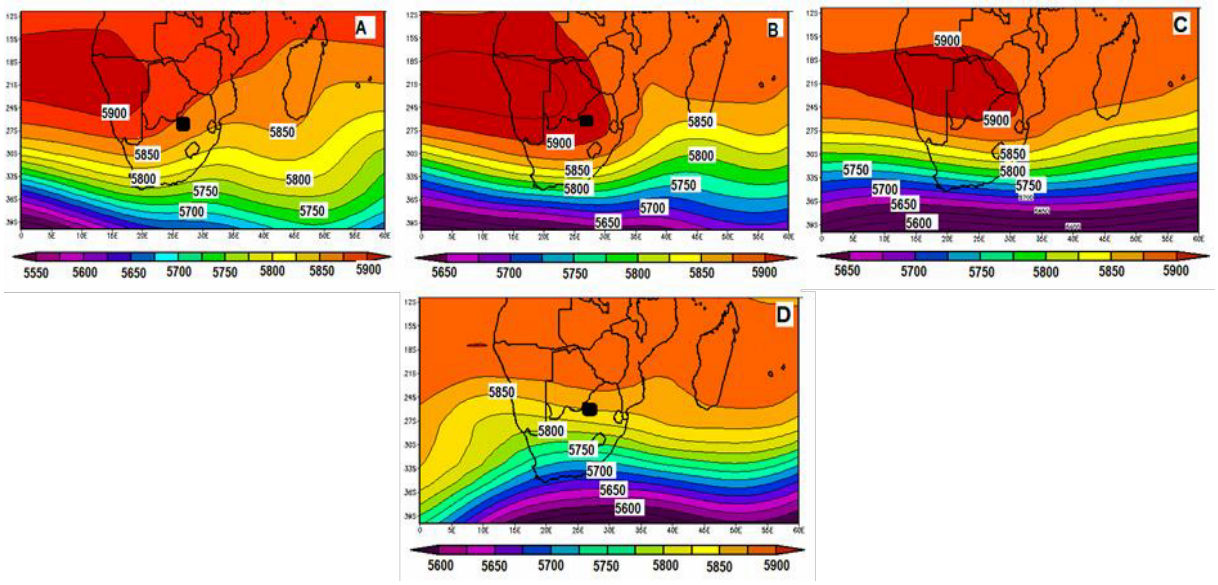

Figure 5.11: Mean geopotential height (gpm) at 500 hPa over the North West province during the 5–day lasting heat wave (9–13 November 2014) over Madikwe. (A) - One day prior to the heat wave, (B) - during the first day of the heat wave, (C) - the composite of all of the heat wave days and (D) - a day after the heat wave cessation. Contours are drawn at 25m intervals.

5.2.4 Geopotential height Anomalies – 500 hPa

500-hPa height anomalies for the 2014 heat wave episode are presented in Figure 5.4. A tongue of strong positive height anomalies of >20 gpm was approaching from the Atlantic Ocean towards the South West Coast of Africa a day before the heat wave onset. It intensified and engulfed the NWP and much of South Africa during the first day (9 Nov 2014) of the heat wave. The areas of falling pressures were found in the SWIO of the KwaZulu Natal coast and the southeast of Madagascar a day before the onset. During the onset, the geopotential height decreased drastically to reach <-20 gpm south of Madagascar. The composite anomalies (C) indicate an overall pressure reduction over southern Africa, when compared to the situation on the onset day and a day before onset. On the cessation day, the geopotential heights hugely reduced to less than -80gpm over the southern parts of South Africa.

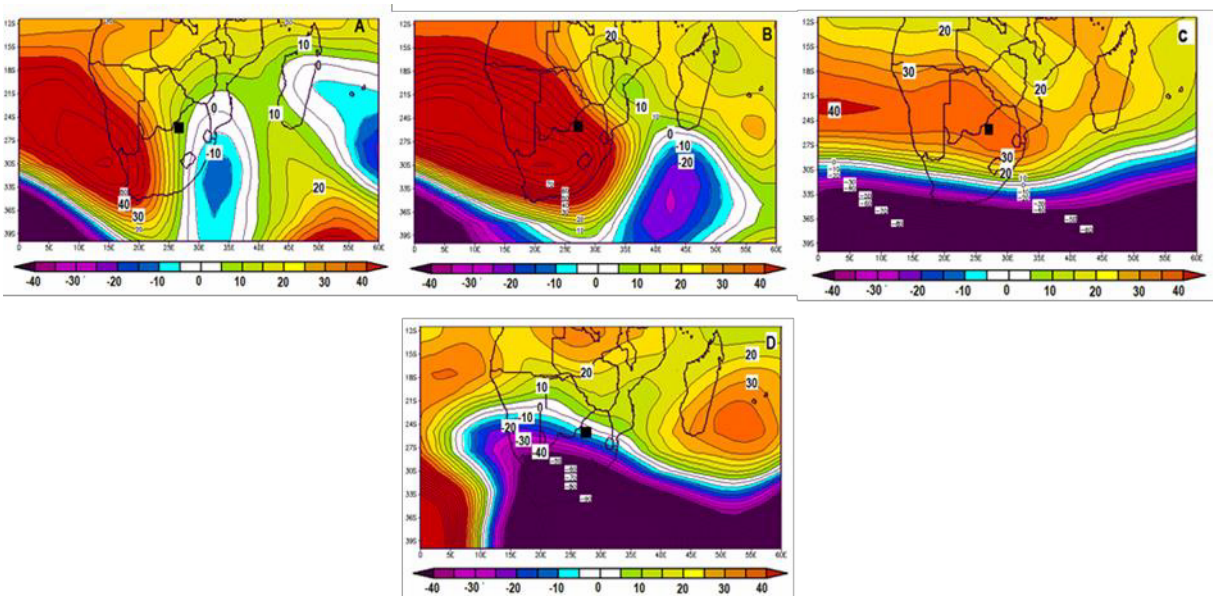

Figure 5.12: Geopotential height Anomalies (gpm) at 500 hPa over the North West province during the 5-day lasting heat wave (9 - 13 November 2014) over Madikwe. (A) - One day prior to the heat wave, (B) - during the first day of the heat wave, (C) - the composite of all of the heat wave days and (D) - a day after the heat wave cessation. Contours drawn at 5 m contour interval.

5.2.5 Mean Geopotential Height – 200 hPa

At 200-hPa, the circulation featured amplified ridges over the south western southern Africa and a trough over the southern Africa with an axis through Zimbabwe to southern Mozambique (Figure 5.5 A). In Figure 5.3 B, the previously observed ridge and trough intensified and relaxed a day later. The composited (Figure 5.5 C) heat wave days, exhibit relaxed parallel geopotential contours, signifying a smooth westerly flow from the Atlantic Ocean aloft. A westerly flow from the southwest Atlantic Ocean generally advects dry air into the interior of the southern Africa and especially over the study area, which was among the first recipients of that kind of flow.

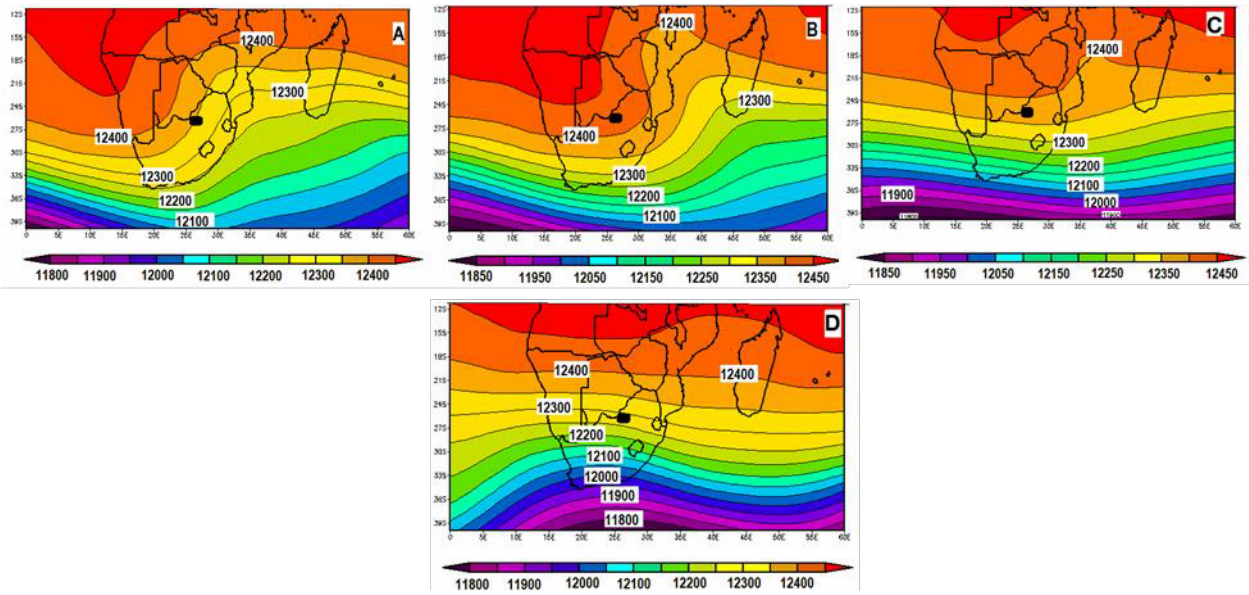

Figure 5.13 Mean Geopotential height (gpm) at 200 hPa over the North West province during the 5- day lasting heat wave (9 - 13 November 2014) over Madikwe. (A) - One day prior to the heat wave, (B) - during the first day of the heat wave, (C) - the composite of all of the heat wave days and (D) - a day after the heat wave cessation. Contours are drawn at 50 m intervals.

5.2.6 Geopotential height Anomalies – 200 hPa

Figure 5.6 shows an evolution of the upper troposphere geopotential height anomalies. Areas of larger negative height anomalies are observed along the two oceans and persist at all stages of the heat episode. During day prior to (A) and onset (B), these heights spread over the continent along the north eastern side. At stage C, the negative heights from the south Atlantic and those over the Indian Ocean, which are observed in A and B, merged up and reaching the south western tip of the country, while the study area maintained very high positive height anomalies through the A, B and C stages of the heat wave episode. Positive height anomalies were then displaced by the deepening

of negative heights from the south, covering the whole of South Africa, parts of Namibia and Botswana (D).

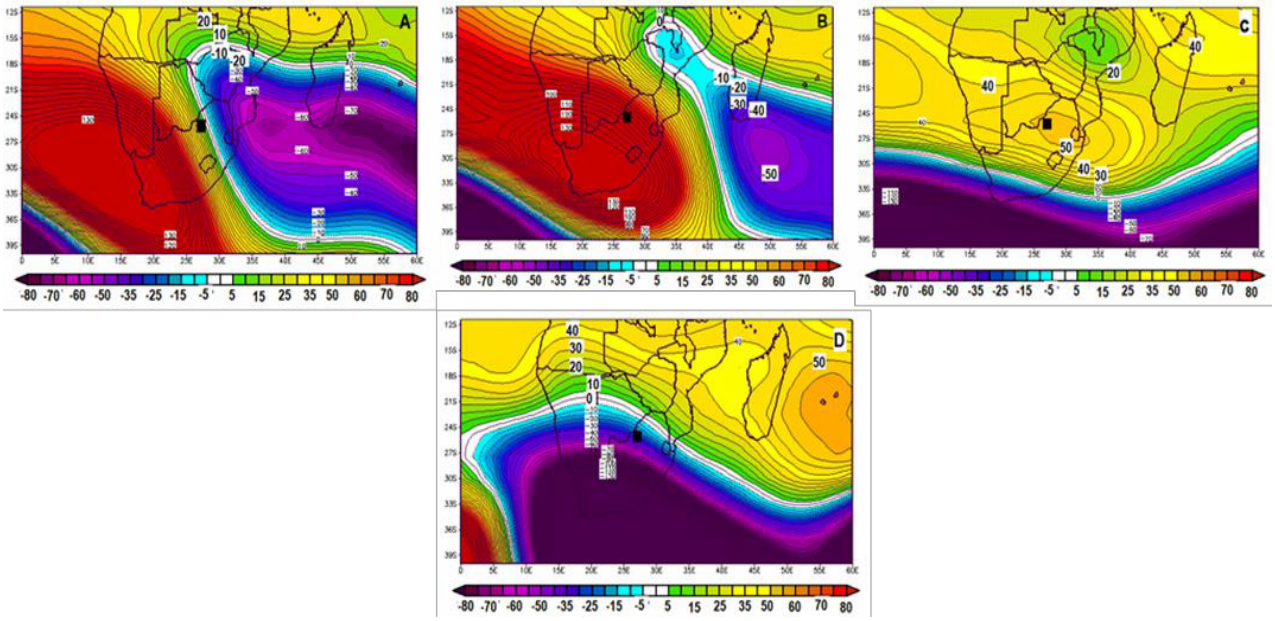

Figure 5.14: Geopotential height anomalies (gpm) at 200 hPa over the North West province during the 5–day lasting heat wave (9-13 November 2014) over Madikwe. (A) - One day prior to the heat wave, (B) - during the first day of the heat wave, (C) - the composite of all of the heat wave days and (D) - a day after the heat wave cessation. Contours drawn at 5 m intervals.

5.2.7 Mean Vector Winds – 850 hPa

Vector winds at 850 hPa during the November 2014 - heat wave are presented in Figure

5.7. Winds with magnitude of ≤ 5 ms^{-1} were evident in all events (one day prior to, onset, during and after heat wave events. During the heat wave onset (Figure 5.7B), northerly winds were observed over the Mozambique Channel and the north eastern part of the country, including the study area. As the flow progressed over the study area, it was diverted to the eastern side, leaving the area with winds of ~4 ms^{-1}. The wind pattern could confirm the advection of the dry continental wind and later likely to result in an increased near-surface moisture advection in the study area. A South westerly flow was maintained over the study area throughout the monitoring period. In the adjacent ocean (Atlantic and Indian Ocean), an anticyclonic flow was retained during the observation period.

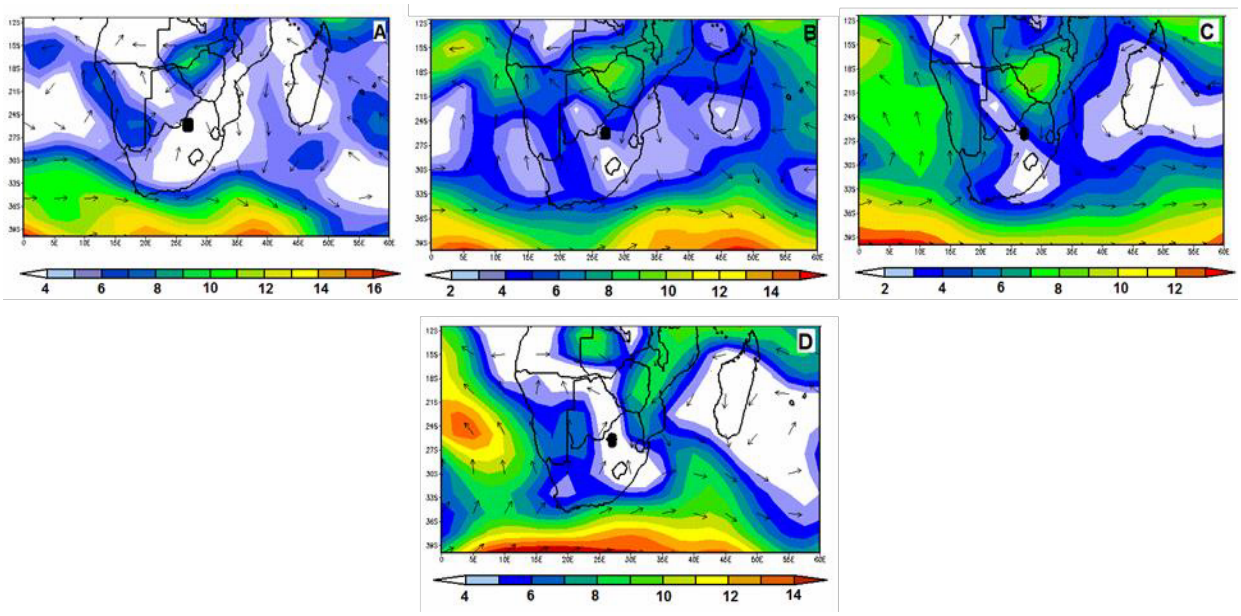

Figure 5.15: Mean vector winds (ms^{-1}) at 850 hPa over the North West province during the 5–day lasting heat wave (9-13 November 2014) over Madikwe. (A) - One day prior to the heat wave, (B) - during the first day of the heat wave, (C) - the composite of all of the heat wave days and (D) - a day after the heat wave cessation.

5.2.8 Vector winds Anomalies – 850 hPa

The main flow that arrived over the study area a day before the onset of heat wave, was mainly south westerly. It emanated from the south east Atlantic Ocean and developed a curvature near the border of South Africa and Namibia. Over the study area, it maintained a magnitude of approximately 4 ms^{-1}. The flow converged over the east coast of South Africa. The convergence area expanded to engulf the study area by the time of the heat wave onset (10 Nov 2014) and the origin of the main flow was still from the south westerly and the Atlantic Ocean. The southerly flow was experienced over the study area during the cessation time with a curvature north of the study area in Zimbabwe. The composite wind vector patterns over the NWP and its neighboring areas resemble those of the cessation time.

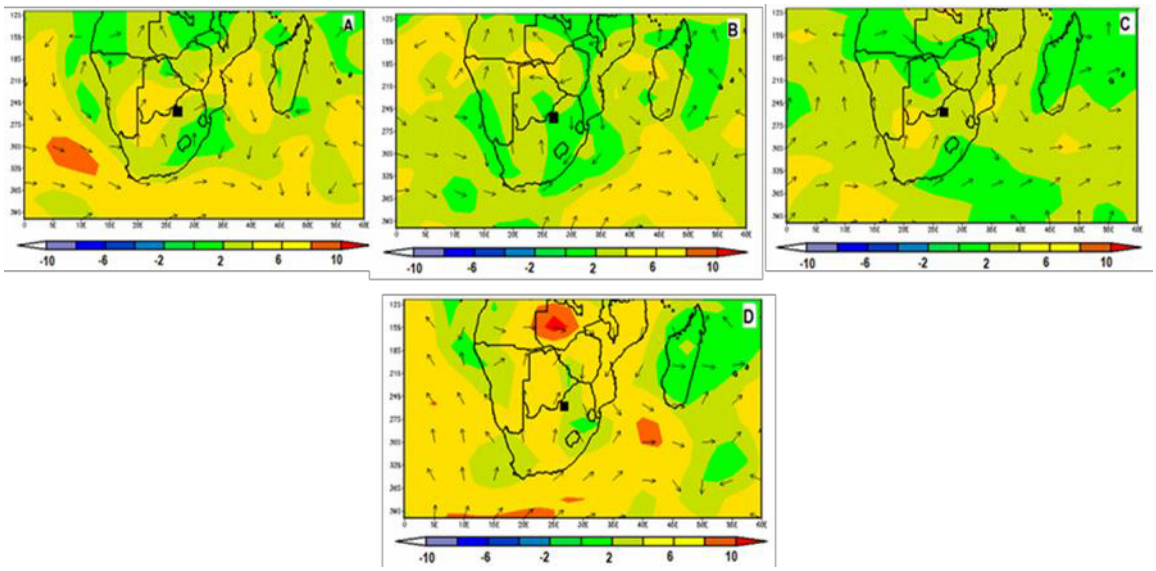

Figure 5.16: Vector winds anomalies (ms^{-1}) at 850 hPa over the North West province during the 5–day lasting heat wave (9-13 November 2014) over Madikwe. (A) - One day prior to the heat wave, (B) - during the first day of the heat wave, (C) - the composite of all of the heat wave days and (D) - a day after the heat wave cessation - Contours drawn at 2 $m.s^{-1}$ intervals.

5.2.9 Mean vector winds - 200 hPa

Mean 200 hPa vector winds are shown in Figures 5.9 (A, B, C and D). Distinctive characteristics observed one day prior to the heat wave onset and during the heat wave commencement, was the upper level anticyclonic flow with a curvature over the study area. The winds were very strong to equal a weak jet stream southward of the study area. While during the heat wave onset, the light winds prevailed northward of the area. The composite of heat wave days, feature an anticyclonic flow of light winds that provided the parallel flow over the study area and a curvature over Madagascar. Winds of 45-50 ms^{-1} maximum magnitude were centered poleward of the Western Cape.

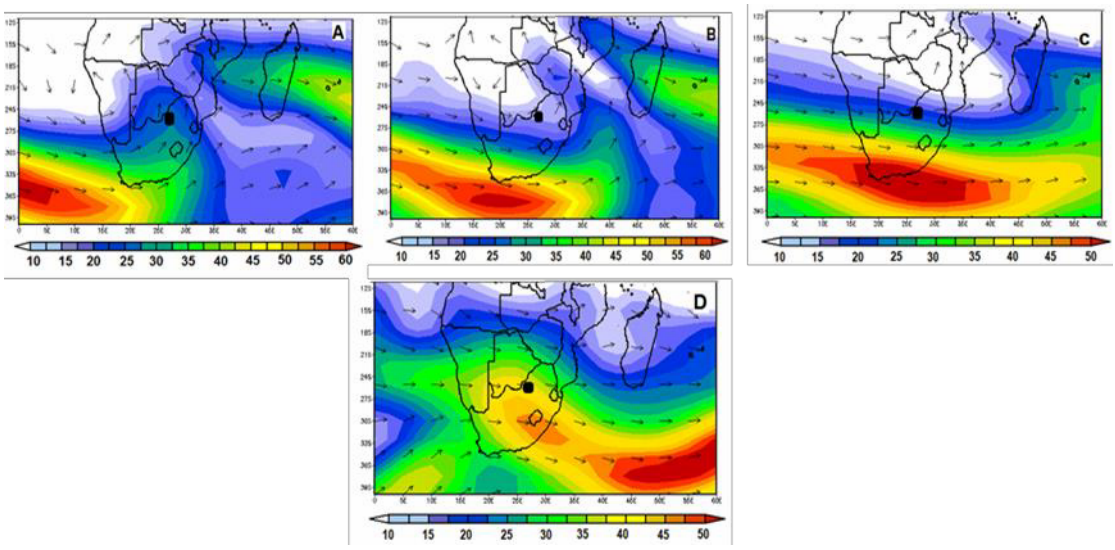

Figure 5.17: Vector winds (ms^{-1}) at 200 hPa over the North West province during the 5–day lasting heat wave (9 - 13 November 2014) over Madikwe. (A) - One day prior to the heat wave, (B) - during the first day of the heat wave, (C) - the composite of all of the heat wave days and (D) - a day after the heat wave cessation.

5.2.10 Vector winds anomalies – 200 hPa

Patterns of vector winds anomalies at 200 hPa are illustrated in the Figure 5.10. The prominent feature that occupied the southern Africa a day prior to the onset and during the beginning of the heat wave is the anti-cyclonic gyre of vector winds from the SEAO through the SWIO – curving over the Limpopo Province and back to the Atlantic Ocean.

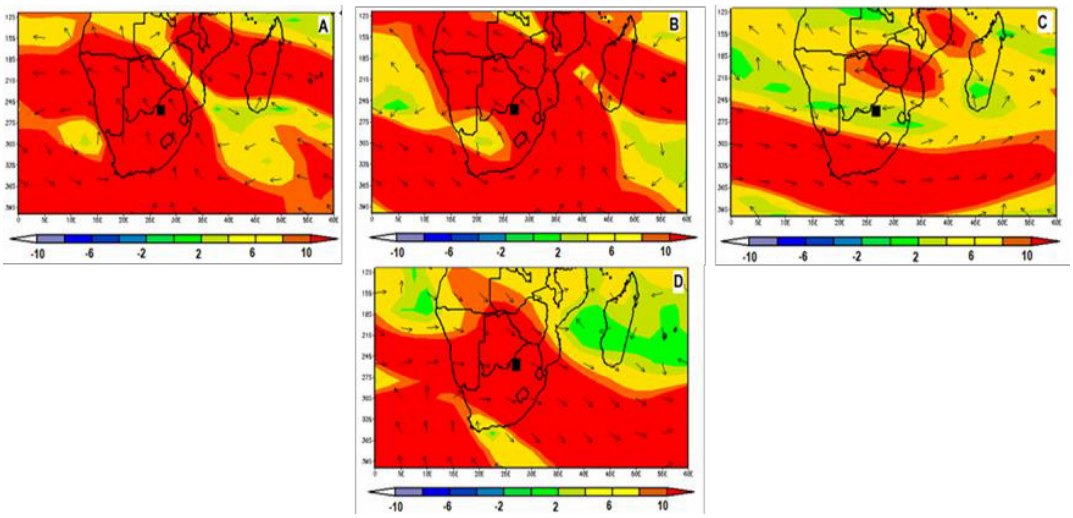

Figure 5.18: Vector winds anomalies (ms^{-1}) at 200 hPa over the North West province during the 5-day lasting heat wave (9 - 13 November 2014) over Madikwe. (A) - One day prior to the heat wave, (B) - during the first day of the heat wave, (C) - the composite of all of the heat wave days and (D) - a day after the heat wave cessation. Contours drawn at 2 m s^{-1} intervals.

Along that trajectory, the wind speed magnitude was ≥ 10 ms^{-1}.The 200 hPa level wind vector anomalies during the composite days, portrayed an easterly flow over the NWP of magnitude ≈ 6 ms^{-1}. Strong anomalies were found further south of the study area. On the day of cessation, a cyclonic flow was observed south ward of the study area; meanwhile a strong westerly flow advanced toward the NWP.

5.2.11 Mean Specific Humidity - 700 hPa

Mean specific humidity at 700 hPa is represented in Figure 5.11. Reference to the figure is the entire part of South Africa (Figure 5.11A), north of the 30°S was under a moisture of ≥ 5 g/kg - this included the study area. The Mozambique Channel depicted dry air ≤ 1g/kg, while north of the 20°S equatorward, the air is moist (≥ 8g/kg) with a centre over Angola. In Figure 5.11B (heat wave onset), the moisture was reduced (≤ 3g/kg) over the study area.

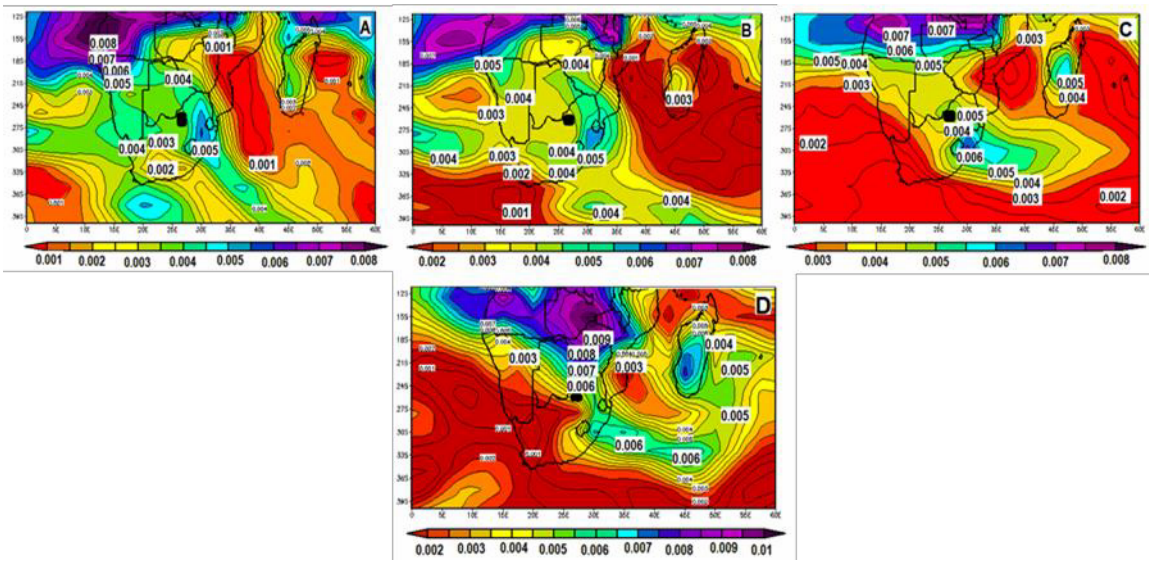

Figure 5.19: Mean specific humidity (g/kg) at 700 hPa over the North West province during the 5-day lasting heat wave (9-13 November 2014) over Madikwe. (A) - One day prior to the heat wave, (B) - during the first day of the heat wave, (C) - the composite of all of the heat wave days and (D) - a day after the heat wave cessation.

The dryness observed previously in the South West Indian Ocean (SWIO) has increased to show very low moisture. Similarly, the Atlantic Ocean south west of the Cape Peninsular moisture was low (≤ 1g/kg). The tropics maintained high moisture. During the first day of the cessation of the heat wave, the south east Atlantic Ocean moisture deficit extended eastward to cover Namibia and south west of South Africa.

Over the study area, the moisture had improved to 6 g/kg. The composite of heat waves (Figure 5.11C) revealed an extension of abundant moisture along the north west – south east orientation over southern Africa that emanated from the tropics – where the maximum moisture is maintained.

5.2.12 Specific Humidity Anomalies – 700 hPa

Specific humidity field (Figure 5.12 for the Nov 2014 heat wave) shows that strong, negative anomalies cell with a centre value of ≈ –4 g/kg over the northeast Zimbabwe one day before the heat wave started. Positive specific humidity anomalies are found in the Atlantic Ocean although they are of weaker magnitude. During the heat wave onset (09 Nov 2014), most areas in the observing domain (40°S – 10°S and 0°E – 60°E), including the study area, experienced weaker specific humidity anomalies. All areas of negative anomalies are indicative of the diminishing moisture regions. Although, the Atlantic Ocean features positive anomalies, the moisture is not available further inland due to its cold characteristics. Thus, the air above it is unable to hold large quantities of vapour.

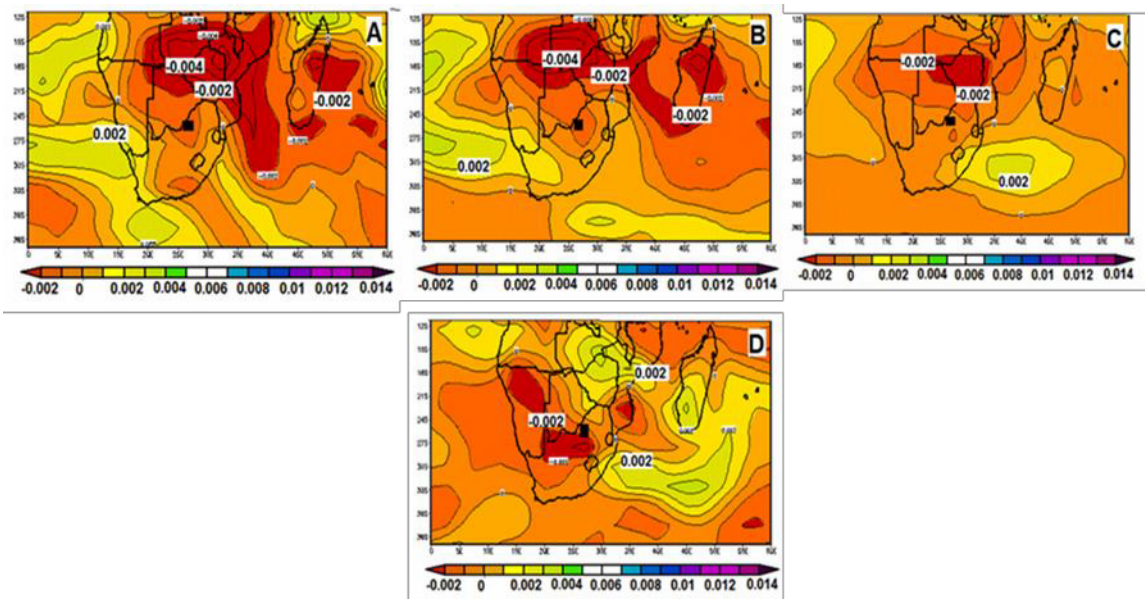

Figure 5.20: Anomalies of specific humidity (g/kg) over the North West province during the 5-day lasting heat wave (9 - 13 November 2014) over Madikwe. (A) - One day prior to the heat wave, (B) - during the first day of the heat wave, (C) - the composite of all of the heat wave days and (D) - a day after the heat wave cessation. Contour interval at 0.001 g/kg.

The composite of heat waves as presented in C, shows a weakening of the specific humidity fields over much of southern Africa, which can be attributed to the south westerly flow through the Kalahari and Namib deserts as observed earlier using the low level geopotential heights (Figure 5.2). During the heat wave cessation (14 Nov 2014), positive anomalies were intensifying in the Indian Ocean around Madagascar and over Zimbabwe and Zambia. Those areas were indicative of moisture evaporative source regions. During this time, the negative humidity anomalies were developing towards the Atlantic Ocean. The target area of study (NWP), was still under low negative humidity anomalies (< -2 g/kg).

5.2.13 Mean Outgoing Longwave Radiation

Figure 5.13 shows the location of the major regions of relatively deep convection (low values of outgoing longwave radiation (OLR) and the relatively clear skies (high values of OLR). In Figure 5.13A, the study area is engulfed by OLR values of around 270 Wm^{-2}, higher values are centred over Namibia and the west part of Madagascar, South West Indian Ocean towards the Mozambique Channel and Angola. In Figure 5.13B, the study area depicts large values of OLR (290Wm^{-2}) a possible indicative of clear skies and high level or thin middle or low clouds. Active regions of deep activities are situated in the South West Indian Ocean south of Madagascar and north of the borderline of the monitoring domain in the tropics.

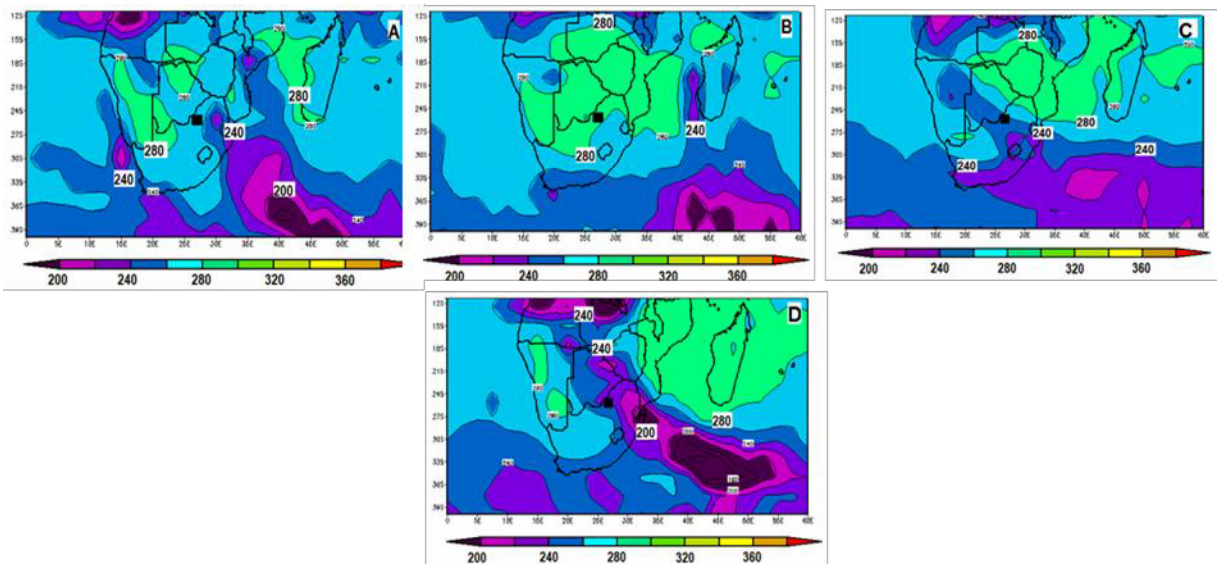

Figure 5.21: Mean Outgoing longwave radiation (Wm^{-2}) over the North West province during the 5-day lasting heat wave (9-13 November 2014) over Madikwe. (A) - One day prior to the heat wave, (B) - during the first day of the heat wave, (C) - the composite of

all of the heat wave days and (D) - a day after the heat wave cessation. Contour intervals are 5-10 Wm^{-2}.

During the end of the heat wave events (Figure 5.13D), large values of OLR occupied Mozambique and extended to Madagascar through the Mozambique Channel. South of the Mozambique Channel and Angola, depicts deep convective areas (< 200 Wm^{-2}). In Figure 5.13C (the composite of heat wave days), SWIO convective activities intensified, extending westward to the south of South Africa.

5.2.14 Outgoing Longwave radiation Anomalies

Figure 5.14 illustrates the OLR anomaly sequence for the November 2014 heat wave event. Major zones of convection are readily described as regions with low OLR departures and those of high OLR are areas of subsidence. The notable feature, which was observed a day before the heat wave, is the extended positive departures from the north (Zimbabwe) through the study area to SWIO. The study area observed departures of ≈30 Wm^{-2}. A negative OLR departure occupied the Mozambique Channel southwards along 40°E. On the first day of the heat wave, the NorthWest Province maintained positive OLR anomalies (≈ 30 Wm^{-2}). This observation suggests that the area experienced sinking air for the two days consecutively, thus drying most of the study area. The convective actions are found in the Mozambique Channel and further south over SWIO. From the heat waves composite patterns, high OLR were sustained over the highveld and north towards Zimbabwe. The study area received high OLR anomalies too. A day after the heat wave ended (Figure 5.14D), the study area portrayed low negative OLR anomalies. The strong centre of convective actions was in the Indian Ocean south of Madagascar. During this period, much of the southern part of Angola, northern Zimbabwe and Mozambique maintained high positive (≥ 30 Wm^{-2}) OLR anomalies

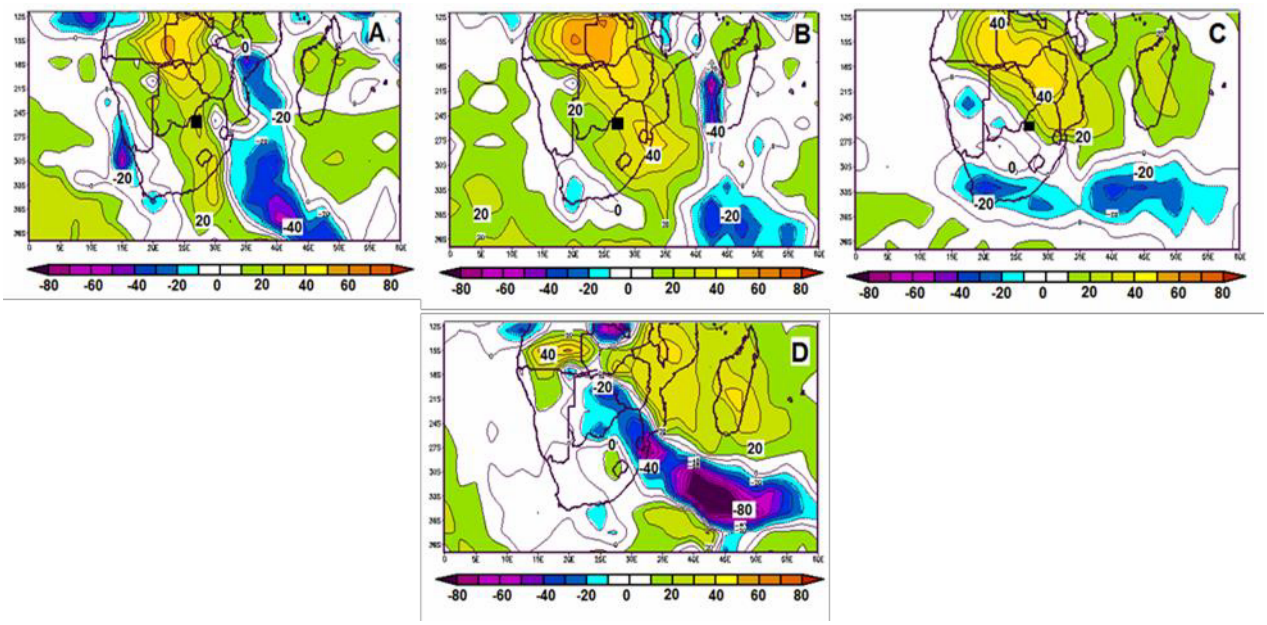

Figure 5.22: Anomalies of Outgoing longwave radiation (OLR Wm^{-2}) over the North West province during the 5-day lasting heat wave (9 - 13 November 2014) over Madikwe. (A) - One day prior to the heat wave, (B) - during the first day of the heat wave, (C) - the composite of all of the heat wave days and (D) - a day after the heat wave cessation. Contour intervals are 10 Wm^{-2}.

5.2.15 Mean Vertical Motion (Omega)

An evolution of 500 hPa vertical motion is analysed in Figure 5.15. On day prior to the event (Figure 5.15 A), a strong ascending motion is evident over South of Namibia, the adjacent Atlantic Ocean, parts of South Africa and south of the Atlantic Ocean. This was maintained up to the onset day except the displacement of SAO ascent by a moderate SAO descent motion. Areas of descending were observed over the Mozambique Channel and South Indian Ocean with centre values of 0.05 Pa s^{-1} and 0.2 Pa s^{-1} respectively. During the onset day, the previously observed descent over the Mozambique Channel intensified, reaching a centre value of 0.1 Pa s^{-1} . It stretched over Zambia, Zimbabwe and south of Mozambique. Along the east of Madagascar, an ascending motion was still maintained. The study area maintained a slight ascending motion. During the composite days of the heat wave (Figure 5.15 C), the ascending motion over Namibia and the bigger part of SA was still maintained. Areas of descent were largely spread over the Atlantic and Indian Oceans with centre values >0.09 Pa s^{-1} and 0.06 Pa s^{-1} respectively. During this period, the study area experienced a rising motion of ~ 0.06 Pa s^{-1}. On the day of cessation, a slight descent was still maintained

over the adjacent oceans while a tongue of ascending motion from the SAO entered through South of Southern Africa.

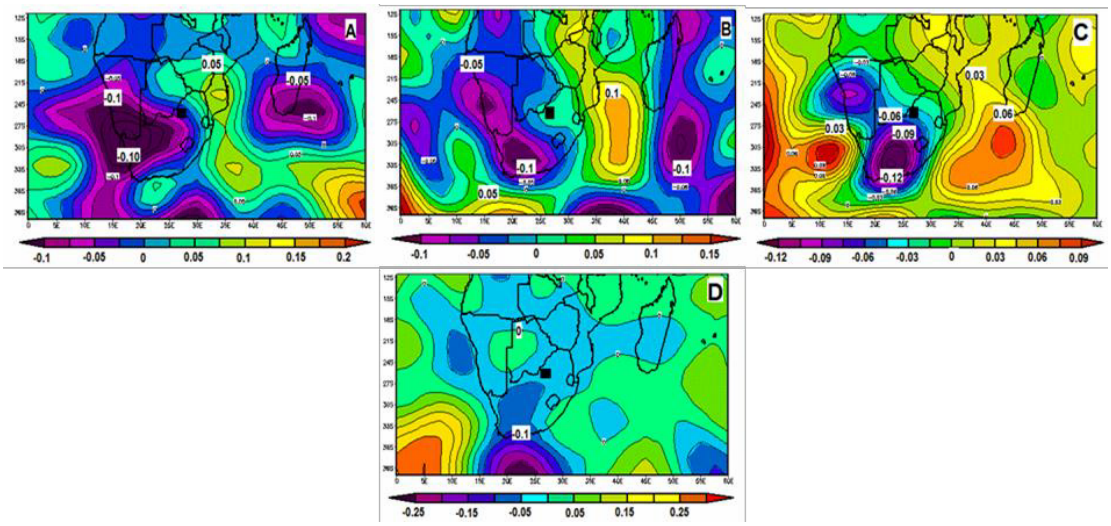

Figure 5.23: Mean vertical motion (Pa s^{-1}) over the North West province during the 5-day lasting heat wave (9-13 November 2014) over Madikwe. (A) - One day prior to the heat wave, (B) - during the first day of the heat wave, (C) - the composite of all of the heat wave days and (D) - a day after the heat wave cessation.

5.2.16 Vertical Motion Anomalies

According to Kabanda (2004), vertical velocity anomalies are complicated to interpret. The problem arises when, for example, a negative anomaly does not necessarily mean an upward motion or a positive anomaly does not mean a downward motion. Therefore, in this section, the attention is then restricted to composite days when a heat wave occurred for 5 days consecutively (Figure 5.16 C). The most conspicuous features are a centre of negative anomalies southward of the study area and positive anomalies over the northeast of the study area. The positive anomalies areas indicate enhanced subsidence areas and the negative anomalies patterns are convective (upward motion) areas.

However, the NWP is located where the two systems meet, which implies that some parts of the province experience a rising motion and the other part, a sinking motion, but each of low magnitudes - because the area experiences the transition of the two extremes.

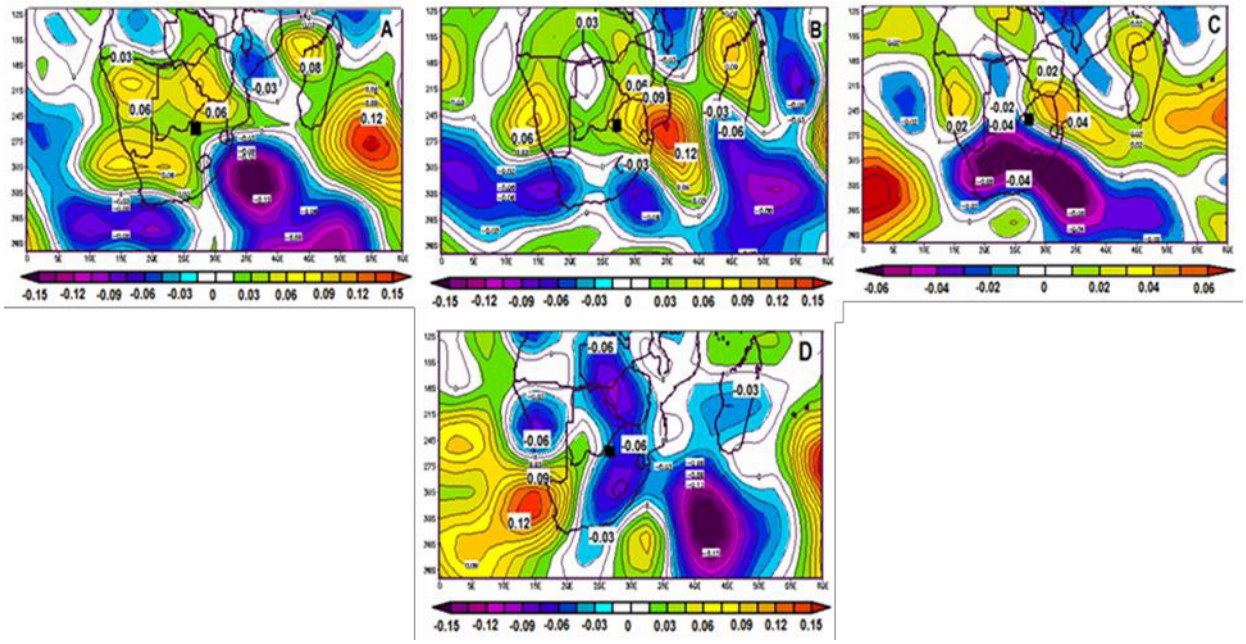

Figure 5.24: Anomalies of vertical motion (Pa s^{-1}) over the North West province during the 5-day lasting heat wave (9-13 November 2014) over Madikwe. (A) - One day prior to the heat wave, (B) - during the first day of the heat wave, (C) - the composite of all of the heat wave days and (D) - a day after the heat wave cessation.

5.3 Meteorological Parameter analysis: 5-7 December 2014 heat wave over Taung

This section deals with a heat wave that occurred in December 2014 and was reported by one station (Taung). However, during that episode, the mean maximum temperature over the station superseded any other temperature reported during the December heat waves under consideration. Its temperature was 37.5°C. Therefore, it was found appropriate to consider it in this analysis.

5.3.1 Mean Geopotential Height – 850 hPa

In Figure 5.17 A, the larger part of southern Africa and the adjacent ocean experienced very high geopotential heights (≥ 1530 gpm). This situation changed a day later (the first day of the heat wave-Figure 5.17B), when the central geopotential heights dropped by about 20 gpm to reach 1520 gpm. This situation was also experienced over Madagascar and a large area of the eastern Indian Ocean. While the Atlantic Ocean

was dominated by higher values of the geopotential height (center value was 1560gpm). The influence of high geopotential fields were experienced in the north eastern South Africa, its origin seems to be south West Indian Ocean. Of notable pattern during days of the heat wave and its first day, is the existence of the Congo trough joined with the one from the southern Africa at stage B and D

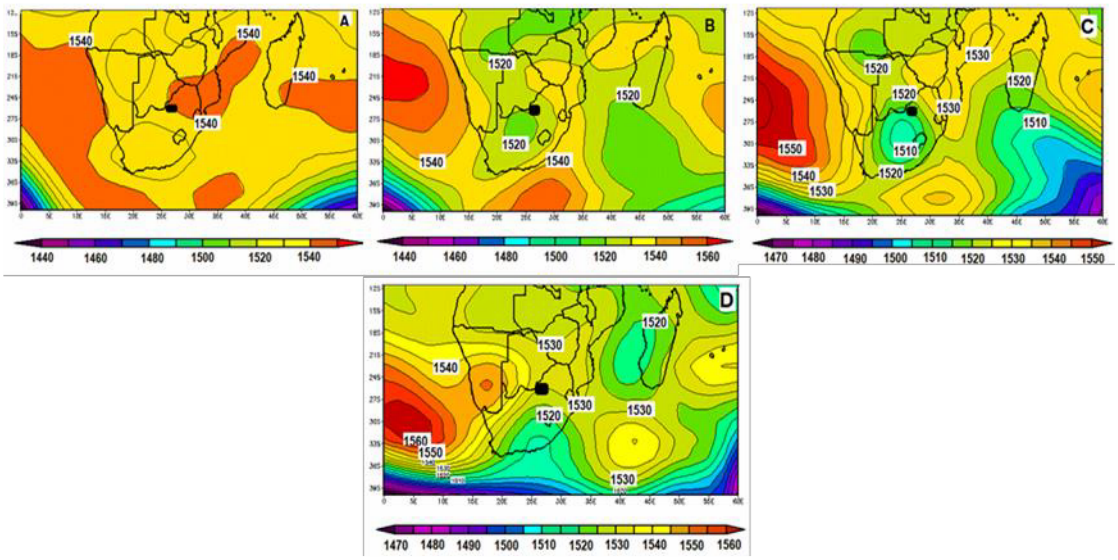

Figure 5.25: Mean geopotential height (gpm) at 850 hPa over the North West province during the 3-day lasting heat wave in Taung from 5-7 December 2014. (A) - One day prior to the heat wave, (B) - during the first day of the heat wave, (C) - the composite of all of the heat wave days and (D) - a day after the heat wave cessation. Contours are drawn at 10 m intervals.

5.3.2 Geopotential height Anomalies – 850 hPa

Anomaly sequences for the low level geopotential height during the three-day heat wave event in December 2014 is explained in Figure 5.18. On the day prior to the onset (Figure 5.18A), the Atlantic Ocean closer to the Namibian coast; there existed a positive geopotential field with a central anomaly of 30 gpm. The study area featured 20 gpm departures from the long term mean. During the onset, the anomaly near the Namibian Coast that were mentioned earlier, intensified to reach a central height anomalies of 40 gpm, which is situated at 18°S and 10°E in the AO. Meanwhile, a tongue of falling pressure with respect to the mean, extended from the SWIO to reach the study area. Thus, rendering the study area to experience a weak positive anomaly (~5 to 10 gpm). The geopotential height anomaly patterns of the composite during the heat waves days (Figure 5.18C) resemble the patterns observed during the onset time – although with a steep falling geopotential height (-30 gpm) southeast of Madagascar. In addition, the

subcontinent experienced a widespread of weakening pressures. The weakening of the pressures were enhanced by the approaching of negative fields from the IO. On the day after the heat wave events (Figure 5.18D), showed a very strong resemblance of the situations experienced a day before the heat wave onset with high (central value of 40 gpm) positive geopotential field anomalies centred South of Namibia.

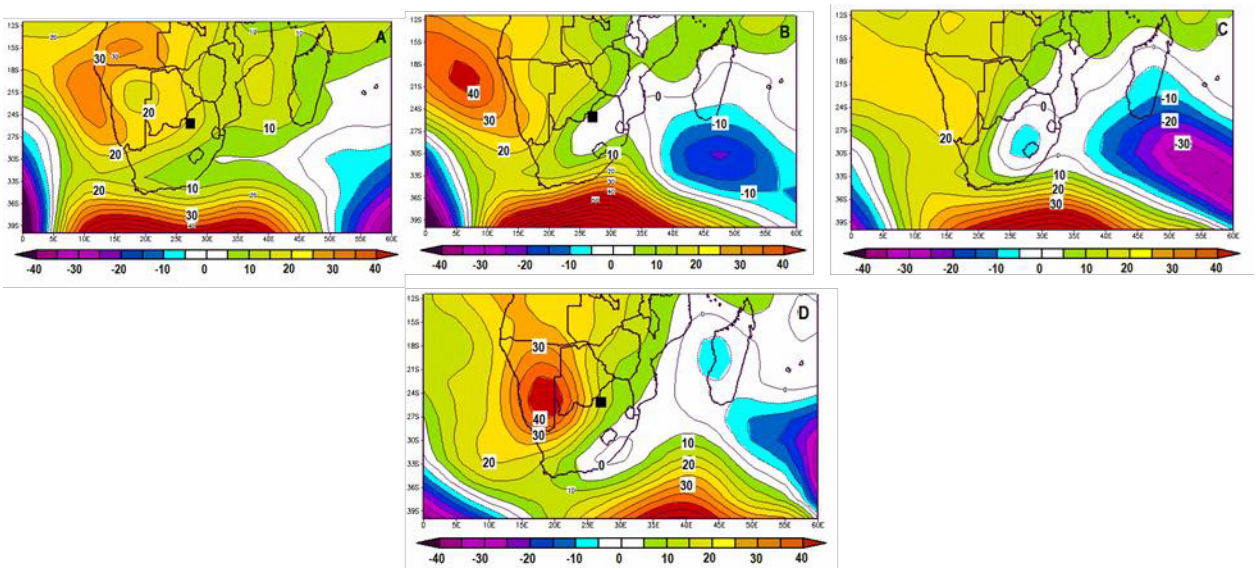

Figure 5.26: Anomalies of geopotential height (gpm) at 850 hPa over the North West province during the 3-day lasting heat wave in Taung from 5-7 December 2014. (A) - One day prior to the heat wave, (B) - during the first day of the heat wave, (C) - the composite of all of the heat wave days and (D) - a day after the heat wave cessation. Contours drawn at 5 m intervals.

5.3.3 Mean Geopotential Height – 500 hPa

An intense geopotential height with a centre value of 5900 gpm was observed a day prior to the heat wave onset (Figure 5.19A), it was centred over the southern Namibia and surrounded the study area. A weak trough developing over the coast of the south eastern South Africa was evident a day before the heat wave event. On the first day of the heat wave episode (Figure 5.19B), the trough reported earlier, deepened with a meridional fetch that maintained its axis over the Mozambique Channel. A wave pattern of geopotential heights was observed south of 30°S especially from stages B, C and D. This situation suggests that the controlling systems (high pressure and troughs) are moving slowly hence the persistence of extreme temperatures, which resulted in the development of heat wave conditions that lasted more than three consecutive days.

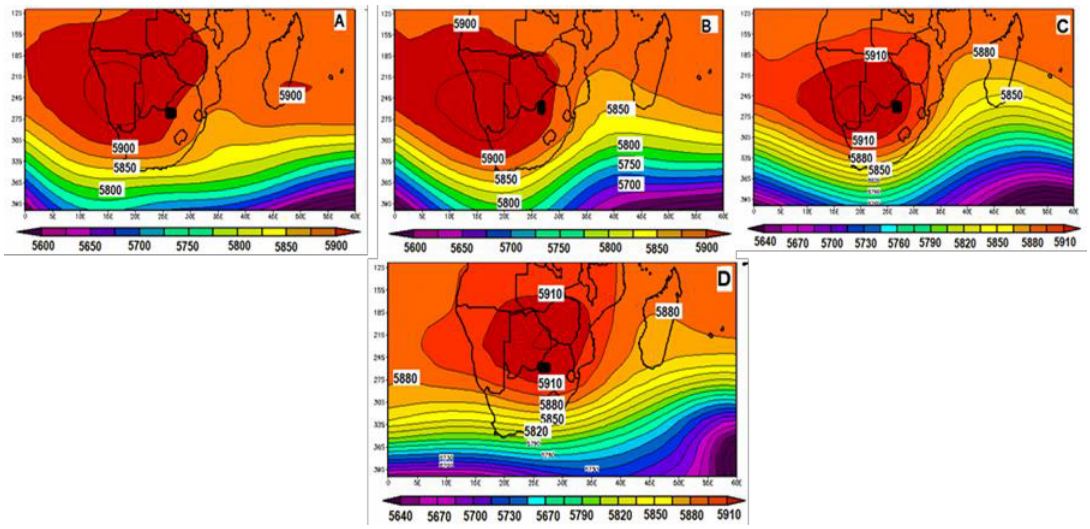

Figure 5.27: Mean geopotential height (gpm) at 500 hPa over the North West province during the 3-day lasting heat wave in Taung from 5-7 December 2014. (A) - One day prior to the heat wave, (B) - during the first day of the heat wave, (C) - the composite of all of the heat wave days and (D) - a day after the heat wave cessation. Contours are drawn at 30 and 100 m intervals.

5.3.4 Geopotential height – 500 hPa

The geopotential height anomalies over the 500 hPa during the day prior to the onset, during the onset and the heat wave composite days are presented in Figure 5.20 A, B and C respectively. From their quasi-identical patterns, it is evident that a dipole feature existed, whereby strong positive geopotential height anomalies are covering much of SEAO, Namibia, Botswana and South Africa; while the strong negative anomalies occupied much of the SWIO that included the Mozambique Channel.

The day after the heat wave events (Figure 5.20 D), strong pressure anomalies occupied the central part of the southern Africa – this is manifested by a closed pressure system with a centre high of 50 gpm that was centred over the subcontinent, including the study area. Strong negative anomalies remained over the SWIO.

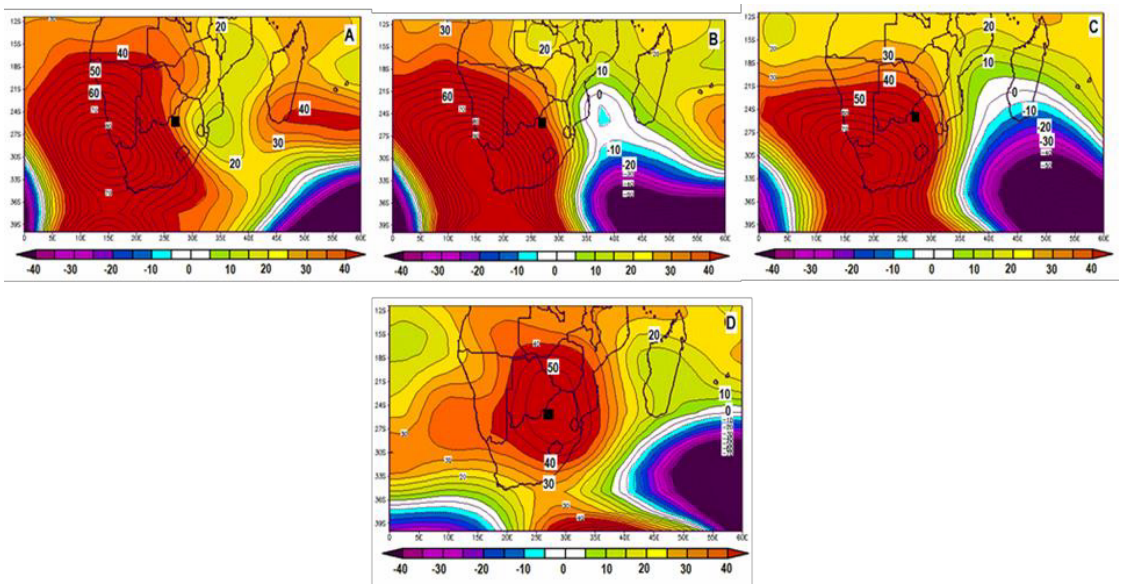

Figure 5.28: Anomalies of geopotential height (gpm) at 500 hPa over the North West province during the 3-day lasting heat wave in Taung from 5-7 December 2014. (A) - One day prior to the heat wave, (B) - during the first day of the heat wave, (C) - the composite of all of the heat wave days and (D) - a day after the heat wave cessation. Contours drawn at 5 m intervals

5.3.5 Mean Geopotential Height – 200 hPa

Mean 200 hPa geopotential height circulation presented the development of upper level troughs and ridges through the heat wave evolution.

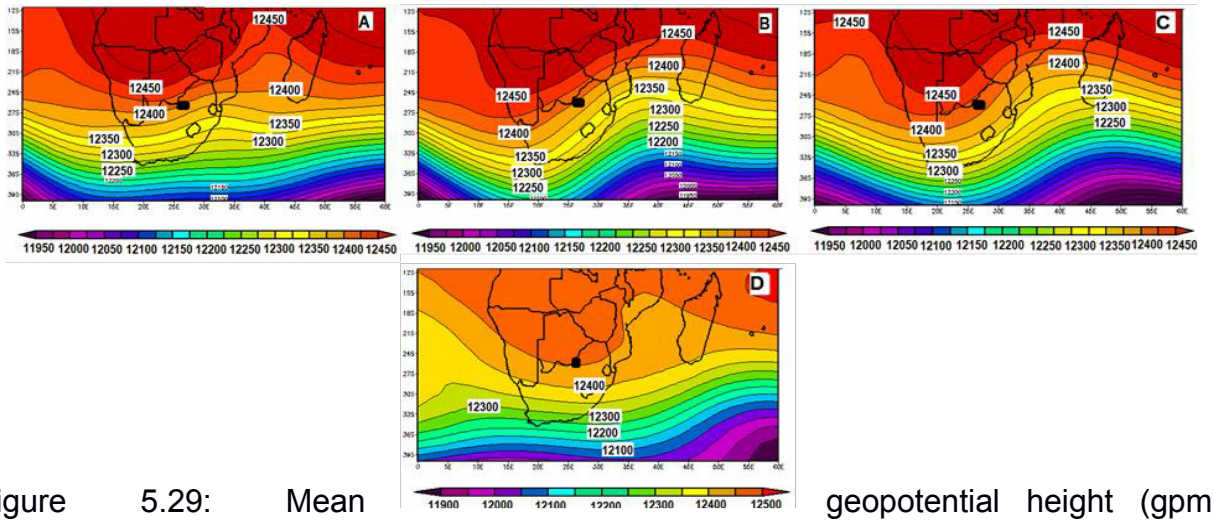

Figure 5.29: Mean geopotential height (gpm) at – 200 hPa over the North West province during the 3-day lasting heat wave in Taung from 5-7 December 2014. (A) - One day prior to the heat wave, (B) - during the first day of the heat wave, (C) - the composite of all of the heat wave days and (D) - a day after the heat wave cessation. Contours are drawn at 100 m intervals.

In Figure 5.21A, B and C, an upper level high pressure cell developed over the central subcontinent with centre values of 12450 gpm. As it extended further south, a ridge covered South Africa while a trough over the Indian Ocean deepened. In Figure 5.21C, the composite of heat wave days shows a deep wave pattern that extended from the Atlantic Ocean to the Indian Ocean; with a deep trough over the Mozambique Channel followed by a strong ridge behind (over southern Africa).

5.3.6 Geopotential height Anomalies – 200 hPa

Upper tropospheric geopotential height anomalies are presented in Figure 5.22. On the day prior to the start of the heat wave, a centre of a high positive anomaly was observed over the Atlantic Ocean, covering the south-west of South Africa and south of Namibia. During the onset (Figure 5.22B) and heat wave composite days (Figure 5.22C), an extended system of falling pressures from the SWIO through the Mozambique Channel were observed. A tongue of the negative geopotential height anomalies extended to reach the north of Limpopo in South Africa, and the adjacent countries (Zimbabwe, Mozambique and Madagascar).

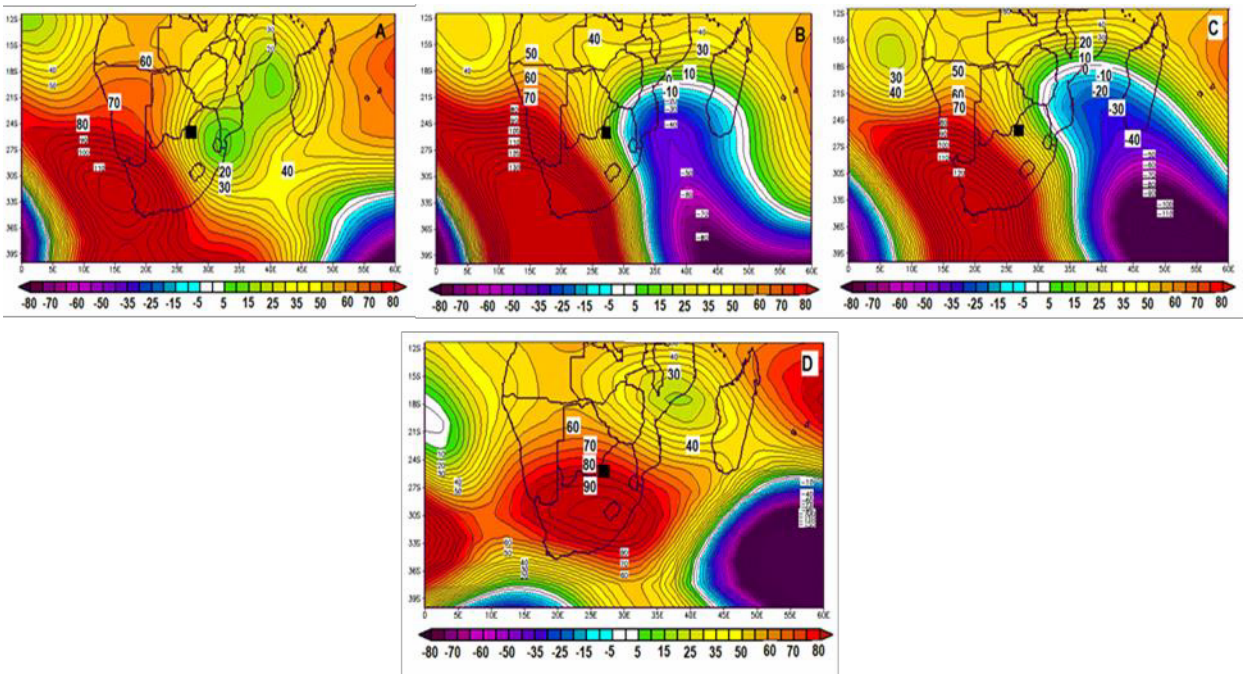

Figure 5.30: Anomalies of geopotential height (gpm) at 200 hPa over the North West province during the 3-day lasting heat wave in Taung from 5-7 December 2014. (A) - One day prior to the heat wave, (B) - during the first day of the heat wave, (C) - the composite of all of the heat wave days and (D) - a day after the heat wave cessation. Contours drawn at 5 m intervals.

The system of strong positive anomalies that occupied the SEAO, southern Namibia and western part of South Africa, which was observed in the last section (Figure 5.22), was maintained at the upper level (200 hPa). The systems featured a slight displacement to the west that gave way to the negative geopotential height to follow suit. In addition, a cell of closed strong positive anomalies over the interior were observed on the day after the heat wave (Figure 5.22D).

5.3.7 Mean Vector Winds – 850 hPa

Patterns of vector winds in the lower levels of the atmosphere during the evolution stages of the December heat wave are illustrated in Figure 5.23. In a day prior to, some light winds (≤ 4 ms^{-1} were observed over the entire sub-continent. On the onset day and heat wave days (Figure 5.23B, C), some westerly flow winds over the study area were diverted northward, leaving the study area with light winds < 4 $m.s^{-1}$. This is likely to result to an increased near-surface moisture advection in the study area. Over the SWIO, the incoming south easterlies make a curvature around the 30 – 40°E with a southward direction along the Mozambique Channel. Over Madagascar, some of these winds diverted cyclonically over the Indian Ocean. A counter-clockwise diversion over the sub-continent was observed as the southerly winds began to divert over the south of Mozambique.

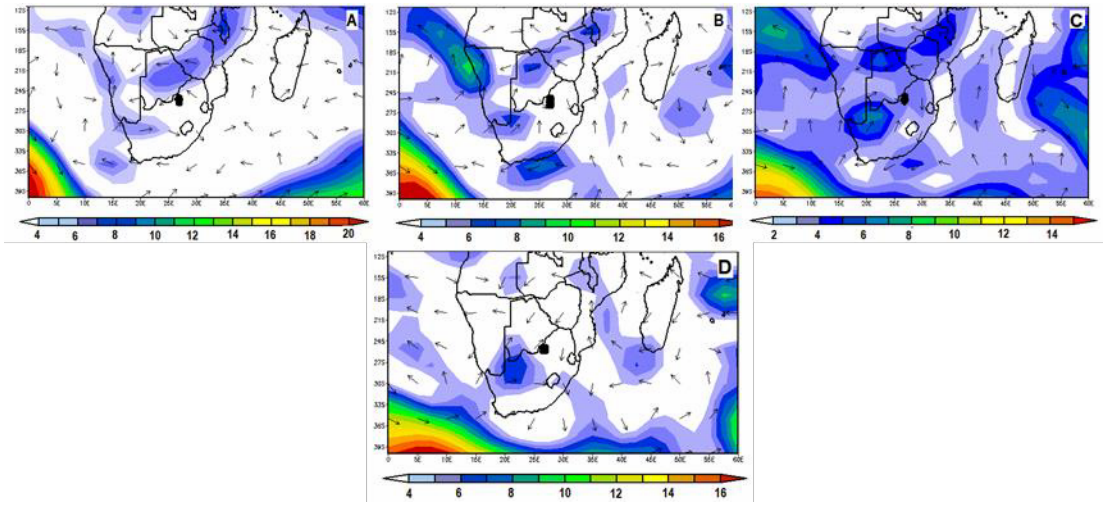

Figure 5.31: Mean vector winds (ms^{-1}) at 850 hPa over the North West province during the 3-day lasting heat wave in Taung from 5-7 December 2014. (A) - One day prior to the heat wave, (B) - during the first day of the heat wave, (C) - the composite of all of the heat wave days and (D) - a day after the heat wave cessation.

5.3.8 Vector Winds Anomalies – 850 hPa

Patterns of 850 hPa low level wind vector anomalies are presented in Figure 5.24. On the day prior to the onset of the heat wave, a flow with a magnitude of 6m.s^{-1} originating from the AO was observed coming through the west of South Africa right across the country to the IO. Strong divergence of winds with a magnitude of 6ms^{-1} over the study area were also observed during the heat wave days composite (Figure 5.24C). The continuous divergence of winds away from the area might likely transport moisture away as well. At the same, time a cyclonic flow over the Indian Ocean, was experienced. On the day of cessation, a convergence of westerly and easterly flow at about 30°E was observed, which then flowed southwards over the AO. In all stages, the NWP was under positive wind anomalies of 2-6ms^{-1}.

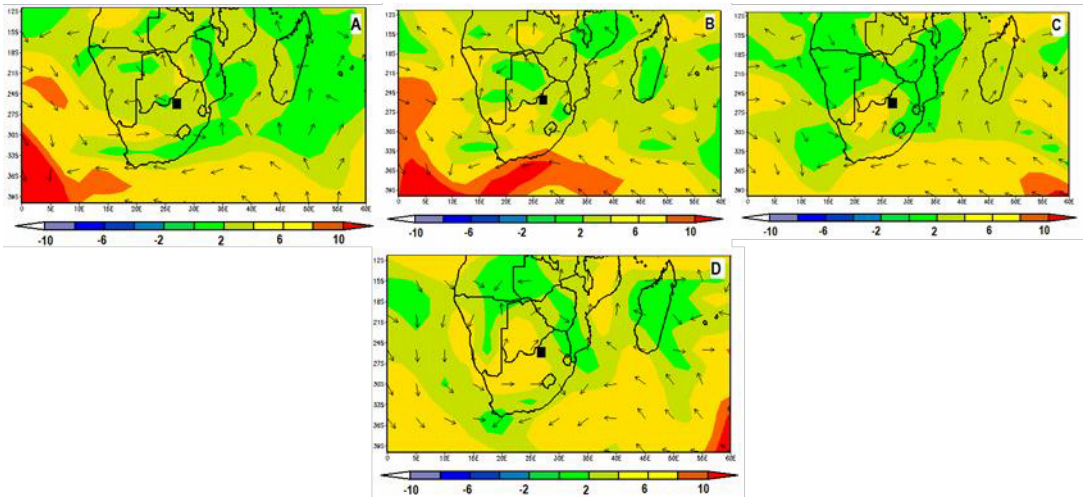

Figure 5.32: Anomalies of vector winds (ms^{-1}) at 850 hPa over the North West province during the 3-day lasting heat wave in Taung from 5-7 December 2014. (A) - One day prior to the heat wave, (B) - during the first day of the heat wave, (C) - the composite of all of the heat wave days and (D) - a day after the heat wave cessation. Contours drawn at 2 ms^{-1} intervals.

5.3.9 Mean Vector Winds – 200 hPa

A smooth parallel flow of the westerly winds were observed in Figure 5.25A with strong to storm winds of ~25 – 30 ms^{-1} over the study area. Light winds (< 10 ms^{-1}) were experienced over the Mozambique Channel, central sub-continent, and west of Atlantic Ocean. During the heat wave days (Figure 5.25C), a parallel flow of light winds over the study area was observed while along the southern parts of the Indian and Atlantic ocean, winds with a maximum magnitude of 40 ms^{-1} were maintained in all events (day

prior to, onset, composite of the heat wave days and on the day of the cessation). A westerly flow was observed over the study area for the entire observation period. This brought up the persistence of dry conditions over the study area as winds from the west are usually dry.

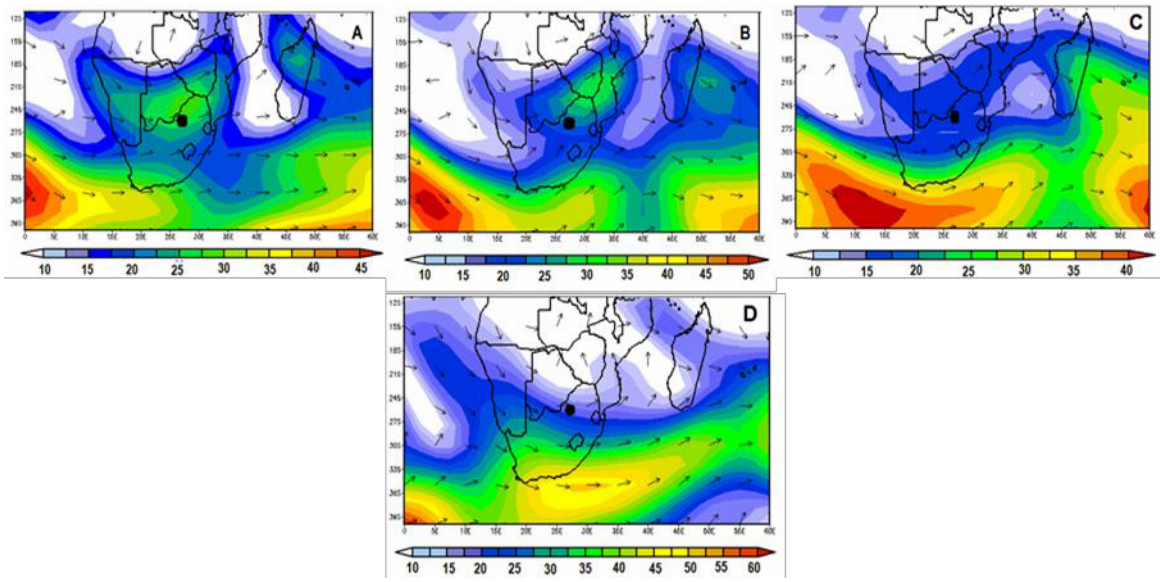

Figure 5.33: Mean vector winds (ms^{-1}) at 200 hPa over the North West province during the 3-day lasting heat wave in Taung from 5-7 December 2014. (A) - One day prior to the heat wave, (B) - during the first day of the heat wave, (C) - the composite of all of the heat wave days and (D) - a day after the heat wave cessation.

5.3.10 Vector winds Anomalies – 200 hPa

Upper level wind vector anomalies are presented in Figure 5.26. Over the north of Madagascar at about 12°S, wind anomalies of ≥ 10 ms^{-1} were evident a day before the start of the heat wave. These wind anomalies were part of the cyclonic flow that depicted a curvature from the south easterly to the south westerly over the study area. During the first day of the heat wave, a flow of ≥10 ms^{-1} magnitude from the SAO originating along the 20°E and 40°E entered through the south of South Africa, propagating further north and reaching the study area with the same magnitude. It passed the study area reaching Botswana, Zimbabwe and Mozambique through the Mozambique Channel. Over the western side of the subcontinent, an anticyclonic flow with a curvature over Namibia, was observed. Positive wind anomalies ≥ 10 ms^{-1} over the study area were maintained since the day prior to the start of the heat wave to the last day of the episode. A slight decrease, reaching a magnitude ≥ 6 ms^{-1} over the NWP, was observed during the day after the heat wave (Figure 5.26D).

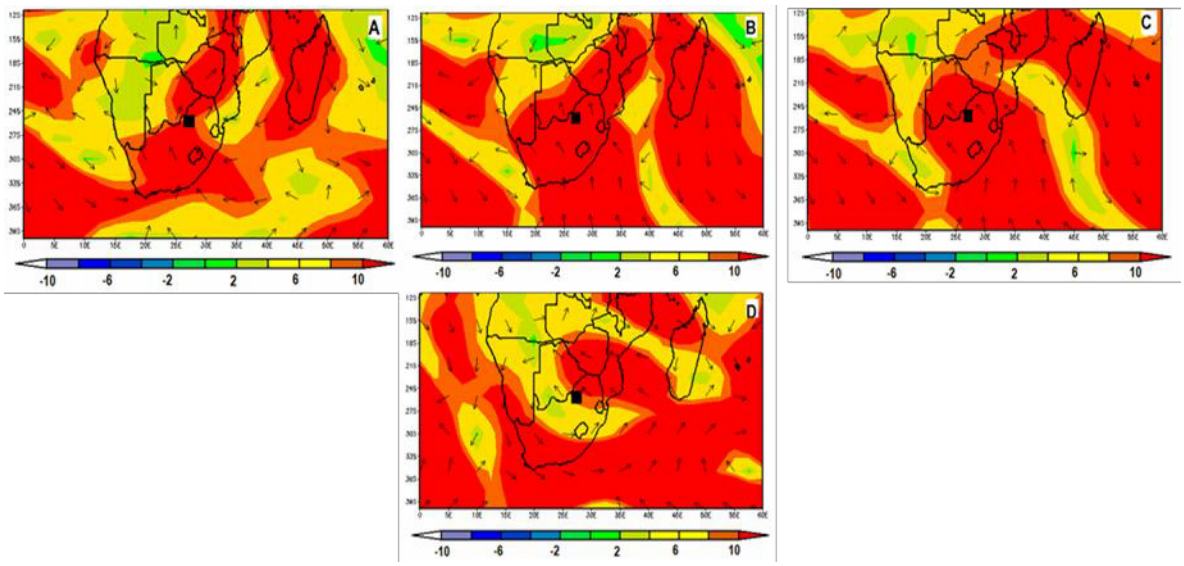

Figure 5.34: Anomalies of vector winds (ms^{-1}) at 200 hPa over the North West province during the 3-day lasting heat wave in Taung from 5-7 December 2014. (A) - One day prior to the heat wave, (B) - during the first day of the heat wave, (C) - the composite of all of the heat wave days and (D) - a day after the heat wave cessation. Contours drawn at 2 m s^{-1} intervals.

5.3.11 Mean Specific Humidity – 700 hPa

Conditions of humidity during the heat wave of December - 2014 are presented in Figure

5.27.

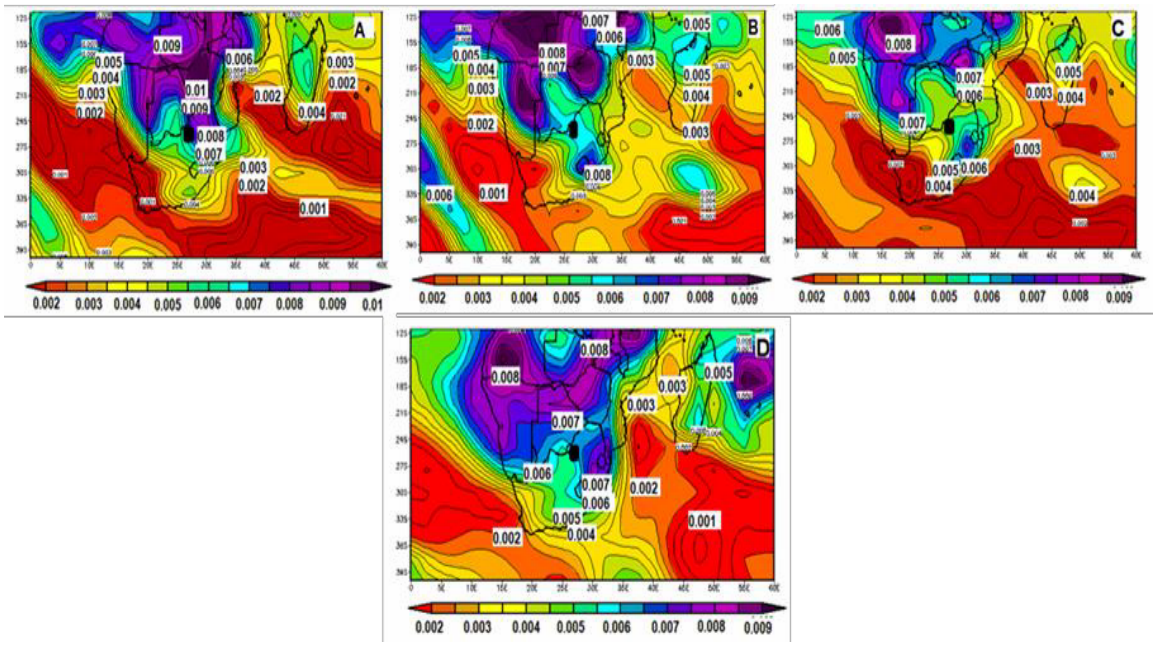

Figure 5.35: Mean specific humidity (g/kg) at 700 hPa over North West province during the 3-day lasting heat wave in Taung from 5-7 December 2014. (A) - One day prior to the heat wave, (B) - during the first day of the heat wave, (C) - the composite of all of the heat wave days and (D) - a day after the heat wave cessation.

It is shown that high levels of moist air (>5 g/kg) from the tropics moved further south, bringing mostly moist air over the north-eastern parts South Africa. Over the adjacent oceans, areas of low humidity were observed whereas over South Africa, a low humidity centre along the south Atlantic was situated over cape Peninsula.

5.3.12 Specific Humidity Anomalies - 700 hPa

Figure 5.28 presents the specific humidity anomalies during the December 2014 heat waves episode. In all stages presented (A, B and C), the study area experienced relatively low negative anomalies of the specific humidity (≤ -1 g/kg). This indicates that relatively little moisture was available during the heat wave evolution. Also worth mentioning is that the adjacent oceans depicted a dryer atmosphere except for some non-significant pockets, where the specific humidity anomalies were relatively greater than -2 g/kg.

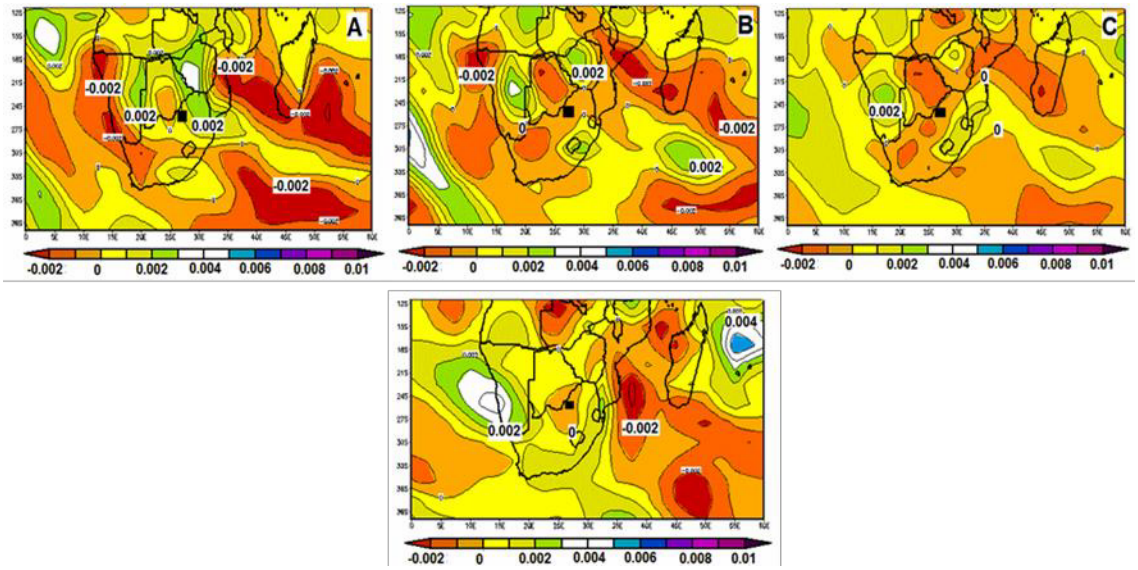

Figure 5.36: Anomalies of specific humidity (g/kg) at 700 hPa over the North West province during the 3-day lasting heat wave in Taung from 5-7 December 2014. (A) - One day prior to the heat wave, (B) - during the first day of the heat wave, (C) - the composite of all of the heat wave days and (D) - a day after the heat wave cessation. Contour intervals at 0.001 g/kg.

5.3.13 Mean Outgoing Longwave Radiation (OLR)

Deep convective areas were found north of the sub-continent in all stages of the heat wave episode. A day prior to (Figure 5.29A), large OLR values over land were found

over Namibia and extended to the northernmost part of the Northern Cape in South Africa. During the same period (stage), high values of OLR along the north Indian Ocean over the Mozambique Channel and east of Madagascar were also observed. During the onset (Figure 5.29B) and heat wave days (Figure 5.29C), OLR values over the study area had reached values of ~270Wm^{-2}. The day after the episode South Africa experienced significantly low OLR values with a centre value of 160 Wm^{-2}. Over the Mozambique Channel, values of >280 Wm^{-2} were maintained in all stages.

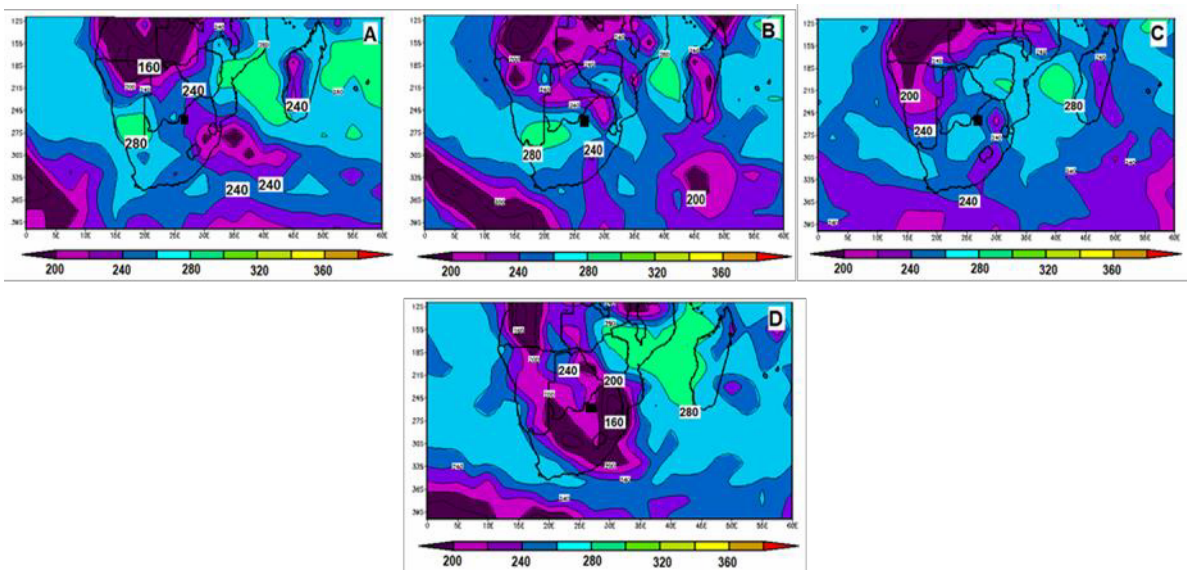

Figure 5.37: Mean Outgoing longwave radiation (OLR Wm^{-2}) over the North West province during the 3-day lasting heat wave in Taung from 5-7 December 2014. (A) - One day prior to the heat wave, (B) - during the first day of the heat wave, (C) - the composite of all of the heat wave days and (D) - a day after the heat wave cessation.

5.3.14 Outgoing Longwave Radiation (OLR) Anomalies

Outgoing longwave radiation anomalies for December 2014 heat wave are illustrated in Figure 5.30. One day prior to the beginning of the heat wave, areas of convective activity were found over the south of the Mozambique Channel, SAO and north of Namibia. A centre of strong subsidence was over Mozambique with values >40 Wm^{-2}. In this period, the study area observed weaker positive departures. During the onset day and heat wave composite days (Figure 5.30B & C), the study area received high OLR anomalies ≥ 20 Wm^{-2} which can be associated with clear skies. From this observation, it is evident that during the heat wave days (5th to 7th December 2014), the study area experienced three consecutive days of strong subsidence. On the day after the heat wave episode, most of South Africa, including the study area, experienced negative OLR anomalies.

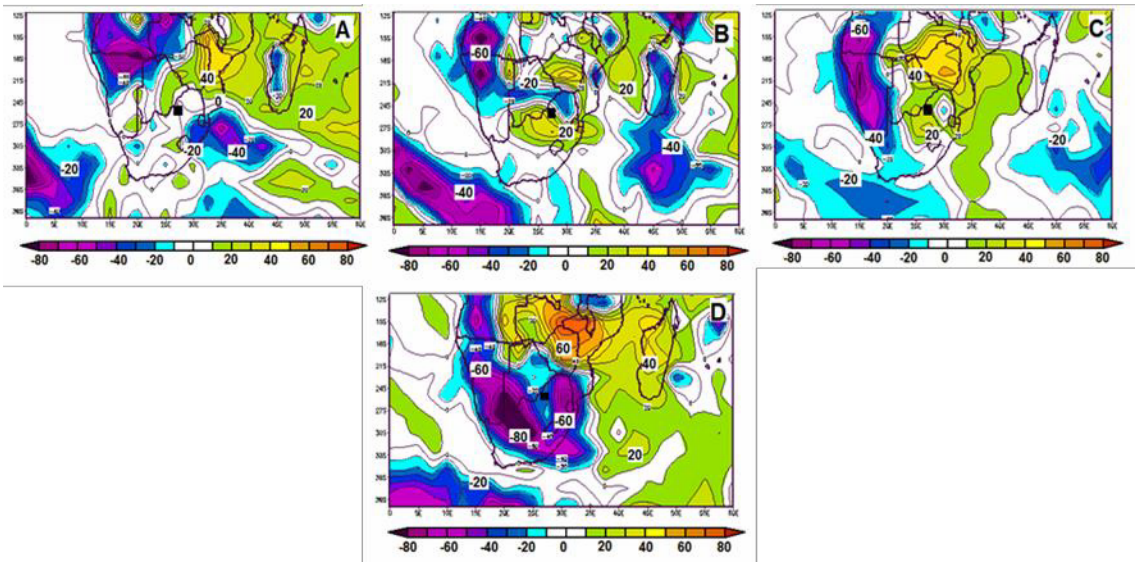

Figure 5.38: Anomalies of the Outgoing longwave radiation (OLR Wm^{-2}) over the North West province during the 3-day lasting heat wave in Taung from 5-7 December 2014. (A) - One day prior to the heat wave, (B) - during the first day of the heat wave, (C) - the composite of all of the heat wave days and (D) - a day after the heat wave cessation. Contour intervals drawn at 10 Wm^{-2}.

5.3.15 Mean Vertical Motion (Omega)

During the day before the initiation of the heat wave Figure 5.31A, the Atlantic Ocean represented an amplified subsidence with a tongue stretching across the southern Africa to the SIO. During the onset and composite days of the heat wave (Figure 5.31B &C), areas of sinking motion were observed along the Mozambique Channel extending to the northeastern part of South Africa, Botswana, Mozambique and Zimbabwe. The strong activity of this motion was centred over the south of Mozambique. Behind this pattern over the Indian Ocean, a rising motion was evident. The study area maintained a sinking motion in all stages of the heat wave development. This was not the case on the day of cessation, where a rising motion with a north-south orientation, passed through the NWP with a centre values ~ -0.09 Pa $s^{-1,}$ situated over Lesotho.

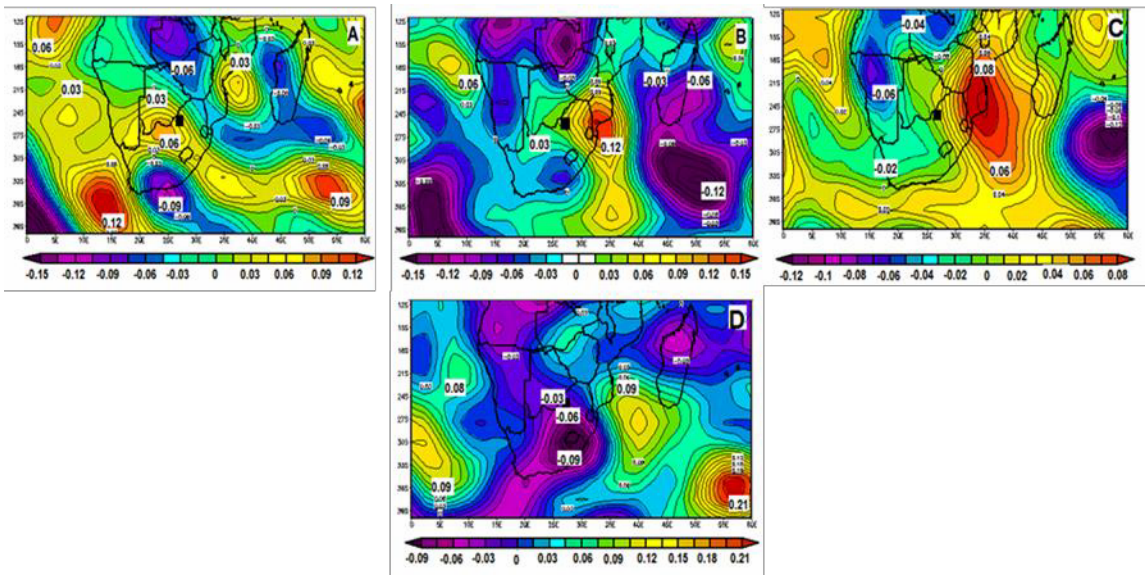

Figure 5.39: Mean vertical motion (Pa s^{-1}) over the North West province during the 3-day lasting heat wave in Taung from 5-7 December 2014. (A) - One day prior to the heat wave, (B) - during the first day of the heat wave, (C) - the composite of all of the heat wave days and (D) - a day after the heat wave cessation.

5.3.16 Vertical Motion Anomalies

Patterns of vertical motion anomalies are presented in Figure 5.32. A day before the start of the heat wave (Figure 5.32A), the scenario displayed a sinking motion with a magnitude of >0.06 Pa s^{-1} over the south of Namibia, Botswana and parts of South Africa. While areas of rising and sinking motion were also observed over the Indian Ocean whereas an area of strong rising motion was evident over the SAO. On the day of the heat wave, an area of sinking motion with a centre magnitude of 0.12 Pa s^{-1} was observed over the boarder of South Africa, Mozambique and the study area. Meanwhile, areas of a strong rising motion were found over the Atlantic and Indian Oceans, with a central magnitude of ~0.15 Pa s^{-1}. The composite days (Figure 5.32C), show that there was a continuous sinking motion during the three days (5^{th} and 7^{th} December 2014) of the event and over the east of the study area and Mozambique. The condition changed on the day after the event when the study area experienced some rising motion. Over the south eastern corner of the diagram (Figure 5.32D), a sinking motion with a central magnitude of 0.18 Pa s^{-1} was evident.

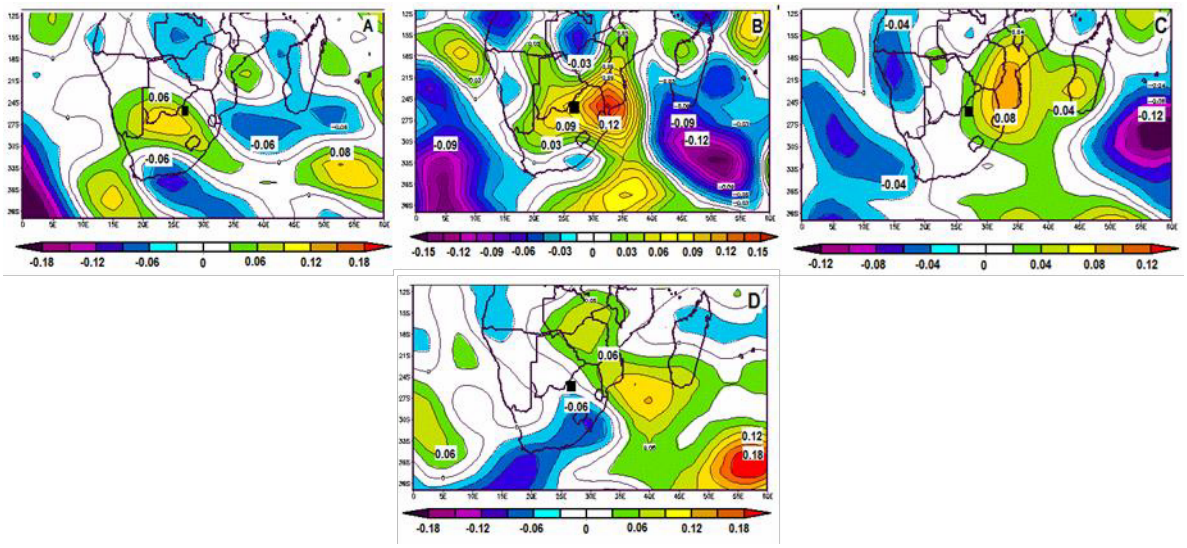

Figure 5.40: Anomalies of vertical motion (Pa s^{-1}) over the North West province during the 3- day lasting heat wave in Taung from 5-7 December 2014. (A) - One day prior to the heat wave, (B) - during the first day of the heat wave, (C) - the composite of all of the heat wave days and (D) - a day after the heat wave cessation.

5.4 Meteorological Parameter analysis: 3- 9 January 2016 heat wave in Taung

From the results analysis displayed in Table 4.1, the summer season of 2015-2016 January reported numerous and extreme heat wave events by more than half of the stations that featured in the analysis of this work. All the reported events in this season reached temperatures of >40°C, in different periods. The duration of events varied from 3 to 4 consecutive days in some area, while a single event that lasted for 7 days, was reported at Taung. Regardless of the duration of the heat event in Taung, the highest maximum temperature of 46°C during the entire season was reported by Tosca during its 3 consecutive days of heat wave.

5.4.1 Mean Geopotential Height – 850 hPa

A strong 850 hPa geopotential height for the January 2016 heat wave is presented, showing its evolution characteristics during this period. An anti-cyclonic flow from the south West Atlantic Ocean was visible proceeding into the country on the western side with a high pressure field of 1560 gpm (Figure 5.33A). Ahead of it and through the centre of the country, a trough was also observed. During the first day (Figure 5.33B), an 850 hPa pressure field intensified, creating another pressure field along the eastern side of the country, with its axis over Zimbabwe and central Mozambique. Because of these two pressure fields adjacent to the country, a trough in South Africa was formed. The study area was engulfed between these two adjacent high pressure cells and a

thus within a deep trough. The worth mentioning prominent patterns during this episode are the Indian Ocean Anti- cyclone (IOA), which persisted at the B, C, D stages and the Atlantic Ocean anti-cyclone (AOA), which was persistent at all the stages (A, B, C, D), though its intensity over land and ocean varied with time as the heat wave evolved.

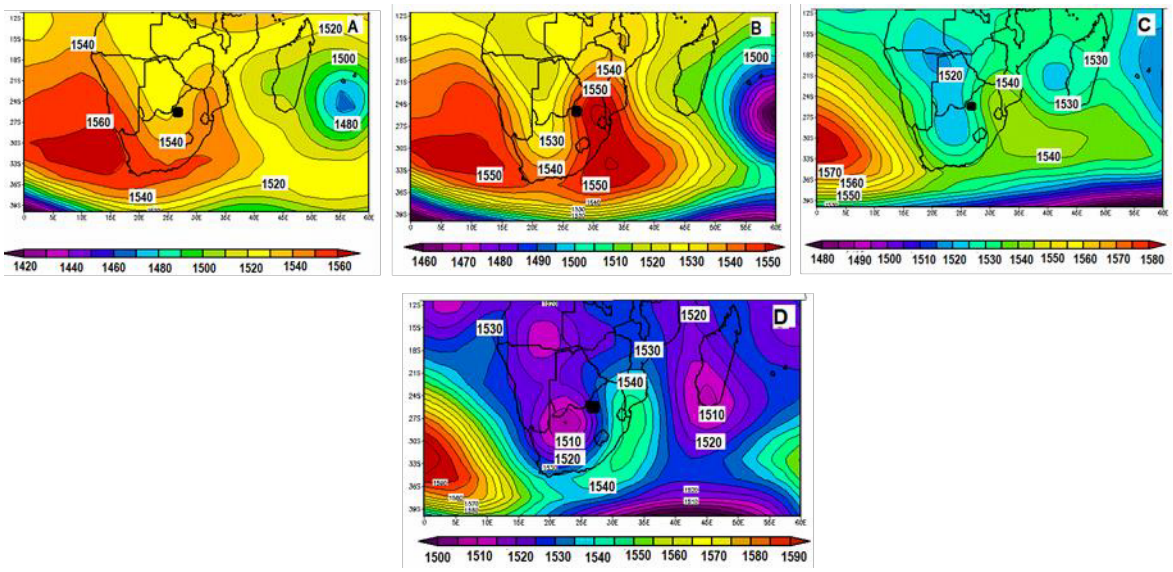

Figure 5.41: Mean geopotential height (gpm) at 850 hPa over the North West Province during the 7-day lasting heat wave (3-9 January 2016) over Taung. (A) One day prior to the heat wave, (B) during the first day of the heat wave, (C) the composite of all of the heat wave days and (D) a day after the heat wave cessation. Contours are drawn at 10 m levels.

5.4.2 Geopotential height Anomalies Lower – 850 hPa

Figure 5.34 represents some geopotential heights at 850hPa during the 2016 heat wave episode. On the day before the start of the heat wave, a centre of positive anomalies with a magnitude of 30 gpm was found on western part of the subcontinent and the immediate adjacent ocean. In Figure 5.34 A &B, a centre of falling pressures (> -40 gpm) was found over the Indian Ocean - south-east of Madagascar. During this period, the study area maintained positive height anomalies of ≤ 20gpm. The pattern of the composite days (Figure 5.34C), reveals that the positive geopotential height anomalies exerted over the subcontinent, including the study area, the AO and greater part of the IO.

On the day after the heat wave (Figure 5.34D), weaker negative geopotential anomalies were observed south of Madagascar in the Indian Ocean. The study area maintained weak positive geopotential anomalies.

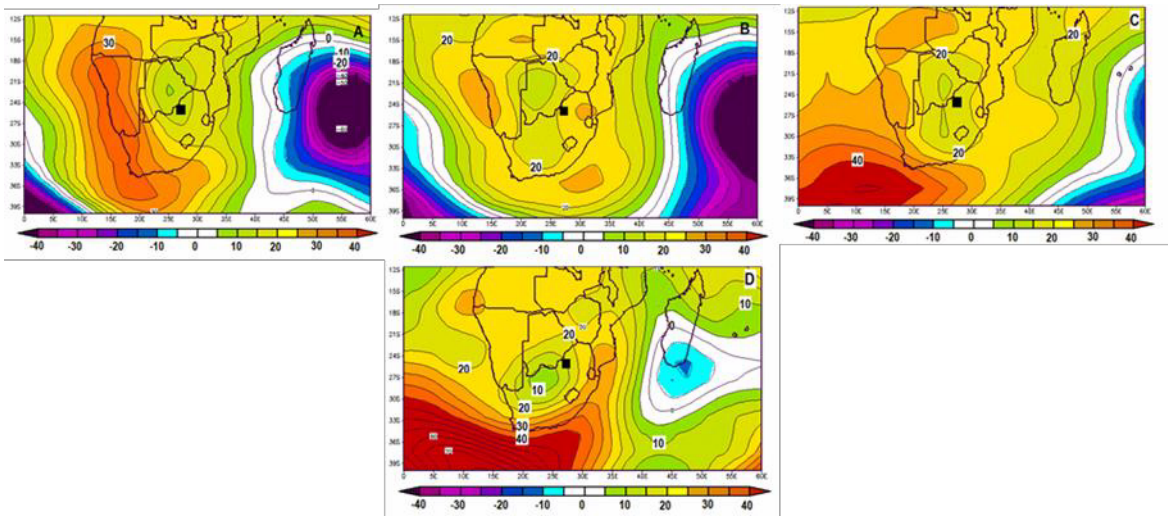

Figure 5.42: Anomalies of geopotential height (gpm) at 850 hPa over the North West Province during the 7-day lasting heat wave (3-9 January 2016) over Taung. (A) One day prior to the heat wave, (B) during the first day of the heat wave, (C) the composite of all of the heat wave days and (D) a day after the heat wave cessation. Contours drawn at 5 m intervals.

5.4.3 Mean Geopotential Height – 500 hPa

Figure 5.35 represents life stages of a 500 hPa geopotential height during January 2016 heat wave episode. Through all stages (A, B, C, D), a strong 500 hPa geopotential, extending from the Atlantic Ocean towards the continent, was observed with a centre high of 5940 gpm. A ridge over the adjacent landmass on the eastern side of the country, with its tongue extending over the north eastern side of the country in all developmental stages of heat wave event was evident. The noticeable weak pressure gradient over land was especially an encouraging slow movement of winds, which were mainly obstructed by the trough ahead, and that resulted to more blocking, clear skies and high surface temperatures.

The southward movement of a strong 500 hPa brought about some warm and dry conditions from the Kalahari Desert over the country, covering much of the western side of the study area. The development of the strong Atlantic Ocean anticyclone showed some spatial variations over the entire heat wave episode. During heat wave days (Figure 5.35C), its common oscillation was between 18 and 27°S and extending up to 30°E, with a centre high of 5940 gpm, and covering the areas of Mafikeng and Tosca that are among the stations that recorded strong heat waves during this period.

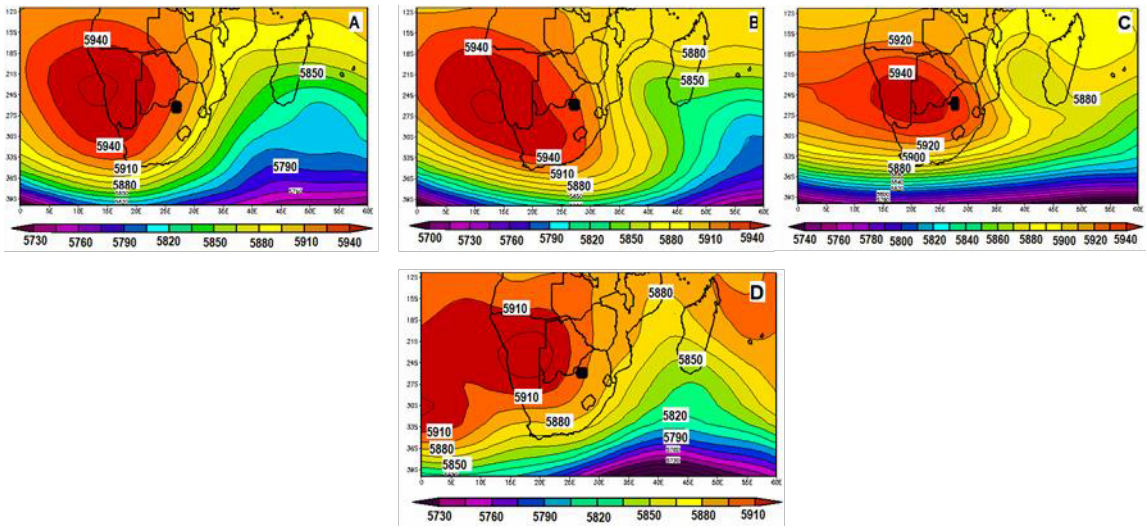

Figure 5.43: Mean geopotential height (gpm) at 500 hPa over the North West Province during the 7-day lasting heat wave (3-9 January 2016) over Taung. (A) One day prior to the heat wave, (B) during the first day of the heat wave, (C) the composite of all of the heat wave days and (D) a day after the heat wave cessation. Contours are drawn at 30 m intervals.

5.4.4 Geopotential height Anomalies – 500 hPa

Middle tropospheric geopotential height anomalies are presented in Figure 5.36. On the day prior to the onset and the start of the heat wave, an area of strong positive height anomalies with a magnitude ≥90 gpm were visible over the South Atlantic Ocean and south- western part of South Africa. Whilst a centre of negative height anomalies were visible over the IO, south east of Madagascar. During the composite days (Figure 5.36C), positive anomalies over the study area and other areas of South Africa intensified, reaching a maximum magnitude >60gpm. In this period, the Mozambique Channel and Indian Ocean (south east of Madagascar) observed relatively weaker positive heights of ≈20 gpm. On the day after the heat wave event (Figure 5.36D), geopotential heights over the IO, south of Madagascar, decreased to reach a centre magnitude of ≥ -15gpm. The NWP was still under positive height anomalies of ≤ 50 gpm. Strong positive anomalies over the SAO were still maintained.

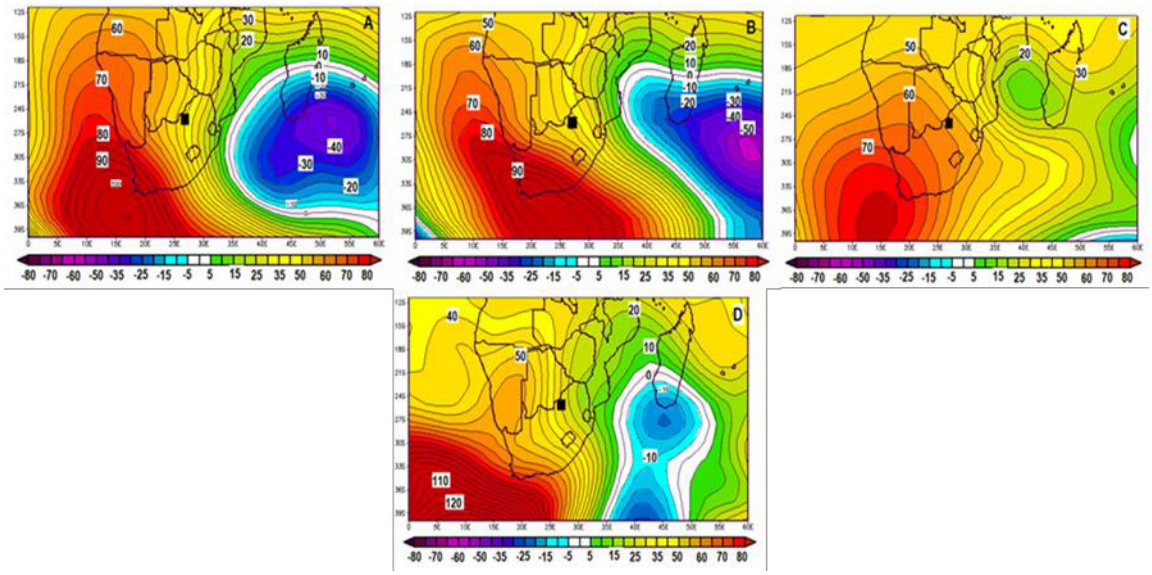

Figure 5.44: Anomalies of geopotential height (gpm) at 500 hPa over the North West Province during the 7-day lasting heat wave (3-9 January 2016) over Taung. (A) One day prior to the heat wave, (B) during the first day of the heat wave, (C) the composite of all of the heat wave days and (D) a day after the heat wave cessation. Contours drawn at 5 m intervals.

5.4.5 Mean Geopotential Height – 200 hPa

Figure 5.37 shows the development of the upper-tropospheric – 200 hPa geopotentials. An upper level - anti-cyclonic cell over Botswana with a centre high of 12550 gpm was at a developing stage at a day prior to and on the onset (Figure 5.37A and B) of a heat wave episode. During the heat wave days (C), it spread over the Atlantic Ocean on the western side, the central African countries and through Madagascar over the eastern side. A ridge ridging further south and an intensified trough over the central and eastern parts of the sub–continent were observed. A high subsidence over the area was highly to result from slow moving air from the west, blocked by the persistent trough over the Indian Ocean.

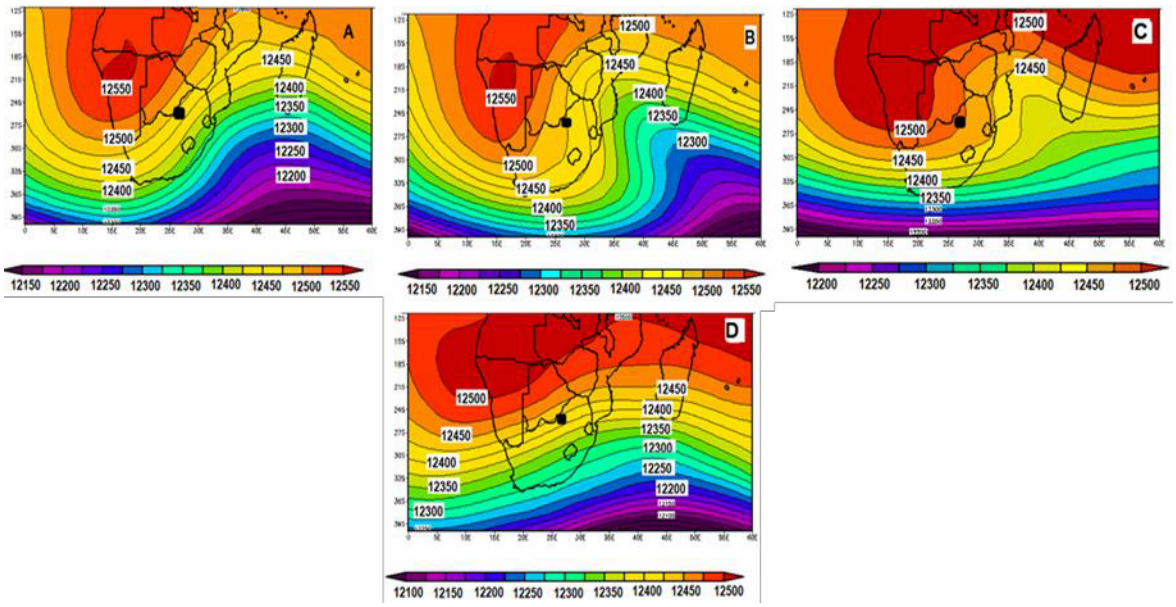

Figure 5.45: Mean geopotential height (gpm) at 200 hPa over the North West Province during the 7-day lasting heat wave (3-9 January 2016) over Taung. (A) One day prior to the heat wave, (B) during the first day of the heat wave, (C) the composite of all of the heat wave days and (D) a day after the heat wave cessation. Contours are drawn at 50 m intervals.

5.4.6 Geopotential height Anomalies– 200 hPa

Patterns of upper level geopotential height anomalies are illustrated in Figure 5.38. A day before the start of the heat wave, a high pressure system was visible over the south west coast of Southern Africa with a positive centre value of ≥120 gpm. While an area of falling pressures with a centre low of – 80 gpm was observed over the IO, south of Madagascar. During the heat wave onset, the positive geopotential anomalies from the Atlantic Ocean extended further inland to engulf almost half of South Africa. However, the study area was still experiencing weak positive anomalies. Patterns of the composite days in Figure 5.38C present increased positive geopotential heights over the IO. The observed patterns in the mid-tropospheric level during this period, are similar to the patterns of this 200 hPa level. That implies a continuous warming in the vertical structure of the atmosphere through the mid-high level. On the day after the event, the falling pressures from the IO, south of Madagascar, were visible and extending through south-eastern side of the subcontinent, reaching the study area as well. Also, a high pressure system over the SAO was maintained in all stages (Figure 5.38 A, B, C, and D).

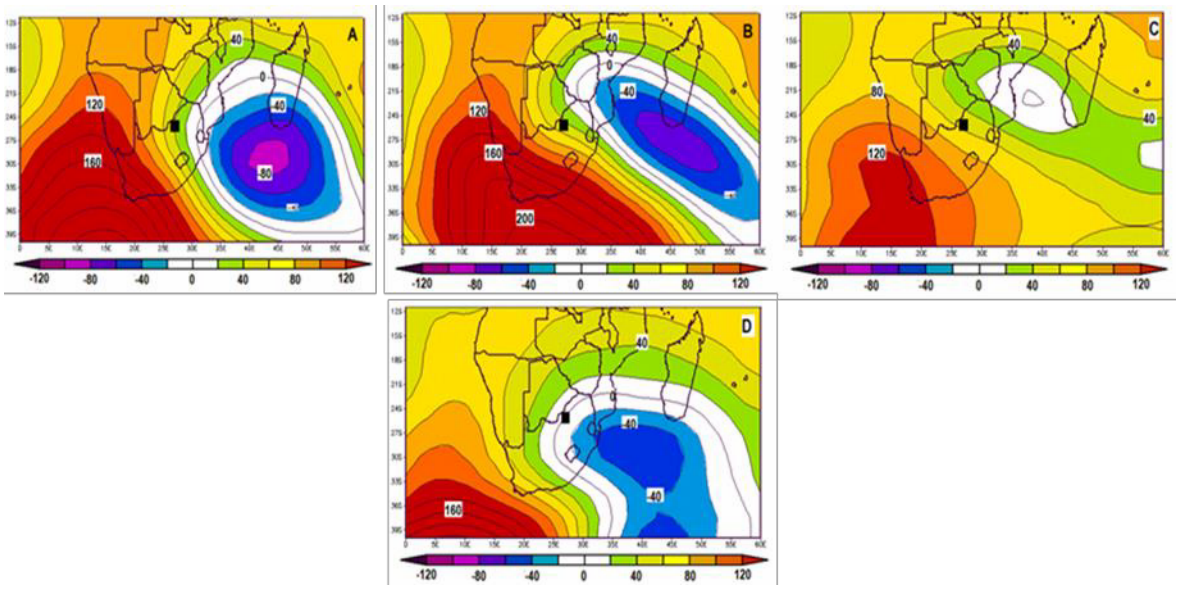

Figure 5.46: Anomalies of geopotential height (gpm) at 200 hPa over the North West Province during the 7-day lasting heat wave (3-9 January 2016) over Taung. (A) One day prior to the heat wave, (B) during the first day of the heat wave, (C) the composite of all of the heat wave days and (D) a day after the heat wave cessation. Contours drawn at 20 m intervals.

5.4.7 Mean Vector Winds – 850 hPa

Very light winds over the study area were observed one day before the beginning of the heat wave event. An anticyclonic flow of light winds over South Africa with a curvature along the SWIO was also evident during this very same onset (Figure 5.39B). Ahead of this curvature, winds of > 6 ms^{-1} magnitude over the Indian Ocean were also evident.

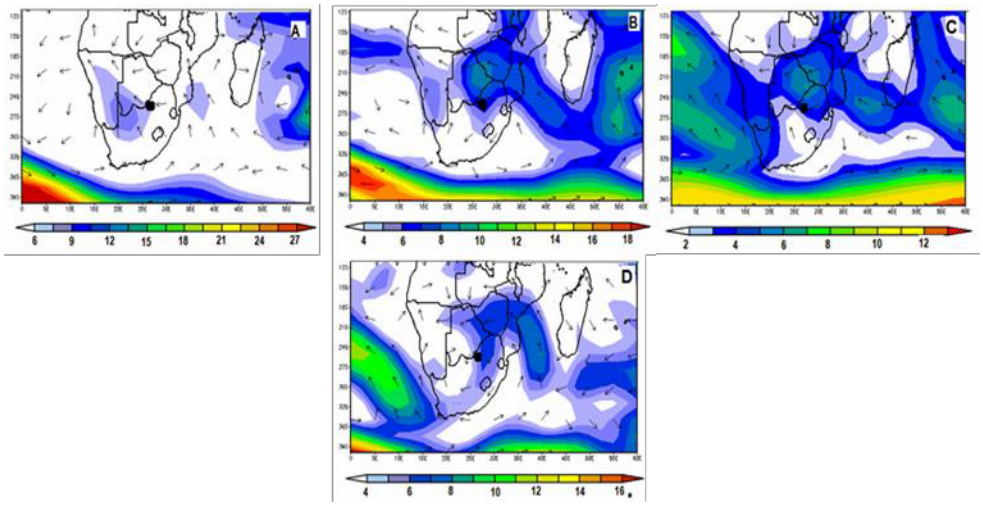

Figure 5.47: Mean vector winds (m s^{-1}) at 850 hPa over the North West Province during the 7-day lasting heat wave (3-9 January 2016) over Taung. (A) One day prior to the heat wave, (B) during the first day of the heat wave, (C) the composite of all of the heat wave days and (D) a day after the heat wave cessation.

Strong westerly winds were maintained along the south Atlantic Ocean to the SWIO at all stages. On the days of the heat wave episode (Figure 5.39C), the north easterly part of the area (NWP) experienced ≥ 4 ms^{-1} easterly winds.

5.4.8 Vector winds Anomalies – 850 hPa

Lower troposphere vector wind anomalies during the January heat wave are presented in Figure 5.40. In this Figure 5.40 (A & B), an anticyclonic flow of vector wind anomalies was observed over southern Africa; while a cyclonic flow was evident east of the Madagascar. Generally, this situation was observed in the vector wind anomalies patterns presented in Figure 5.42 and could infer areas of subsidence and the uplifting of air mass respectively.

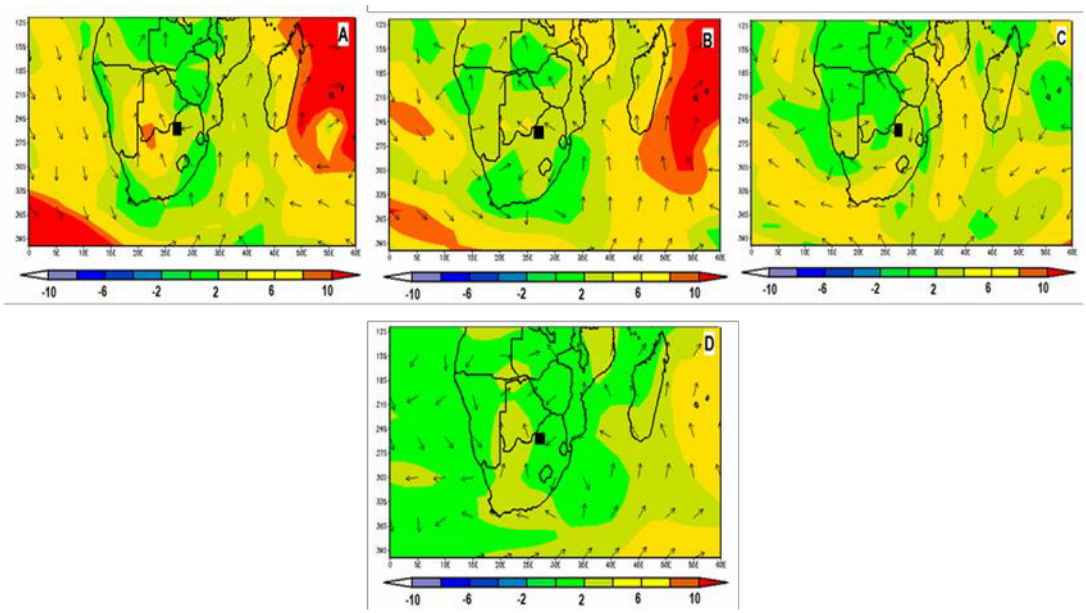

Figure 5.48: Anomalies of vector winds (ms^{-1}) at 850 hPa over the North West Province during the 7-day lasting heat wave (3-9 January 2016) over Taung. (A) One day prior to the heat wave, (B) during the first day of the heat wave, (C) the composite of all of the heat wave days and (D) a day after the heat wave cessation. Contours drawn at 2 ms^{-1} intervals.

5.4.9 Mean Vector Winds – 200 hPa

During the day prior to the onset of the heat wave, South Africa experienced a strong anticyclonic flow. Above 24°E, an inflow of strong southerly winds along the SWIO acted as a barrier of the incoming westerly winds, resulting them diverging counter-clockwise over the interior, leading to strong subsidence. On the first day of the heat episode

(Figure 5.41B), winds over the study area had decreased reaching values of ≤ 10 ms^{-1} . However, the previously observed anticyclonic flow was maintained up to the composite days of the heat waves (Figure 5.41 C). On the day of cessation, strong parallel westerly winds across the southern part of the sub-continent were observed while a curvature of low magnitude was situated over Angola.

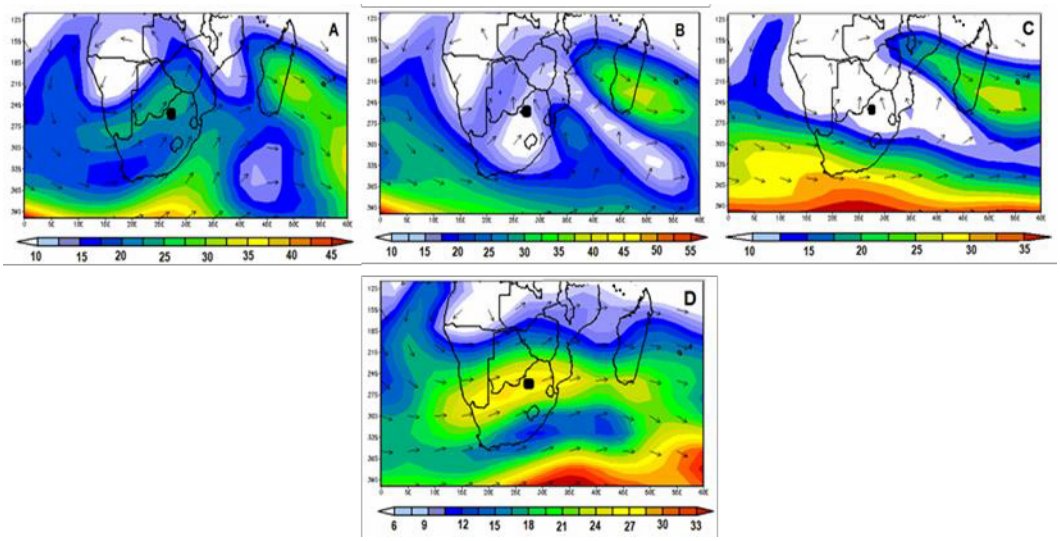

Figure 5.49: Mean vector winds (m s^{-1}) at 200 hPa over the North West Province during the 7-day lasting heat wave (3-9 January 2016) over Taung. (A) One day prior to the heat wave, (B) during the first day of the heat wave, (C) the composite of all of the heat wave days and (D) a day after the heat wave cessation.

5.4.10 Vector Winds Anomalies – 200 hPa

Patterns of vector wind anomalies at 200 hPa are shown in Figure 5.42. The day before the start of the heat wave revealed winds of ≥10 $m.s^{-1}$ over the southern Africa, including the study area. Also, Figure 5.42A presents a cyclonic gyre of vector winds from the south of the two Oceans (AO and IO) curving over Mozambique and back to the IO. On the first day of the heat wave, an anticyclonic flow with winds originating from the same area, was observed over South Africa, including the study area. During the composite days, the 200 hPa level wind vector anomalies portrayed a dominance of cyclonic flow over the study area with a magnitude of ~10 ms^{-1}. An inflow of positive vector winds from the IO to the study area was observed a day after the heat wave episode.

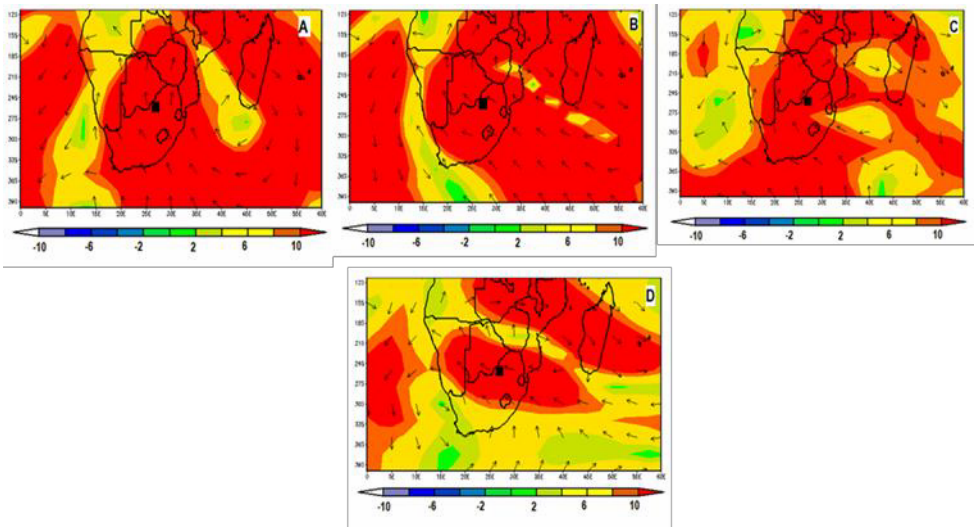

Figure 5.50: Anomalies of vector winds (ms^{-1}) at 200 hPa over North West Province during the 7-day lasting heat wave (3-9 January 2016) over Taung. (A) One day prior to the heat wave, (B) during the first day of the heat wave, (C) the composite of all of the heat wave days and (D) a day after the heat wave cessation. Contours drawn at 2 ms^{-1} intervals.

5.4.11 Mean Specific Humidity - 700 hPa

During the January 2016 heat wave, high levels of humidity existed over areas at the central part of the continent. These areas are known as the centre pool of humidity. The southward movement of this high moisture centres resulted into increased levels reaching 9g/kg specific humidity over the centre of the NWP during this period (Figure 5.43 A and B). A prominent decrease of humidity levels with latitude was also observed at all stages. Regardless of this and at the tropics, higher values of around 9 g/kg (prior to and during the onset), 7 g/kg, 8 g/kg during and after respectively of heat wave episode were maintained.

Low levels of dry air engulfed the country along the eastern, western and southern parts prior to, during and after the period of the heat wave. Along the north eastern side, dry air of around 3 g/kg from the Mozambique Channel emanated the north eastern part of the country during the heat wave episode (Figure 5.43C). This appeared to dry up the north eastern part of South Africa, resulting into a slight decrease in humidity levels to about 6.5 g/kg. Also, the same atmospheric conditions from the South Atlantic Ocean dominated parts of the Western Cape, Northern Cape and Eastern Cape provinces with humidity levels reaching a low of 2g/kg. The prominent pattern during this period was the strong influx of moisture, whose centre high was mainly situated over the tropics. This brought about high humid conditions in the range of 6 to 9 g/kg over the NWP.

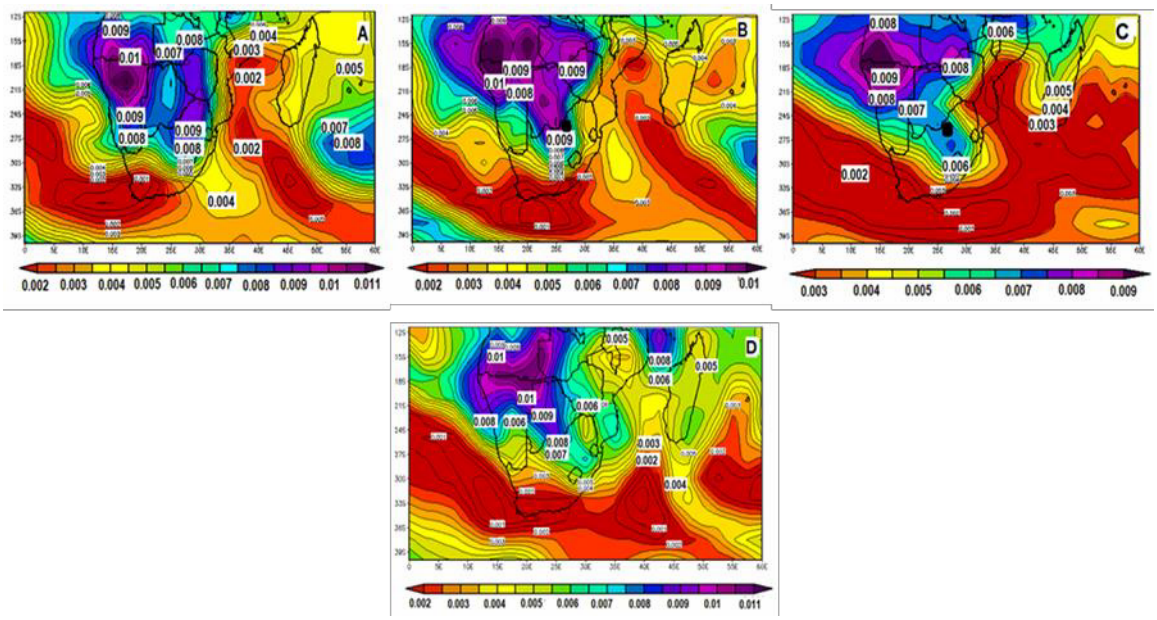

Figure 5.51: Mean specific humidity (g/kg) at 700 hPa over the North West province during the 7-day lasting heat wave (3-9 January 2016) over Taung. (A) One day prior to the heat wave, (B) during the first day of the heat wave, (C) the composite of all of the heat wave days and (D) a day after the heat wave cessation.

5.4.12 Specific Humidity Anomalies - 700 hPa

Specific humidity anomalies for the Jan 2016 heat wave are illustrated in Figure 5.44. In this Figure (A), most areas of the subcontinent including the study area, experienced positive anomalies (moisture increase), with two centre cells - one over Namibia and the other one over the northernmost part of Limpopo in South Africa. Between these two centres is the study area with positive anomaly values of around 2g/kg. Areas with a negative specific humidity were found over Mozambique, the Mozambique Channel, south of Madagascar and the SAO in both stages (A and B) – this could be inferred to mean that the atmosphere over those areas was dry. During the beginning of the heat wave, the moisture deficiency over the Mozambique Channel extended to cover most of the eastern side of the subcontinent. The composite of heat waves showed a moisture deficiency over the north-eastern side of the study area while adequate moisture was found over the western side. A day after the heat wave event, depicted an increase in moisture to the study area from south of Botswana. The AO, IO and some parts of the southeast of South Africa, experienced patches of negative anomalies, which implied that dryness prevailed.

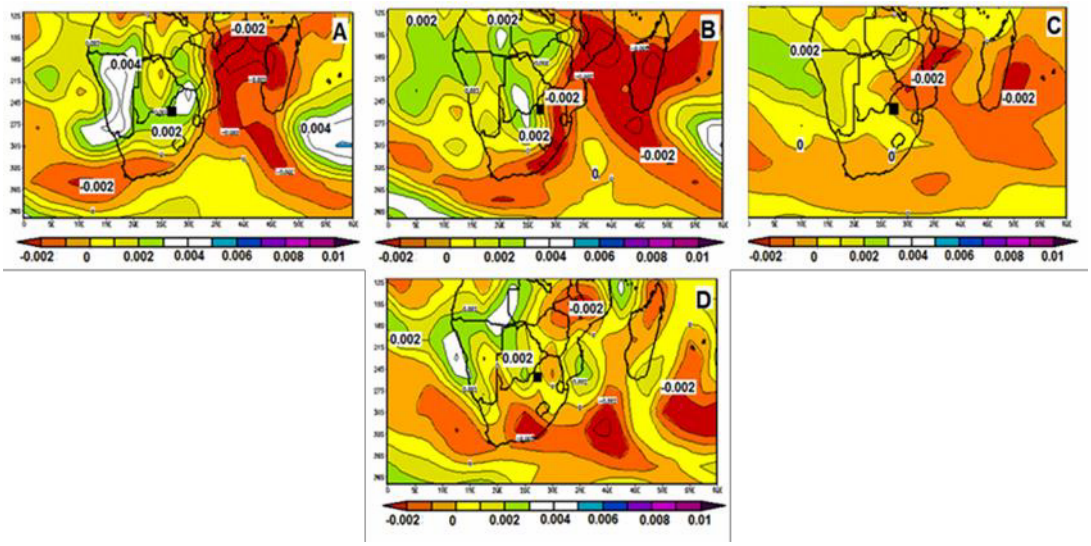

Figure 5.52: Anomalies of specific humidity (g/kg) at 700 hPa over the North West province during the 7-day lasting heat wave (3-9 January 2016) over Taung. (A) One day prior to the heat wave, (B) during the first day of the heat wave, (C) the composite of all of the heat wave days and (D) a day after the heat wave cessation. Contours are drawn at 0.001 g/kg.

5.4.13 Mean Outgoing Longwave radiation (OLR)

Outgoing longwave radiation (OLR) values for the January 2016 heat wave episode are presented in the Figure 5.45. Areas of strong subsidence were evident above the two adjacent Oceans (Indian and Atlantic Ocean). While a region of deep convection was cantered over Angola, stretching towards Madagascar on the eastern side and to parts of the Atlantic Ocean on the western side. A day prior to the episode, the study area had OLR values ~ 240 Wm^{-2}. During the onset of (Figure 5.45 B) and days of the heat wave episode (Figure 5.45C), the condition changed, OLR reached higher values of ~ 280 Wm^{-2}. A slight decrease in the OLR values were observed on the north eastern part of the province after the heat wave event but a significant subsidence still remained in some parts of the whole country and along the adjacent oceans.

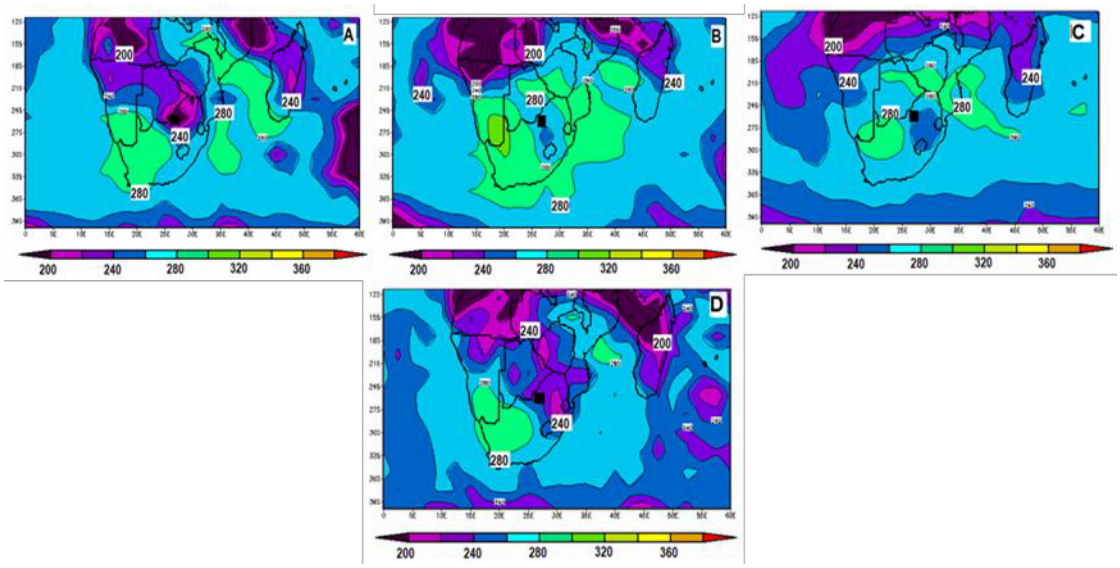

Figure 5.53: Mean Outgoing longwave radiation (OLR Wm^{-2}) over the North West province during the 7-day lasting heat wave (3-9 January 2016) over Taung. (A) One day prior to the heat wave, (B) during the first day of the heat wave, (C) the composite of all of the heat wave days and (D) a day after the heat wave cessation.

5.4.14 Outgoing Longwave radiation (OLR) Anomalies

Patterns of OLR anomalies for the January 2016 heat wave are displayed in Figure 5.46. In this Figure (A), areas of the positive OLR anomaly were found over Zambia, Mozambique and Zimbabwe with a centre value of 80 Wm^{-2}. In this period, the study area maintained weak negative (convective) anomalies of ~-40 Wm^{-2}. During the beginning of the heat wave, the greater part of South Africa, including the study area, experienced some increased OLR values. While areas of convective activity were found over Angola and Namibia with a centre magnitude of ~80 Wm^{-2}. As is shown in Figure 5.46C (composite days), the study area, the Mozambique Channel and parts of the IO were under high OLR values with a maximum magnitude >45 Wm^{-2}. Negative OLR values of ~10 Wm^{-2} over the study area were observed the day after the heat wave event. The most noticeable pattern observed from stages A to D in this period is the persistence of a centre of positive anomalies over Mozambique, Zambia and Zimbabwe.

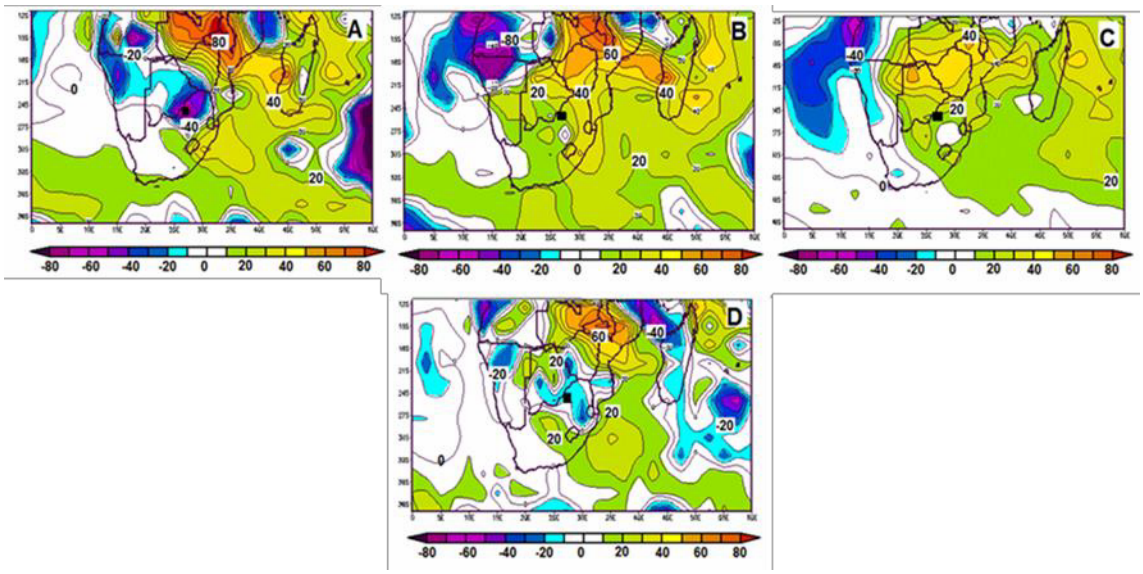

Figure 5.54: Anomalies of outgoing longwave radiation (OLR Wm^{-2}) over the North West Province during the 7-day lasting heat wave (3-9 January 2016) over Taung. (A) One day prior to the heat wave, (B) during the first day of the heat wave, (C) the composite of all of the heat wave days and (D) a day after the heat wave cessation. Contour intervals drawn at 10 Wm^{-2}

5.4.15 Mean Vertical Motion (Omega)

Vertical velocity patterns for the January 2016 heat wave episode are presented in Figure 5.47. On a day prior to the onset of the heat wave (Figure 5.47A), an amplified sinking motion was observed over the entire southern Africa and the adjacent oceans with centre values of 0.05 Pa s^{-1} . A descent motion from the AO, crossing the southern Africa in a west eastern orientation was evident during the onset day. Areas of ascent were depicted over Namibia and the Channel with -0.03 Pa s^{-1} and -0.06 Pa s^{-1} magnitudes respectively. During the composite days of the heat wave, the rising motion over the tropics extended eastward, emerging with that over the channel. Along south of the southern Africa, another centre of ascent was evident. However, the study area was still under weak subsidence. A relatively strong subsidence during this period was observed over the SOA. On the day of cessation, a sinking motion over the SOA, Namibia, and Indian Ocean is presented by distinct areas of the descent cells. The area of decent situated over Botswana, extended further south, reaching the NWP, and resulting into a sinking motion over the study area with values of 0.03 Pa s^{-1}.

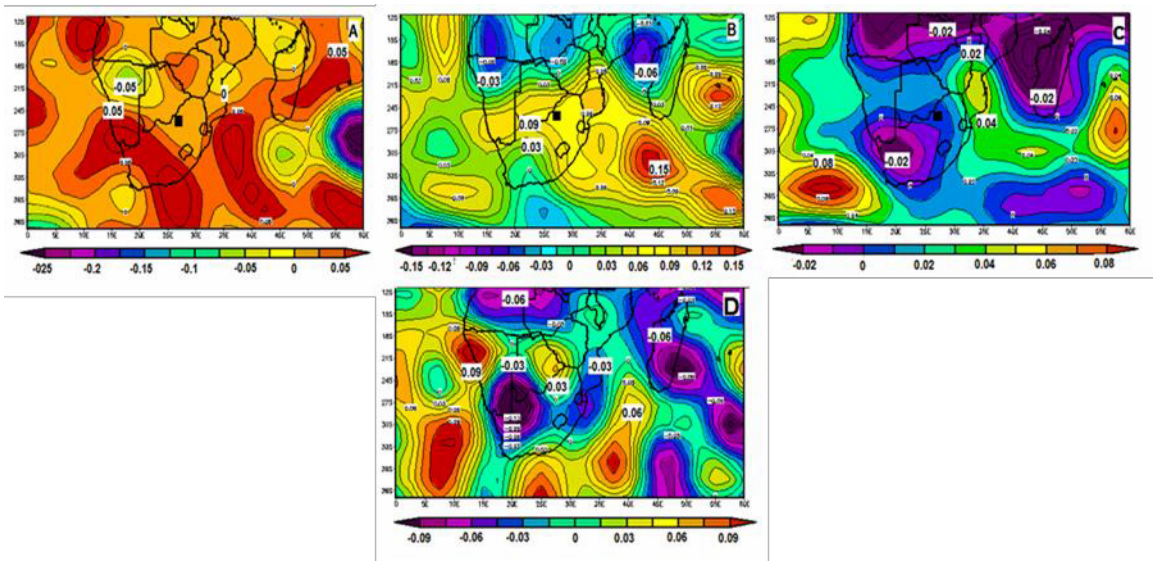

Figure 5.55: Mean vertical motion (Pa s^{-1}) over the North West province during the 7-day lasting heat wave (3-9 January 2016) over Taung. (A) One day prior to the heat wave, (B) during the first day of the heat wave, (C) the composite of all of the heat wave days and (D) a day after the heat wave cessation.

5.4.16 Vertical Motion Anomalies

Patterns of vertical motion for the January 2016 heat wave event are illustrated in Figure 5.48. The day before the start of the heat wave displayed a tongue of weak rising motion with a northwest-southeast orientation passing through the study area with its centre high over Namibia. Another centre of strong rising motion was found south of Madagascar (Figure 5.48A) but this was displaced by a sinking motion during the beginning of the heat wave (Figure 5.48B). The study area and other areas over the subcontinent also observed a sinking motion during this period. The composite pattern (Figure 5.48C), represent two areas of strong sinking motion with a magnitude of ≥0.6 Pa s^{-1} over the IO, south east of Madagascar and one over Mozambique and Zimbabwe, with a centre value ≥0.4 Pa s^{-1}. Also, strong positive OLR anomalies over Zimbabwe and south of Madagascar were observed. This situation then corresponded to the sinking motion also observed over this area.

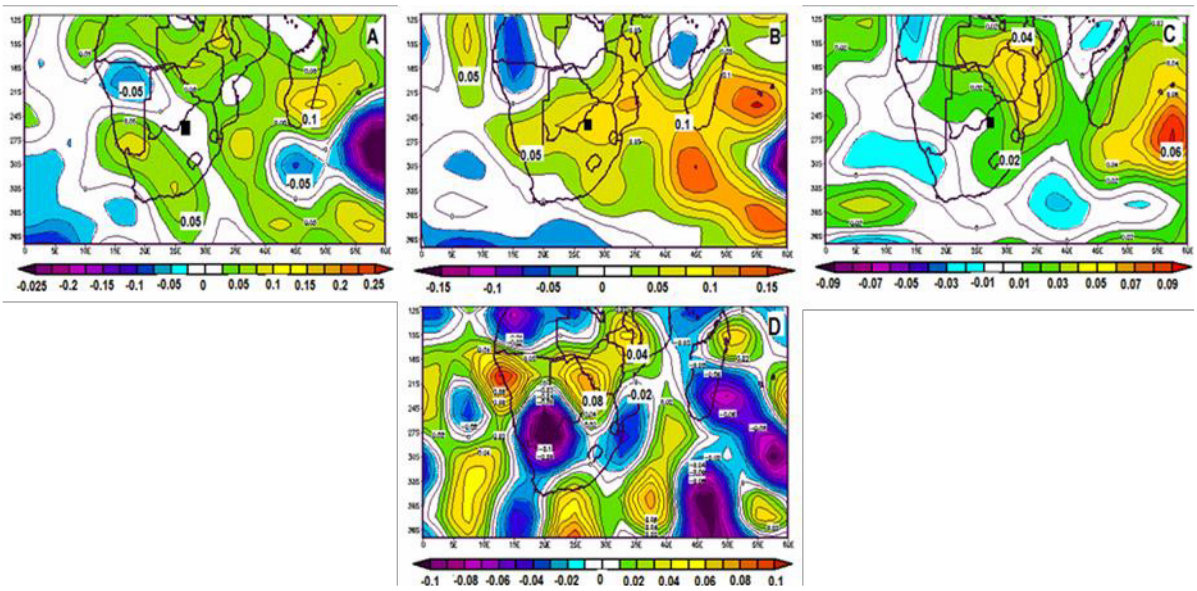

Figure 5.56: Anomalies of vertical motion (Pa s^{-1}) over the North West province during the 7-day lasting heat wave (3-9 January 2016) over Taung. (A) One day prior to the heat wave, (B) during the first day of the heat wave, (C) the composite of all of the heat wave days and (D) a day after the heat wave cessation.

5.5 Chapter Summary

5.5.1 Mean Atmospheric Patterns

In this chapter mean meteorological patterns for 2015 and 2016 heat wave episodes were presented using NCEP/NCAR reanalysis data. At lower geopotential height levels (850hPa) along the west of South Africa, an Atlantic Ocean Anti-cyclonic (AOA) circulation was dominant in all heat wave episodes. While along the south east of southern Africa an Indian Ocean anticyclone (IOA) was maintained. The other observed pattern in this level was the trough situated above the sub-continent. Over the study area, this had a negative influence as it blocked the passage of the incoming westerly winds which are usually warm and dry. A clear view of this flow is presented during a composite of heat wave days (C) in all episodes. Maximum fields of geopotential height at 850 hPa were observed along the centres of AOA and IOA. During the 2015/16 January heat wave episode, of worth mentioning and observed pattern in the low-level geopotential is the deep trough over the interior. The trough was intensified by the existence of strong AOA and IOA that engulfed the country.

Mid – tropospheric level height analysis has shown a strong persistence of geopotentials reaching a maximum of 5900m, 5910m and 5940 m height contours originating from the western side of the sub-continent over Atlantic Ocean. This also suggests that another factor associating heat waves with persistent high and associated anticyclonic flow in the middle troposphere causing descending motion, which leads to surface warming. At the upper level (200hPa), the similar patterns that prevailed at 500hPa were observed. This suggests that within the vertical profile from mid to higher level there is persistence of higher geopotentials. A hanging trough over Mozambique Channel, which is observed in mid and upper mean geopotential levels, reduced the speed of westerly winds.

The analysis of wind motion showed patterns where wind was blowing away and to the study area. However many cases had revealed the anticyclonic curvature above different areas in the interior including the study area. This fairly suggests slow movement of warm westerly wind in the mid and lower levels in the area due to less notable physical features. Due to this effect, these winds tend to slow down as they pass the area. Because they are warm and dry, the longer they take to pass the area, they result to increase surface warming.

Areas of high humidity were found to be in the tropics, while over the oceans low humid levels were dominant. The high levels of humidity were found to decrease with latitude,

this resulting in an inflow of relatively high humidity values to the study area. In this regard, it was speculated that the humidity content increase over NWP was in response to temperature rise and that the majority of this humidity was supplied from the tropics. Patches of higher OLR values (>260 W/m^{-2}) over the adjacent oceans and the continent were observed. The higher OLR values over these areas suggests dry atmospheric conditions and possibly less or no clouds. In addition, the sinking motion, which is detected at geopotential height analysis, has a significant role on the increased OLR values over the study area.

The overall analysis of vertical motion displays significant descent motion over the entire observation area (subcontinent and adjacent oceans) on the day prior to the November heat wave episode. Another observed pattern that occurred in all heat wave episodes is the southward deposition of rising motion from the tropics. Nevertheless, the NWP remained under descent motion throughout the development stages of all heat wave episodes. The possible contributing factor of sinking motion over the study area observed during these episodes is the existence of descent motion along the Mozambique Channel and SWIO. As stated by Cook *et al*. (2004) the Indian Ocean acts as the major source of moisture over southern Africa. The existence of persistent sinking motion over the Indian Ocean implies insufficient moisture transported to the continent especially the northeast of South Africa where it could easily reach the NWP.

5.5.2 Atmospheric Anomalies summary

Meteorological anomalies of the selected atmospheric parameters were analysed and the heat wave occurrences of different periods were inferred. Three episodes of severe heat waves were considered - they include November, December (2015) and January (2016). Unique Patterns of atmospheric anomalies were observed on individual heat waves and some were common on all the heat waves as shown in Table 5.1 where atmospheric anomalies that prevail on the first day of the heat wave is indicated as B and the composite days as C.

Table 5.3: Atmospheric circulation anomalies during heat wave days over the study area

Months	Heat wave Days	Geopotential Height (gpm)			Vector Winds ($m.s^{-1}$)		Specific Humidity (g/kg)	OLR (Wm^{-2})	Vertical Motion (Pa s^{-1})
		850 hPa	500 hPa	200 hPa	850 hPa	200 hPa			
NOV	B	10	>40	>80	≤2	>10	~-2	~30	>0.03
	C	-10	~35	~55	>2	>2	≥-1	10 - 20	>-0.02
DEC	B	10	>40	25	~4	≥10	≤-1	≥20	~0.05
	C	5	>40	25	6	≥10	≤-1	≥20	≥0.04
JAN	B	≤20	>60	60	4	≥10	2	30	0.05
	C	≤20	>60	60	4	≥10	2	30	0.03

More importantly, the investigation in this chapter has revealed the following:

- During the three heat wave episodes, the clear skies over the study area-manifested positive OLR anomalies (≥10 Wm^{-2}). The areas of large magnitude were over Zimbabwe, Mozambique and Zambia.
- On average, all heat wave episodes, there was evidence of subsidence given by positive vertical motion anomalies. It was only during the November episode, where rising motion (>-0.02 Pa s^{-1}) was observed and it corresponded with falling pressures (- 10gpm) at 850hPa level.
- During November and December heat wave episodes, specific humidity anomalies (≤ -1 g/kg) indicated deficiency of moisture over the study area. In January however, positive moisture anomalies prevailed throughout the period of heat wave over the study area.

CHAPTER 6

Summary and Conclusions

6.1 Introduction

The overall objective of this research was to study the climatology of heat waves in the NWP. To accomplish this aim, the following tasks were undertaken in the respective chapters: Chapter 1 entailed the overview of the study, aims and objectives and description of the study area and the motivation for the study. Inclusive of Chapter 2, is the review of the literature, focusing on the local and global extreme temperatures, heat wave background and future expectations on extreme temperatures. Chapter 3 described the basic research plan, data sets used, their sources and specific use in this study as well as the statistical analysis techniques employed. Among the specified objectives of this study was the temporal and spatial analysis of heat waves, and finding the association of heat wave recurrent characteristics in relation to large scale/global circulations. The results of these objectives were then provided in Chapter 4. Chapter 5 dealt with analysing the synoptic-scale atmospheric circulation characteristics associated with the occurrence of heat waves by employing the NCEP/NCAR reanalysis data. Chapters particularly four and five provided the original work of this study and each of those chapters included a concerted summary.

6.2. Summary of Important Findings

6.2.1 Maximum temperatures in North West Province

This study has identified austral summer (September to March of the following year) as the period of heat wave occurrence. The temporal variations of maximum temperatures presented high seasonal variability, where a number of below normal and above normal seasonal levels tended to follow each other. Extreme maximum temperatures have persisted since 2011 and climaxed in the 2015 season that ended in March 2016. The highest maximum temperatures (>40°C) were registered in January 2016 at most stations used in the study, registering the highest number of heat waves in the recorded history. Generally, 2014-2016 summer seasons reported the most pronounced heat waves with the highest maximum temperatures observed. The trend of increasing heat waves and temperatures observed in the North West province corresponds to the results of New et al. (2006) and Kruger and Sekele (2013).

6.2.2 Heat waves in North West Province

The study has identified 25 heat wave events at stations in the North West province. From the period of analysis, the longest heat wave was registered in Taung in January 2016 and lasted for 7 days. At the same period, a heat wave with an intensity of 46°C

was recorded in Tosca. The results of this study have corroborated quite well with other previous research findings that in a future warming climate, with increasing mean temperatures, heat waves will not only become more frequent but also their duration and intensity are very much likely to intensify (e.g., Min *et al*., 2011; Coumou & Rahmstorf, 2012 & IPCC, 2013).

With respect to frequency among the 13 stations analysed, 6 of them experienced at least one heat wave event for the study period. The maximum occurrence was experienced at two stations, Tosca with 4 events and Marico with 5 events. The data has also shown that the occurrence of heat waves in the North West province are spatially variable. A heat wave recoded at one station does not mean that other stations in the province will also experience the same conditions. Stations with the highest frequency of occurrence of heat waves are located in the western and southern parts of the province. This is possibly due the different topography found across the eastern and western sides of the province. The influence of the steep escarpment only benefits areas lying on the eastern side while moist air is hindered to reach the western areas, hence dry and hot conditions are mainly on the western side. Stations with minimum number of heat waves (2-3 events) were found across the central and eastern part of the North West province.

This study also investigated the cyclic nature of heat wave occurrence. The results revealed return periods of 12-years, 4.8 years and 2.1 years. These cycles are mostly associated with sunspot activity (capable of planetary forcing), El Nino- Southern Oscillation (ENSO), and quasi-biennial oscillation (QBO) respectively. These observations dissertation validate several previous findings/theories related to the climatology of southern Africa (e.g., Makarau, 1995; Kabanda, 2004 and Jury, 2018).

6.2.3 Synoptic Conditions Associated with Heat Waves in North West Province

Apart from reaffirming previous findings, this study has also succeeded to highlight the understanding influence of the synoptic circulation on heat waves over the North West province. The important findings include: Persistent clear skies associated with continental high pressure systems (manifested by higher positive OLR anomalies) that dominated the circulation during the observed heat waves. These conditions are associated with no rainfall. Strong subsidence as observed from the vertical motion patterns. This subsidence is also a characteristic feature of continental high pressure

conditions. Increased temperatures over the NWP can also be associated with anomalies over the Indian Ocean (For example; the persistent dry conditions over the Indian Ocean and SAO as observed on specific humidity anomalies and the corresponding wind patterns). This has the negative influence over Southern Africa since larger amounts of atmospheric moisture to the continent originates from the Indian Ocean and reach the continent through the onshore air currents.

Over the 850 hPa, heat waves occurrences were associated with the advection of the near surface warm and dry air from Namibia and Botswana towards the northwestern part of the province.

The distinctive circulation pattern observed in all heat wave cases involved the persistent Atlantic high pressure system, propagating into a south-west, south–east direction, and coupled with low humidity values over the NWP. In general, the strong Atlantic Ocean anticyclone at 500 hPa, which extended to a greater part of the study area, was observed in all heat wave occurrences, and this is an associated high pressure system. With regards to the extreme temperatures observed over Tosca and Marico, stations that recorded the longest and strongest heat wave, it is safe to conclude that they were caused by both the subsiding air from the AOA and the near surface warm air advection from nearby areas as was observed over 850 hPa.

Heat waves over the NWP are connected to strong mid latitude AOA (high pressure systems) propagating on a south-west, south-east direction. Situated at the interior of the country, heat waves in the North West province are mainly triggered by the (positive anomalies) subsidences at the 500 hPa level, the warm and dry continental winds. This fairly corresponds with previous studies over a large scale, whereby by Tyson and Preston-Whyte (2000) found that an anticyclonic weather/circulation is the cause of almost all prolonged heat waves over southern Africa. From other parts of the world, related work by Kunkel *et al*., 1996; Fischer *et al.,* 2007; Lau & Nath, 2012; Zittis *et al.,* 2014 established that prolonged heat waves are associated with anticyclonic conditions. Hence, it is safe to conclude that heat waves are generally generated by the descending air in the middle level of the high pressure system. In addition, the 500 hPa anomalies displayed an anomalous blocking over the Indian Ocean, which generally blocked the pathway of the AOA and made it to be more persistent over the interior. This coincides with Barnes *et al*., 2014 & Photiadou *et al.,* 2014, who reported that regardless of the difficulty in measuring the blocking anticyclones, but they can

significantly reduce weather variability at synoptic timescales, allowing heatwaves the time to build.

Although in this study there is no other season and/or another area (e.g., coastal area) to compare with, the heat wave duration in Taung, which lasted for 7 days, qualifies the results of the other previous studies, which stated that heat waves over interior can last for 4 days and even more. The results of a study by Tyson and Preston-Whyte (2000) indicate that over the interior, heat waves often last 4 days with temperatures exceeding 5°C and highly influenced by the presence of a strong continental anticyclone.

6.3 Limitations of the study

Like all other scientific studies, this study has faced a number of limitations. Although the limitations have not necessarily weakened the dissertation in achieving the targeted objectives it is worth stating the major ones, to acknowledge the problems encountered and validate the lack of depth/completeness in certain areas. Two main limitations have particularly been identified in this study: Firstly, the data issues (i.e., the commencement of temperature observations in the study area varied from station to station and in some stations, the period was very short). Secondly, theoretical basis (i.e., there are very few studies (literature) that have been conducted previously and are specifically related to southern Africa and in North West province in particular, especially with respect to the large-scale meteorological circulation in terms of heat wave - although there are many studies, which have been undertaken in other parts of the world).

6.4 Concluding remarks

As it has been mentioned earlier on in this study that there is little research on heat waves in South Africa, therefore, their impact on crops, water supplies and human health is still not well understood. It is therefore, a required action for all the relevant organizations to participate in furthering heat waves research in order to make better decisions for the country. The concept and methodology applied in this dissertation should provide the basis for further scientific research, and the outcomes derived from this study could be used in various practical applications such as early warnings to the society. Also, more active research will enable to improve precautionary measures on and future forecasting of heat waves.

REFERENCES

Asnani, G.C. 1993. Tropical meteorology. Noble Printers, Pune

Baldwin, M., Gray, L., Dunkerton, T., Hamilton, K., Haynes, P., Randel, W., Holton, J., Alexander, M., Hirota, I. & Horinouchi, T. 2001. The quasi-biennial oscillation. reviews of geophysics, 39(2):179-229.

Barbu, N., Georgescu, F., Ştefanescu, V., & Stefan, S. 2014. Large-scale mechanisms responsible for heat waves occurrence in Romania. Rom. J. Phys, 59(9-10), 1109-1126.

Barriopedro, D., Fischer, E.M., Luterbacher, J., Trigo, R.M. & García-Herrera, R. 2011. The hot summer of 2010: redrawing the temperature record map of Europe. Science, 332(6026):220-224.

Barnes, E.A., Slingo, J., & Woollings, T. 2012. A methodology for the comparison of blocking climatologies across indices, models and climate scenarios. Clim Dyn.;38:2467–81. doi: 10.1007/s00382-011-1243-6.

Barry, R.G. & Chorley, R.J. 2009. Atmosphere, weather and climate: Routledge.

Bengtsson, L., 2010: The global atmospheric water cycle. Environ. Res. Lett., 5, 025202, doi:10.1088/1748-9326/5/2/025202.

Beniston, M. 2004. The 2003 heat wave in Europe: A shape of things to come? An analysis based on Swiss climatological data and model simulations. Geophysical Research Letters, 31(2).

Beniston, M., Stephenson, D. B., Christensen, O. B., Ferro, C. A., Frei, C., Goyette, S., Koffi, B. 2007. Future extreme events in European climate: an exploration of regional climate model projections. Climatic Change, 81(1), 71-95.

Binder, P. & Schär, C. 1996. MAP design proposal. Mesoscale Alpine Programme Rep.

Black, P.E. 1996. Watershed hydrology: Wiley Online Library.

Blignaut, J., Ueckermann, L. & Aronson, J. 2009. Agriculture production's sensitivity to changes in climate in South Africa. South African Journal of Science, 105(1-2):61-68.

Bluestein, H.B. 1992. Synoptic-dynamic Meteorology in Multitudes: Observations and theory of weather systems. Vol. 2: Taylor & Francis.

Bommier, E. 2014. Peaks-Over-Threshold Modelling of Environmental Data (pp. 22-27).

Brabson, B.B., Lister, D.H., Jones, P.D. and Palutikof, J.P. 2005. Soil moisture and predicted spells of extreme temperatures. J. Geophys. Res., 110, D05104, doi: 10.1029/2004JD005156.

Ceballos, J.C., Lima, W.F.A. & Souza, J.M.d. 2003. Outgoing longwave radiation at the top of the atmosphere: preliminary assessment using GOES-8 imager data. Revista Brasileira de Geofísica, 21(1):53-64.

Ceccherini, G., Russo, S., Ameztoy, I., Marchese, A.F. & Carmona-Moreno, C. 2017. Heat waves in Africa 1981–2015, observations and reanalysis. Natural Hazards and Earth System Sciences, 17(1):115-125.

Chang, F.-C. & Wallace, J.M. 1987. Meteorological conditions during heat waves and droughts in the United States Great Plains. Monthly Weather Review, 115(7):1253-1269.

Chikoore, H. 2016. Drought in southern Africa: structure, characteristics and impacts. PhD thesis, University of Zululand.

Coles, S., Bawa, J., Trenner, L. & Dorazio, P. 2001. An introduction to statistical modeling of extreme values. Vol. 208: Springer.

Coles, S., Bawa, J., Trenner, L., & Dorazio, P. 2001. An introduction to statistical modeling of extreme values (Vol. 208): Springer.

Conradie, D.C. 2012. South Africa's climatic zones: today, tomorrow.

Cook, C., Reason, C. J., & Hewitson, B. C. 2004. Wet and dry spells within particularly wet and dry summers in the South African summer rainfall region. Climate research, 26(1), 17-31.

Coumou, D. & Rahmstorf, S. 2012. A decade of weather extremes. Nature Climate Change, 2(7):491-496.

Croitoru, A.E., Antonie, R. & Rus, A. 2014. Heat waves and their estimated socio-economic impact in Bucharest city, Romania. 14th SGEM GeoConference on Energy and Clean Technologies, 2(SGEM2014 Conference Proceedings, ISBN 978-619-7105-16-2/ISSN 1314-2704, June 19-25, 2014, Vol. 2):367-374 pp.

Dai, A. 2006. Recent climatology, variability, and trends in global surface humidity. Journal of Climate, 19(15):3589-3606.

de Villiers, B. & Mangold, S. 2002. The biophysical environment. North West Province state of the environment report. Directorate of Environment and Conservation Management, North West Department of Agriculture, Conservation and Environment, Mmabatho.

Della-Marta, P.M., Haylock, M.R., Luterbacher, J. & Wanner, H. 2007. Doubled length of western European summer heat waves since 1880. Journal of Geophysical Research: Atmospheres, 112(D15).

Deo, R.C., Syktus, J., McAlpine, C., Lawrence, P., McGowan, H. & Phinn, S.R. 2009. Impact of historical land cover change on daily indices of climate extremes including droughts in eastern Australia. Geophysical research letters, 36(8).

Department of Environmental Affairs. 2013. Biome-based Adaptation Framework: Vulnerability Assessment of Climate Change Impacts on South African Biomes. Department of Environmental Affairs, Pretoria.

Department Of Water Affairs & Forestry. 2004. National Water Resources Strategy, 1st edition. Department of Water Affairs and Forestry, Pretoria.

Department of health & Department of Environmental Affairs, 2016. National Climate Change & Health Adaptation Plan 2014/2019.

Easterling, D.R., Evans, J., Groisman, P.Y., Karl, T.R., Kunkel, K.E. & Ambenje, P. 2000. Observed variability and trends in extreme climate events: a brief review. Bulletin of the American Meteorological Society, 81(3):417-425.

Engelbrecht F.A. & Landman W. 2014. A brief description of South Africa's present-day climate, South African Risk and Vulnerability Atlas. ISBN: 978-0-620-45659-3

Francois Engelbrecht et al 2015.Projections of rapidly rising surface temperatures over Africa under low mitigation Environ. Res. Lett.10 085004.

Ekstrom, M., Fowler, H. J., Kilsby, C. G., & Jones, P. D. 2005. New estimates of future changes in extreme rainfall across the UK using regional climate model integrations. 2. Future estimates and use in impact studies. Journal of Hydrology, 300(1-4), 234-251. doi:10.1016/j.jhydrol.2004.06.019.

Fauchereau, N., Pohl, B., Reason, C., Rouault, M. & Richard, Y. 2009. Recurrent daily OLR patterns in the Southern Africa/Southwest Indian Ocean region, implications for South African rainfall and teleconnections. Climate Dynamics, 32(4):575-591.

Feng, L., Li, T., & Yu, W. 2014. Cause of severe droughts in Southwest China during 1951–2010. Climate Dynamics, 43(7-8), 2033-2042.

Fischer, E. M., Seneviratne, S. I., Lüthi, D., & Schär, C. 2007. Contribution of land-atmosphere coupling to recent European summer heat waves. Geophysical Research Letters, 34, L06707.

Fischer, E.M. 2014. Climate science: autopsy of two mega-heatwaves. Nature Geoscience, 7(5):332-333.

Fisher, M., Abate, T., Lunduka, R.W., Asnake, W., Alemayehu, Y. & Madulu, R.B. 2015. Drought tolerant maize for farmer adaptation to drought in sub-Saharan Africa: Determinants of adoption in eastern and southern Africa. Climatic change, 133(2):283-299.

Frich, P., Alexander, L.V., Della-Marta, P., Gleason, B., Haylock, M., Tank, A.K. & Peterson, T. 2002. Observed coherent changes in climatic extremes during the second half of the twentieth century. Climate research, 19(3):193-212.

Furrer, E.M., Katz, R.W., Walter, M.D. & Furrer, R. 2010. Statistical modeling of hot spells and heat waves. Climate research, 43(3):191-205.

Giles, B.D., Balafoutis, C. & Maheras, P. 1990. Too hot for comfort: the heatwaves in Greece in 1987 and 1988. International Journal of Biometeorology, 34(2):98-104.

Gong, S. 2012. Estimation of hot and cold spells with extreme value theory.

Gruber, A. & Krueger, A.F. 1984. The status of the NOAA outgoing longwave radiation data set. Bulletin of the American Meteorological Society, 65(9):958-962.

Grundstein et al., (2013). Exceedance of wet bulb globe temperature safety thresholds in sports under a warming climate. Climate Research. 58. 183-191. 10.3354/cr01199.

Hansen, J., Ruedy, R., Sato, M. & Lo, K. 2010. Global surface temperature change. Reviews of Geophysics, 48(4).

Hart, N.C.G., Reason, C.J.C. & Fauchereau, N. Clim Dyn 2013 41: 1199.

Hart, N., Reason, C.J.C. & Fauchereau, N. 2010. Tropical-extratropical interactions over southern Africa: three cases of heavy summer season rainfall. Monthly Weather Review, 138:2608–2623

Hartmann, D. L., & Recker, E. E. 1986. Diurnal variation of outgoing longwave radiation in the tropics. Journal of Climate and Applied Meteorology, 25(6), 800-812.

Hartmann, D.L. & Recker, E.E. 1986. Diurnal variation of outgoing longwave radiation in the tropics. Journal of Climate and Applied Meteorology, 25(6):800-812.

Hatzaki, M., Flocas, H.A., Simmonds, I., Kouroutzoglou, J., Keay, K. & Rudeva, I. 2014. Seasonal aspects of an objective climatology of anticyclones affecting the Mediterranean. Journal of Climate, 27(24):9272-9289.

Hennessy, K. & Pittock, A. 1995. Greenhouse warming and threshold temperature events in Victoria, Australia. International Journal of Climatology, 15(6):591-612.

Hernández-Ceballos, M., Brattich, E. & Cinelli, G. 2016. Heat-wave events in Spain: air mass analysis and impacts on 7Be concentrations. Advances in Meteorology, 2016.

Hewitson, B. C., & Crane, R. G. 2006. Consensus between GCM climate change projections with empirical downscaling: precipitation downscaling over South Africa. International Journal of Climatology, 26(10), 1315-1337. doi:10.1002/joc.1314.

Hewitson, B.C. & Crane, R.G. 2006. Consensus between GCM climate change projections with empirical downscaling: precipitation downscaling over South Africa. International Journal of Climatology, 26(10):1315-1337.

Hill, M., Held, A., Leuning, R., Coops, N., Hughes, D. & Cleugh, H. 2006. MODIS spectral signals at a flux tower site: Relationships with high-resolution data, and CO2 flux and light use efficiency measurements. Remote Sensing of Environment, 103(3):351-368.

Hinze, S., Reiss, T. & Schmoch, U. 1997. Statistical analysis on the distance between fields of technology: Fraunhofer-Inst. Systems and Innovation Research.

Holton, J. R. 1979. Introduction to Dynamic Meteorology (Volume 23).

Horton, R.M., Mankin, J.S., Lesk, C. et al. Curr Climb Change Rep 2016 2: 242.

Horton, R.M., Mankin, J.S., Lesk, C., Coffel, E. & Raymond, C. 2016. A Review of Recent Advances in Research on Extreme Heat Events. Current Climate Change Reports, 2(4):242-259.

Huber, D.G. & Gulledge, J. 2011. Extreme weather and climate change: understanding the link, managing the risk: Pew Center on Global Climate Change Arlington.

Hughes SH, Balling RC. 1996. Urban influences on South African temperature trends. International Journal of Climatology 16: 935–940.

Hunt, B.G. 2007. A Climatology of Heat Waves from a Multimillennial Simulation. Journal of Climate, 20(15):3802-3821.

Iizumi, T. & Ramankutty, N. 2015. How do weather and climate influence cropping area and intensity? Global Food Security, 4:46-50.

Intergovernmental Panel on Climate Change, 2001. Special Report on Emissions Scenarios: A special report of Working Group III of the Intergovernmental Panel on Climate Change (eds. Nakićenović, N., and Swart, R.), Cambridge University Press, Cambridge, United Kingdom and New York, NY, USA.

Intergovernmental Panel on Climate Change, 2013. Climate Change 2013: The Physical Science Basis. Contribution of Working Group I to the Fifth Assessment Report of the Intergovernmental Panel on Climate Change. IPCC, Geneva, Switzerland.

Ioannidou, L. & Yau, M. 2008. A climatology of the Northern Hemisphere winter anticyclones. Journal of Geophysical Research: Atmospheres, 113(D8).

IPCC Workshop on Changes in Extreme Weather and Climate Events, workshop report, Beijing, China, 11-13 June, 2002, pp. 107

Jentsch, A. & Beierkuhnlein, C. 2008. Research frontiers in climate change: Effects of extreme meteorological events on ecosystems. Comptes Rendus Geoscience, 340(9):621-628.

Jury, M.R. 2013. Climate trends in Southern Africa. S Afr J Sci. 2013; 109(1/2)

Jury, M.R. 2018. Climate trends across South Africa since 1980. Water SA, 44(2), 297-307.

Kabanda, T.A. 2004. Climatology of long-term drought in the northern region of the Limpopo Province of South Africa. PhD thesis, University of Venda.

Kalnay E, Kanamistu M, Kistler R, Collins W, Deaven D, Gandin L, Iredell M, Saha S, White G, Woollen J, Zhu Y, Leoma A, Reynolds R, Chelliah M, Ebisuzaki W, Higgins W, Janowiak J, Mo KC, Ropelewski C, Wang J, Jenne R, Joseph D.1996. The NMC/NCAR 40-Year Reanalysis Project. Bull Am Meteorol Soc 77:437–471

Karl, T.R. & Knight, R.W. 1997. The 1995 Chicago heat wave: How likely is a recurrence? Bulletin of the American Meteorological Society, 78(6):1107-1119.

Karl, T.R., Jones, P.D., Knight, R.W., Kukla, G., Plummer, N., Razuvayev, V., Gallo, K.P., Lindseay, J., Charlson, R.J. & Peterson, T.C. 1993. A new perspective on recent global warming: asymmetric trends of daily maximum and minimum temperature. Bulletin of the American Meteorological Society, 74(6):1007-1024.

Katz, R. W. 2010. Statistics of extremes in climate change. Climatic change, 100(1), 71- 76.

Katz, R. W., & Brown, B. G. 1992. Extreme events in a changing climate: variability is more important than averages. Climatic change, 21(3), 289-302.

Katz, R. W., Parlange, M. B., & Naveau, P. 2002. Statistics of extremes in hydrology. Advances in water resources, 25(8-12), 1287-1304.

Katz, R.W. 2010. Statistics of extremes in climate change. Climatic change, 100(1):71-76.

Katz, R.W. & Brown, B.G. 1992. Extreme events in a changing climate: variability is more important than averages. Climatic change, 21(3):289-302.

Kharin, V.V. & Zwiers, F.W. 2000. Changes in the extremes in an ensemble of transient climate simulations with a coupled atmosphere–ocean GCM. Journal of Climate, 13(21):3760-3788.

Kistler, R., Kalnay, E., Collins, W., Saha, S., White, G., Woollen, J., Chelliah, M., Ebisuzaki, W., Kanamitsu, M., Kousky, V., van den Dool, H., Jenne, R., & Fiorino, M. 2001. The NCEP-NCAR 50 year reanalysis: Monthly means CD-ROM and documentation. Bull. Amer. Meteor. Soc, 82, 247-268.

Kostopoulou, E. 2003. The relationships between atmospheric circulation patterns and surface climatic elements in the eastern Mediterranean (University of East Anglia, Ph.D. thesis). Retrieved from http://ethos.bl.uk/OrderDetails.do?uin=uk.bl.eth os.405217

Kotsiantis, S., Kostoulas, A., Lykoudis, S., Argiriou, A. & Menagias, K. 2006. Filling missing temperature values in weather data banks. 2006:v1-327-v321-327.

Kruger, A. & Sekele, S. 2013a. Trends in extreme temperature indices in South Africa: 1962–2009. International Journal of Climatology, 33(3):661-676.

Kruger, A., Goliger, A.M., Retief, J. & Sekele, S. 2010. Strong wind climatic zones in South Africa.

Kruger, A.C. & Sekele, S.S. 2013b. Trends in extreme temperature indices in South Africa: 1962-2009. International Journal of Climatology, 33(3):661-676.

Kruger, A.C. & Shongwe, S. 2004. Temperature trends in South Africa: 1960–2003. International Journal of Climatology, 24(15):1929-1945.

Kueh, M., Lin, C., Chuang, Y., Sheng, Y. & Chien, Y. 2017. Climate variability of heat waves and their associated diurnal temperature range variations in Taiwan. Environmental Research Letters, 12(7):074017.

Kunkel, K.E., Changnon, S.A., Reinke, B.C. & Arritt, R.W. 1996. The July 1995 heat wave in the Midwest: A climatic perspective and critical weather factors. Bulletin of the American Meteorological Society, 77(7):1507-1518.

Kurz, M. 1998. Synoptic meteorology: Deutscher Wetterdienst.

Kysely, J. & Kim, J. 2009. Mortality during heat waves in South Korea, 1991 to 2005: How exceptional was the 1994 heat wave? Climate research, 38:105-116.

Labitzke, K., & Van Loon, H. 1999. The Stratosphere: Phenomena. History, and Relevance. Springer, 3(4), 41.

Läderach, A. & Raible, C.C. 2013. Lower-tropospheric humidity: climatology, trends and the relation to the ITCZ. Tellus A: Dynamic Meteorology and Oceanography, 65(1):20413.

Landman, S. 2012. A multi-model ensemble system for short-range weather prediction in South Africa.

Lau, N.-C. & Nath, M.J. 2012. A model study of heat waves over North America: Meteorological aspects and projections for the twenty-first century. Journal of Climate, 25(14):4761-4784.

Linacre, E. 1992. Climate data and resources: a reference and guide: Psychology Press.

Lucio, P., Silva, A. & Serrano, A. 2010. Changes in occurrences of temperature extremes in continental Portugal: a stochastic approach. Meteorological Applications, 17(4):404-418.

Lyon, B. 2009. Southern Africa summer drought and heat waves: observations and coupled model behavior. Journal of Climate, 22(22):6033-6046.

Lyon, B. & Mason, S.J. 2007. The 1997-98 summer rainfall season in southern Africa. Part I: Observations. Journal of Climate, 20(20):5134-5148.

M¨uhlenbruch-Tegen A. 1992. Long-term surface temperature variations in South Africa. South African Journal of Science 88: 197–205.

Makarau A. 1995. Intra-seasonal oscillatory modes of the southern Africa summer circulation. PhD thesis, University of Cape Town

Marshall, G.J. & Harangozo, S.A. 2000. An appraisal of NCEP/NCAR reanalysis MSLP data viability for climate studies in the South Pacific. Geophysical Research Letters, 27(19), 3057-3060.

Matzarakis, A. & Mayer, H. 1997. Heat stress in Greece. International Journal of Biometeorology, 41(1):34-39.

McNeil, A.J. & Frey, R. 2000. Estimation of tail-related risk measures for heteroscedastic financial time series: an extreme value approach. Journal of empirical finance, 7(3-4):271-300.

Meehl, G.A. & Tebaldi, C. 2004. More intense, more frequent, and longer lasting heat waves in the 21st century. Science, 305(5686):994-997.

Meehl, G.A., Arblaster, J.M., Matthes, K., Sassi, F. & van Loon, H. 2009. Amplifying the Pacific climate system response to a small 11-year solar cycle forcing. Science, 325(5944):1114-1118.

Meehl, G.A., Karl, T., Easterling, D.R., Changnon, S., Jr., R.P., Changnon, D., Evans, J., Groisman, P.Y., Knutson, T.R., Kunkel, K.E., Mearns, L.O., Parmesan, C., Pulwarty, R., Root, T., Sylves, R.T., Whetton, P. & Zwiers, F. 2000. An Introduction to Trends in Extreme Weather and Climate Events: Observations, Socioeconomic Impacts, Terrestrial Ecological Impacts, and Model Projections. Bulletin of the American Meteorological Society, 81(3):413-416.

Min, S.-K., Zhang, X., Zwiers, F.W. & Hegerl, G.C. 2011. Human contribution to more-intense precipitation extremes. Nature, 470(7334):378-381.

Miralles, D.G., Teuling, A.J., van Heerwaarden, C.C. and VilaGuerau de Arellano, J. 2014. Mega-heat wave temperatures due to combined soil desiccation and atmospheric heat accumulation, Nat. Geosci., 7, 345–349.

Muhlenbruch-Tegen, A. 1992. Long-term surface temperature variations in South Africa. South African Journal of Science, 88, 197-205.

Mulenga, H.M., Rouault, M. & Reason, C.J.C. 2003. Dry summers over NE South Africa and associated circulation anomalies, Climate Research, 25, 29-41. Retrieved from http://www.int-res.com/articles/cr2003/25/c025p029.pdf

Musk, L. 1988. The assessment of local fog climatology for new motorway and major road schemes. (In. Proceedings of the IVth International Conference on Weather and Road Safety, Florence organised by. p. 777-797).

Nenwiini, S.C. 2017. Climatic Anomalies and their influence on Rainfall Trends in Vhembe District South Africa. PhD Thesis, North West University.

New, M., et al. 2006, Evidence of trends in daily climate extremes over southern and West Africa, J. Geophys. Res., 111, D14102.

Newman, M., Sardeshmukh, P.D. & Bergman, J.W. 2000. An assessment of the NCEP, NASA, and ECMWF reanalyses over the tropical west Pacific warm pool. Bulletin of the American Meteorological Society, 81(1), 41.

NOOA/NCEP, Global climate report, accessed 15 October 2016, https://www.ncdc.noaa.gov/sotc/global/201510

Ogallo, L. 1993. Climate change signals over eastern and southern Africa. (In. Proc. 3rd Technical conference on meteorological Research in eastern and southern Africa.

Ogallo, L. 1993. Climate change signals over eastern and southern Africa. Paper presented at the Proc. 3rd Technical conference on meteorological Research in eastern and southern Africa.

Patricola, C.M. & Cook, K.H. 2010. Northern African climate at the end of the twenty-first century: an integrated application of regional and global climate models. Climate Dynamics, 35(1):193-212.

Pantavou, K.,Theoharatos, G., Nikolopoulos, G., Katavoutas, G., & Asimakopoulos, D. 2008. Evaluation of thermal discomfort in Athens territory and its effect on the daily number of recorded patients at hospitals' emergency rooms. Int. J. Biometeorol. 52, 773–778.

Pearce, F. 1989. Turning up the heat: Our perilous future in the global greenhouse: Random House (UK).

Peixoto, J. & Oort, A.H. 1996. The climatology of relative humidity in the atmosphere. Journal of Climate, 9(12):3443-3463.

Perkins, S. & Alexander, L. 2013. On the measurement of heat waves. Journal of Climate, 26(13):4500-4517.

Pezza, A.B., Van Rensch, P. & Cai, W. 2012. Severe heat waves in Southern Australia: synoptic climatology and large scale connections. Climate Dynamics, 38(1-2):209-224.

Planton, S., Déqué, M., Chauvin, F. & Terray, L. 2008. Expected impacts of climate change on extreme climate events. Comptes Rendus Geoscience, 340(9-10):564-574.

Photiadou, C., Jones, M.R., Keellings, D., & Dewes, C.F. 2014. Modeling European hot spells using extreme value analysis. Clim Res;58:193–207. doi: 10.3354/cr01191.

Planton, S., Déqué, M., Chauvin, F., & Terray, L. 2008. Expected impacts of climate change on extreme climate events. Comptes Rendus Geoscience, 340(9-10), 564-574. doi:10.1016/j.crte.2008.07.009.

Potgieter, C.J. 2007. Accuracy and skill of the conformal-cubic atmospheric model in short-range weather forecasting over southern Africa.

Preston-Whyte, R.A. & Tyson, P.D. 1988. Atmosphere and weather of southern Africa: Oxford University Press.

Puckridge, J., Walker, K. & Costelloe, J. 2000. Hydrological persistence and the ecology of dryland rivers. Regulated Rivers: Research & Management, 16(5):385-402.

Quinn, W. H., Neal, V. T., & Mayolo, S. E. A. D. 1987. El Niño occurrences over the past four and a half centuries. Journal of Geophysical Research: Oceans (1978–2012), 92(C13), 14449-14461. Doi: 10.1029/JC092iC13p14449.

Radinović, D. & Ćurić, M. 2012. Criteria for heat and cold wave duration indexes. Theoretical and applied climatology, 107(3-4):505-510.

Radinović, D., & Ćurić, M. 2012. Criteria for heat and cold wave duration indexes. Theoretical and applied climatology, 107(3-4), 505-510.

Ragone, F. & Bouchet, F. 2017. Studying extreme European heat waves and extreme teleconnection patterns with a rare event algorithm. (In. EGU General Assembly Conference Abstracts organised by. p. 15887).

Randel, W.J., Wu, F., & Gaffen, D. J. 2000. Interannual variability of the tropical tropopause derived from radiosonde data and NCEP reanalyses. Journal of geophysical research, 105(D12), 15-509.

Ratnam, J.V., Behera, S.K., Ratna, S.B., Rajeevan, M. & Yamagata, T. 2016. Anatomy of Indian heatwaves. Sci Rep, 6:24395.

Reid, P.A., Jones, P.D., Brown, O., Goodess, C.M. & Davies, T.D. 2001. Assessments of the reliability of NCEP circulation data and relationships with surface climate by direct comparisons with station based data. Climate Research, 17, 247261.

Rhino, P., Rajeevan, M., & Srivastava, A. K. 2016. On the Variability and Increasing Trends of Heat Waves over India. Scientific reports, 6, 26153. Doi: 10.1038/srep26153

Robinson, P. J. 2001. On the definition of a heat wave. Journal of applied Meteorology, 40(4), 762-775.

Robinson, P.J. 2001. On the definition of a heat wave. Journal of applied Meteorology, 40(4):762-775.

Ross, R.J. & Elliott, W.P. 1996. Tropospheric water vapor climatology and trends over North America: 1973–93. Journal of Climate, 9(12):3561-3574.

Ruckstuhl, C., Philipona, R., Morland, J. & Ohmura, A. 2007. Observed relationship between surface specific humidity, integrated water vapor, and longwave downward radiation at different altitudes. Journal of Geophysical Research: Atmospheres, 112(D3).

Russo, S., Marchese, A.F., Sillmann, J. & Immé, G. 2016. When will unusual heat waves become normal in a warming Africa? Environmental Research Letters, 11(5):054016.

Rusticucci, M., Kyselý, J., Almeira, G. & Lhotka, O. 2016. Long-term variability of heat waves in Argentina and recurrence probability of the severe 2008 heat wave in Buenos Aires. Theoretical and applied climatology, 124(3-4):679-689.

Salby, M.L. 1996. Fundamentals of atmospheric physics. Vol. 61: Elsevier.

Sánchez-Lugo, A., Morice, C., Berrisford, P., Argüez, A. 2018. Temperature [in State of the Climate in 2017. Bulletin of the American Meteorological Society, 99(8), S11–S13.

Sarazin, M., Graham, E. & Kurlandczyk, H. 2006. FriOWL: A Site Selection Tool for the European Extremely Large Telescope (E-ELT) Project. The Messenger, 125:44.

Schulze, R. & Maharaj, M. 2006. A-Pan equivalent reference potential evaporation. South African Atlas of Climatology and Agrohydrology, Water Research Commission, Pretoria, South Africa, WRC Report, 1489(1):06.

Scott M. Osprey, N. B., 2 Jeff R. Knight,2 Adam A. Scaife,2,3 Kevin Hamilton,4 James A. Anstey,5 Verena Schenzinger,1 Chunxi Zhang4. 2016. An unexpected disruption of the atmospheric quasi-biennial oscillation. sciencemag.org, VOL 353(ISSUE 6306).

Sfîcă, L., Croitoru, A.-E., Iordache, I. & Ciupertea, A.-F. 2017. Synoptic Conditions Generating Heat Waves and Warm Spells in Romania. Atmosphere, 8(3):50.

Sfîcă, L., Croitoru, A.-E., Iordache, I., & Ciupertea, A.-F. 2017. Synoptic Conditions Generating Heat Waves and Warm Spells in Romania. Atmosphere, 8(3), 50.

Smith, T.T., Zaitchik, B.F. & Gohlke, J.M. 2013. Heat waves in the United States: definitions, patterns and trends. Climatic change, 118(3-4):811-825.

Solomon, S., Plattner, G.-K., Knutti, R. & Friedlingstein, P. 2009. Irreversible climate change due to carbon dioxide emissions. Proceedings of the national academy of sciences, 106(6):1704-1709.

Solomon, S., Plattner, G.-K., Knutti, R., & Friedlingstein, P. 2009. Irreversible climate change due to carbon dioxide emissions. Proceedings of the national academy of sciences, 106(6), 1704-1709.

South African Weather Service, what is a heat wave, accessed 10 May 2016, http://www.weathersa.co.za/learning/weather-questions/346-what-is-a-heat-wave

Steadman, R.G. 1984. A universal scale of apparent temperature. Journal of Climate and Applied Meteorology, 23(12):1674-1687.

Sun, G.-Q., Chakraborty, A., Liu, Q.-X., Jin, Z., Anderson, K.E. & Li, B.-L. 2014. Influence of time delay and nonlinear diffusion on herbivore outbreak. Communications in Nonlinear Science and Numerical Simulation, 19(5):1507-1518.

Taljaard, J.J. & Phil, D. 1996. Atmospheric circulation systems, synoptic climatology and weather phenomena of South Africa: Government Printer, South Africa.

Tan, J., Zheng, Y., Song, G., Kalkstein, L. S., Kalkstein, A. J., & Tang, X. 2007. Heat wave impacts on mortality in Shanghai, 1998 and 2003. International Journal of Biometeorology, 51(3), 193-200.

Theoharatos, G., Pantavou, K., Mavrakis, A., Spanou, G.-K., Efsthatiou, P., Mpekas, P., & Asimakopoulos, D. 2010 Heat waves observed in 2007 in Athens, Greece: Synoptic conditions, bioclimatological assessement, air quality levels and health effects. Environ. Res.110, 152–161.

Todd, M., Washington, R. & Palmer, P.I. 2004. Water vapour transport associated with tropical-temperate trough systems over southern Africa and the southwest Indian Ocean. International Journal of Climatology, 24, 555–568

Trigo, R.M., García-Herrera, R., Díaz, J., Trigo, I.F. & Valente, M.A. 2005. How exceptional was the early August 2003 heatwave in France? Geophysical research letters, 32(10).

Trenberth, K.E., Stepaniak, D.P., Hurrell, J.W. and Fiorino, M. 2001. Quality of Reanalyses in the Tropics. Journal of Climate, 14, 1499-1510

Trigo, R.M., Pereira, J., Pereira, M.G., Mota, B., Calado, T.J., Dacamara, C.C. & Santo, F.E. 2006. Atmospheric conditions associated with the exceptional fire season of 2003 in Portugal. International Journal of Climatology, 26(13):1741-1757.

Tsiropoula, G. 2003. Signatures of solar activity variability in meteorological parameters. Journal of Atmospheric and Solar-Terrestrial Physics, 65(4):469-482.

Tularam, G.A. & Ilahee, M. 2010. Time series analysis of rainfall and temperature interactions in coastal catchments. Journal of mathematics and statistics, 6(3):372-380.

Tyson, P.D. & Preston-Whyte, R.A. 2000. The weather and climate of southern Africa, 2nd edition, Oxford University press southern Africa.

Unkaševica, M. and Tošic, I. 2009. An analysis of heat waves in Serbia. Global and Planetary Change 65, 17–26.

Van den Brink, H., Können, G. & Opsteegh, J. 2004. Statistics of extreme synoptic-scale wind speeds in ensemble simulations of current and future climate. Journal of Climate, 17(23):4564-4574.

Van den Brink, H., Können, G., Opsteegh, J., van Oldenborgh, G. J., & Burgers, G. 2004. Estimating thousands-year return values from ECMWF seasonal forecast ensembles. Int. Journal of Clim.

Van Loon, H. & Labitzke, K. 2000. The influence of the 11-year solar cycle on the stratosphere below 30 km: A review. Space Science Reviews, 94(1-2):259-278.

Vigaud, N., Richard, Y., Rouault, M. & Fauchereau, N. 2007. Water vapour transport from the tropical Atlantic and summer rainfall in tropical southern Africa. Climate dynamics, 28(2-3), 113-123

Vizy, E.K. & Cook, K.H. 2012. Mid-twenty-first-century changes in extreme events over northern and tropical Africa. Journal of Climate, 25(17):5748-5767.

Wallace, J.M. & Gutzler, D.S. 1981. Teleconnections in the geopotential height field during the Northern Hemisphere winter. Mon. Wea. Rev., 109, 784–812.

Wallace, J. M., & Hobbs, P. V. 2006. Atmospheric science: an introductory survey (Vol. 92): Academic press.

Walshaw, D. 1994. Getting the most from your extreme wind data: a step by step guide. Journal of Research-National Institute of Standards and Technology, 99, 399-399.

Wang, W., Zhou, W., Li, X., Wang, X. & Wang, D. 2015. Synoptic-scale characteristics and atmospheric controls of summer heat waves in China. Climate Dynamics, 46(9-10):2923-2941.

Warwick S. Hughes And Robert C. Balling, J. 1995. Urban Influences on South African Temperature Trends. International Journal of Climatology, VOL. 16.

Zampieri M, D'Andrea F, Vautard R, Ciais P, De Noblet-Ducoudré N, Yiou P.2009 Hot European summers and the role of soil moisture in the propagation of Mediterranean drought. J Climate. 22:4747–58.

Zhang, H. 2009. Multifractality ofSunspot Time Series.

Zittis, G., Hadjinicolaou, P. & Lelieveld, J. 2014. Role of soil moisture in the amplification of climate warming in the Eastern Mediterranean and the Middle East. Climate research, 59(1):27-37.